Hip

12

Carlo Martinoli and Stefano Bianchi

CONTENTS

C. Martinoli, MD
Associate Professor of Radiology, Cattedra "R" di Radiologia – DICMI – Università di Genova, Largo Rosanna Benzi 8, 16132 Genova, Italy
S. Bianchi, MD
Privat-docent, Université de Genève, Consultant Radiologist, Fondation et Clinique des Grangettes, 7, ch. des Grangettes, 1224 Genève, Switzerland

12.1 Introduction

US examination of the hip has mostly been dedicated to examination of the infant hip to detect developmental hip dysplasia. More recently, the development and refinement of "small-parts" transducers and the widespread consciousness of the capabilities of US in the assessment of musculoskeletal disorders have increased the number of US examinations of the hip in adults. This chapter deals with the normal anatomy, technique of examination and pathologic findings of the hip joint and hip region.

12.2 Clinical Anatomy

12.2.1 Osseous and Articular Anatomy

The hip is a "ball-and-socket" joint composed of the femoral head and the acetabulum, a cavity made by joining of three pelvic bones: ilium, pubis and ischium (Fig. 12.1). A triangular fibrocartilaginous structure, the acetabular labrum, inserts into the border of the acetabulum. Its main function is to increase the depth and surface of the acetabular cavity, thus allowing a better congruity between it and the femoral head. The articular surface of the

acetabulum has a concave shape and is tilted inferiorly and anteriorly. Its central nonarticular portion is made by a depression of the bony contours filled by fat and containing vessels and the ligamentum teres. The ligamentum teres is a flat cord-like structure which joins the fovea centralis with the lower portion of the acetabulum and houses the vasculature supplying the femoral head. The femoral head is a round structure representing approximately two-thirds of a sphere. It is almost completely covered by articular hyaline cartilage with the exception of the fovea, a small depression located in its center. The cartilage of the femoral head ends at the level of the epiphyseal plate, at the junction between femoral head and femoral neck.

The hip bones give rise to many muscular attachments. Cranial to the acetabulum, the ilium also has two prominent projections on its anterior margin: the anterior superior iliac spine, which may easily be visible through the skin of slender subjects, and the anterior inferior iliac spine (Fig. 12.1a). The first gives insertion to the tensor fasciae latae and sartorius, the second to the rectus femoris. Medially, the iliac fossa is filled by the iliacus muscle. The lower branch of the pubis gives insertion to the adductor magnus and brevis and, more medially, to the adductor longus and the gracilis. On its posterior aspect, the ischium exhibits a rough, blunt projection, the ischial tuberosity, from which the long head of the biceps, the semitendinosus and semimembranosus arise (Fig. 12.1). Then, the proximal femur has two prominent apophyses: the greater and the lesser trochanters (Fig. 12.1). One should remember that the greater trochanter has three facets (anterior, lateral and posterosuperior) for the insertion of the abductor muscles, which are, from anterior to posterior, the gluteus minimus, the anterior and posterior tendons of the gluteus medius – whereas the iliopsoas tendon attaches to the lesser trochanter (Pfirrmann et al. 2001).

12.2.2 Joint and Ligament Complexes

The articulating surface of the head of the femur is located deep inside the bony acetabulum, which

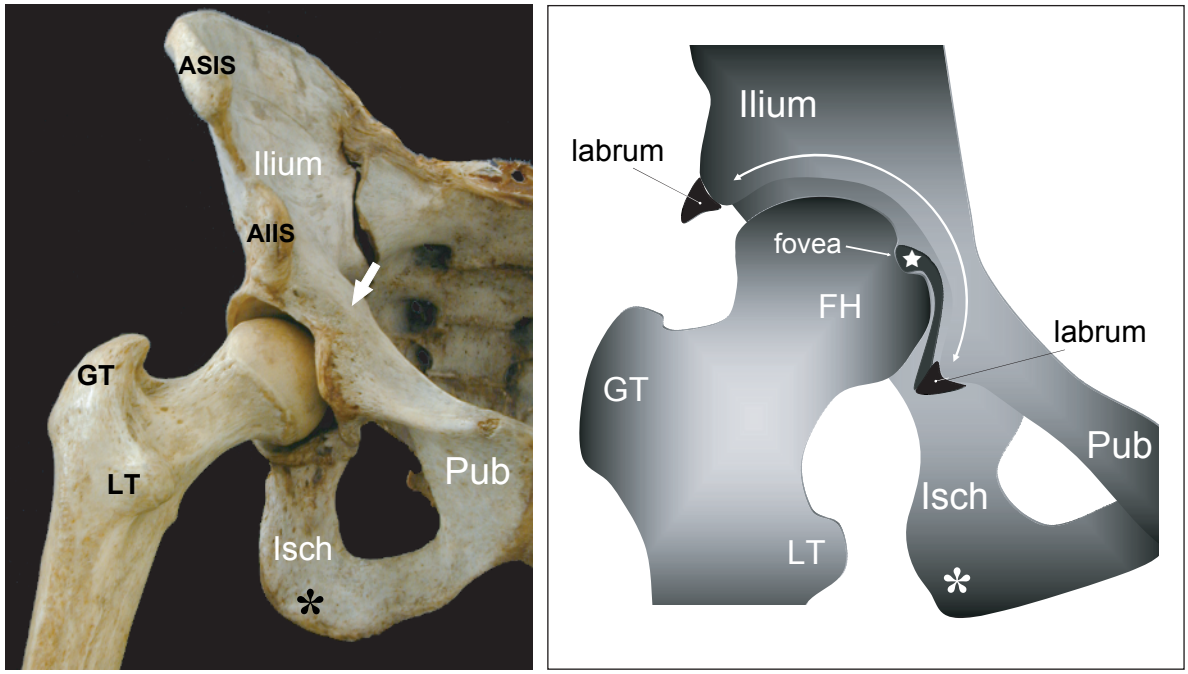

Fig. 12.1a,b. Hip joint. Articular anatomy. **a** Anterior aspect of the hip bones illustrates the relationships of the femoral head with the acetabulum. Observe that the hip is composed of three bones, ilium, ischium (*Isch*) and pubis (*Pub*), which meet at the cup-shaped acetabulum, the socket for the femoral head. Two prominences, the anterior superior (*ASIS*) and anterior inferior (*AIIS*) iliac spines, are visible on the anterior margin of the ilium and a rough, blunt projection, the ischial tuberosity (*asterisk*), can be appreciated on the posteroinferior aspect of the ischium. The two apophyses of the femur, the greater (*GT*) and the lesser (*LT*) trochanters, are also illustrated. These important bony landmarks indicate where most of the hip tendons attach. *Arrow*, iliopectineal eminence. **b** Schematic drawing of a coronal view through the hip shows a closer look at the articular anatomy. The femoral head (*FH*) shows a defect at its internal aspect, the fovea, which gives insertion to the ligament teres (*star*). Note the acetabular labrum, which increases the depth of the acetabular cavity

covers approximately 40% of it at any position of hip motion. This structural design, along with the presence of a strong capsule and of several powerful para-articular ligaments, confers an inherent stability to the coxofemoral joint, which is necessary for the bipedal posture. The fibrous capsule surrounds the acetabulum attaching to the outer surface of the labrum and inserts distally to the intertrochanteric region and the posterior aspect of the femoral neck. Its anterior part is very strong and becomes taut in full extension. The anterior iliofemoral and pubofemoral ligaments reinforce the anterior capsule during extension and abduction of the thigh respectively by joining the ilium and the pubis with the anterior aspect of the proximal metaphysis of the femur. The posterior ischiofemoral ligament covers the posterior aspect of the capsule and, because of its spiral structure, stabilizes the joint during extension. The lateral third of the femoral neck and the trochanters are extra-articular. Despite its stability, the hip joint reveals a considerable range of motion with flexion (135°) and extension (20–30°), internal (20–30°) and external (45–50°) rotation.

12.2.3 Muscles and Tendons

Because many tendons and muscles lie in the soft tissues around the hip, they have been subdivided here, based on their position, into anterior, medial, lateral and posterior groups. In general, anterior and lateral muscles and tendons are readily depicted with US, whereas posterior structures are more difficult to assess with this technique, at least in patients with large body habitus, due to their deep position.

12.2.3.1 Anterior Hip

The muscles and tendons of the anterior hip can be divided in two groups: superficial (sartorius and tensor fasciae latae) and deep (rectus femoris, iliopsoas and pectineus). Superficial muscles can be easily delineated with high US frequencies, whereas deep muscles may require switching the transducer frequency down for an adequate examination.

In the superficial group, the sartorius and tensor fasciae latae arise from the anterior and lateral aspect of anterior superior iliac spine respectively (Fig. 12.2). The sartorius, the longest muscle of the human body, crosses the midline overlying the deep muscles to descend along the medial aspect of the thigh and reach the anteromedial aspect of the proximal leg. It is a weak flexor and contributes to rotating the thigh externally. The tensor fasciae latae is a short muscle that descends to insert distally in the anterior edge of the fasciae latae, a fibrous lamina also referred to as the "iliotibial band" which covers the lateral aspect of the thigh. It is an abductor and flexor of the thigh and tightens the iliotibial band helping to keep the knee extended while standing.

From lateral to medial, the deep layer of anterior muscles includes: the rectus femoris, the iliopsoas and the pectineus (Fig. 12.2). The rectus femoris muscle has three separate proximal tendons: direct (straight), indirect and reflected. The direct tendon originates from the anterior inferior iliac spine and continues down into a superficial aponeurosis which covers the anterior aspect of the proximal muscle (superficial aponeurosis); the indirect tendon arises from the superior acetabular ridge and forms a sagittal-oriented band (central aponeurosis) that is located inside the proximal muscle belly; the thin reflected tendon is directed more medially to merge

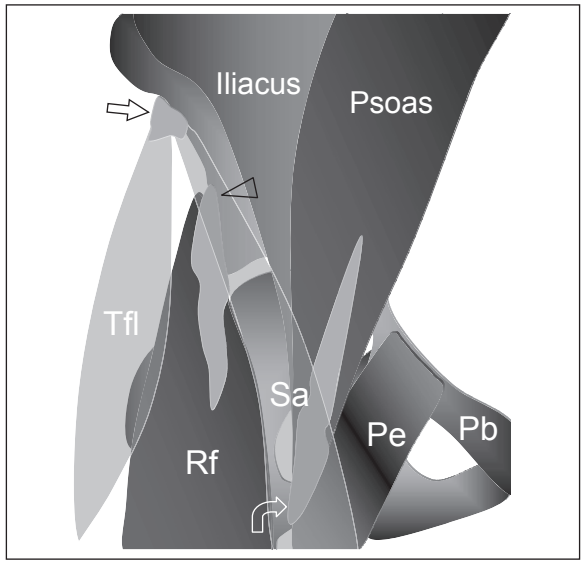

Fig. 12.2. Anatomy of the anterior muscles and tendons of the hip. Schematic drawing of an anterior view through the hip illustrates the relationships of the anterior muscles to each other. The superficial tensor fasciae latae (*Tfl*) and sartorius (*Sa*) arise from the anterior superior iliac spine (*straight arrow*). On a deeper plane, the rectus femoris (*Rf*) originates from the anterior inferior iliac spine (*arrowhead*). Observe the iliacus and the psoas muscles which join distally to insert through a common tendon onto the lesser trochanter (*curved arrow*). Medially to the iliopsoas tendon, the pectineus muscle (*Pe*) can be seen arising from the anterior aspect of the superior ramus of the pubis (*Pb*)

with the anterior capsule of the hip joint. After its origin, the rectus femoris crosses the anterior aspect of the hip joint and expands straight downward in the anterior thigh to insert into the upper pole of the patella. The rectus femoris is part of the quadriceps femoris complex and its primary function is to flex the thigh and extend the leg at the knee joint by pulling on the patella and the patellar tendon. The iliopsoas is composed of two muscles of the posterior abdominal walls: the psoas and iliacus. The psoas muscle arises from the lateral aspect of the bodies and transverse processes of T12 through L5 vertebrae; the iliacus muscle has a wide origin from the iliac crest, the iliac fossa, the ala of the sacrum and the iliolumbar and sacroiliac ligaments. The two muscles join, reflecting over the anterosuperior

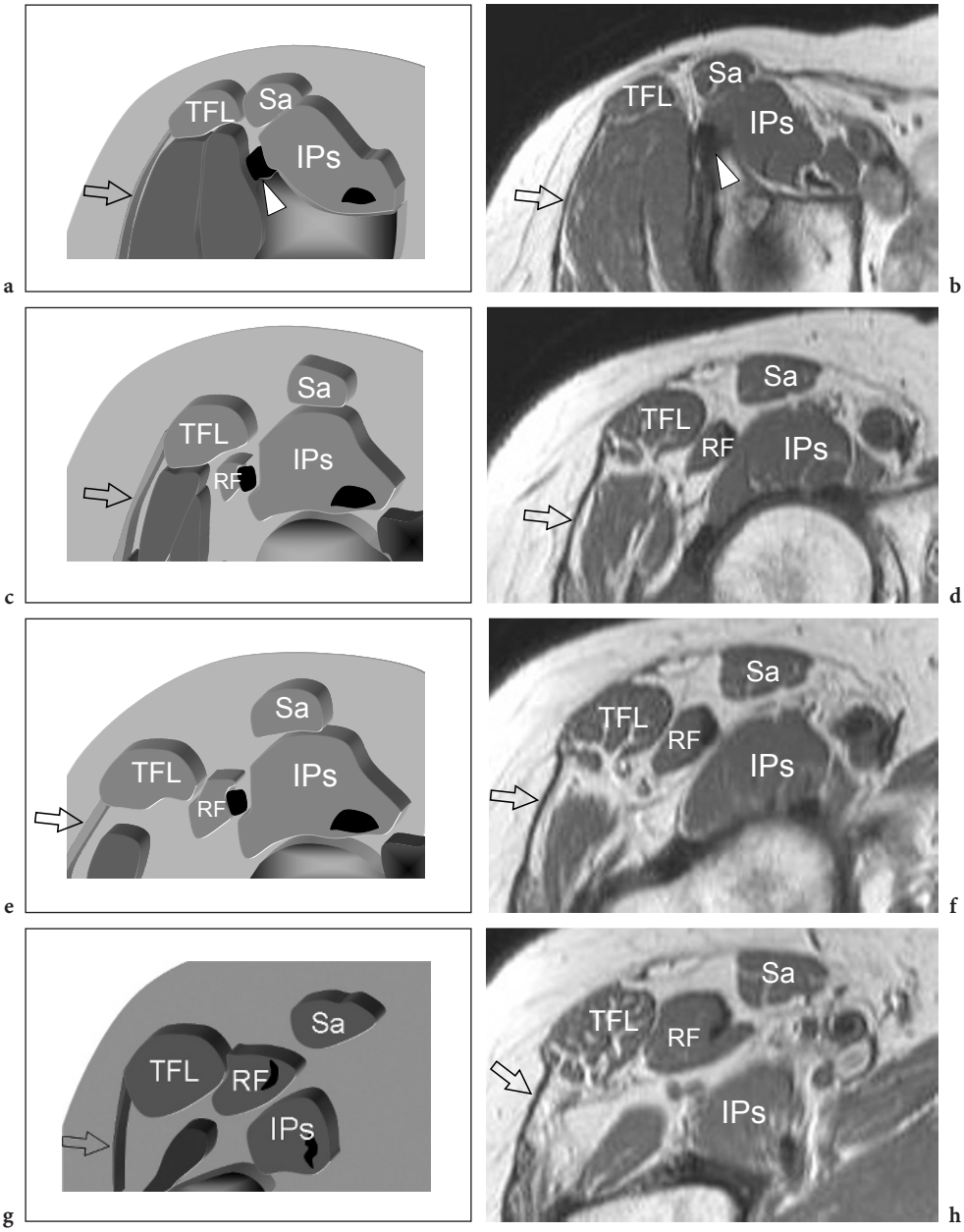

Fig. 12.3a–h. Anatomy of the anterior group (flexors) of muscles and tendons of the hip. Series of schematic drawings (**a,c,e,g**) and corresponding T1-weighted MR images (**b,d,f,h**) illustrate the relationship among the tensor fasciae latae (*TfL*)(TFL), iliopsoas (*IPs*), sartorius (*Sa*) and rectus femoris (*RF*) in transverse planes obtained from proximal to distal. Muscle bellies are represented in *intermediate gray*, tendons in *black*. In **a,b**, a *white arrowhead* indicates the rectus femoris tendon. Note that the sartorius muscle crosses the iliopsoas from lateral to medial as it proceeds downwards. *Arrow*, fasciae latae

aspect of the iliopubic ramus (iliopectineal eminence) to insert into the lesser trochanter through a common broad tendon. The iliopsoas muscle is a flexor of the thigh and, when the thighs are flexed, it is also a flexor of the trunk. On leaving the pelvis, the iliopsoas courses beneath the inguinal ligament, which joins the anterior superior iliac spine with a small tubercle located at the superior aspect of the pubis. The space between the inguinal ligament and the underlying bones (ilium laterally and pubis medially) is divided into two compartments by the iliopectineal ligament. The iliopsoas almost completely fills the lateral compartment, the "lacuna musculorum", whereas the medial compartment, the "lacuna vasorum", contains the common femoral artery and vein surrounded by fat. Two nerves are closely associated with the iliopsoas muscle: the femoral nerve, which courses along its anteromedial aspect passing through the most medial part of the "lacuna musculorum", and the small lateral femoral cutaneous nerve, located anterolaterally in close relationship with the anterior superior iliac spine. The femoral artery lies on the lateral side of the vein and is usually located in a more superficial position. The pectineus muscle is a flat rectangular muscle located medial to the iliopsoas and deep to the common femoral vessels. It forms the floor of the femoral triangle arising from the pubis and inserting to the pectineal line of the femur.

The anatomic relationship among the anterior hip muscles in the transverse plane is shown in Figure 12.3.

12.2.3.2 Medial Hip

In a more medial location, the adductor muscles include the adductor longus, the adductor brevis, the adductor magnus and the gracilis (Fig. 12.4). These muscles may merge with each other. Briefly, the adductor longus lies superficially, in the same plane as the pectineus. It arises from a narrow tendon from the body of the pubis, just inferior to the pubic crest. Deep to the pectineus and the adductor longus and superficial to the adductor magnus, the adductor brevis arises from the inferior branch of the pubis. The deep adductor magnus, the largest of the adductors, belongs in part to the adductors and in part to the hamstrings. It originates from the inferior branch of the pubis, the ramus of the ischium and the ischial tuberosity. The gracilis is the weakest and most medial of the adductors. It is a long strap-like muscle arising from the body and the inferior branch of the pubis. On the whole, the adductor muscles have their main function in the adduction and flexion of the thigh.

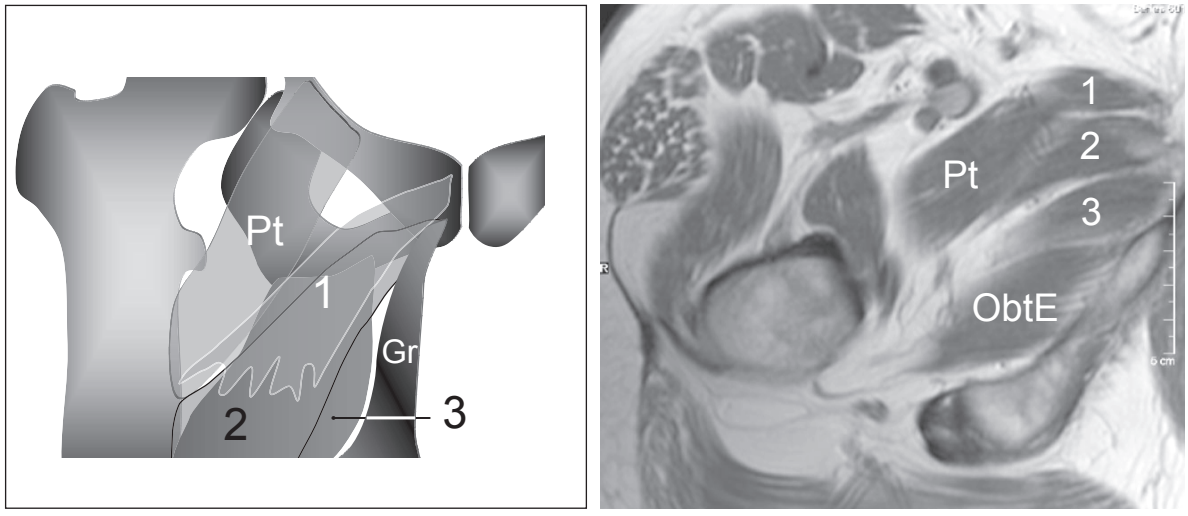

Fig. 12.4a,b. Anatomy of the medial group (adductors) of muscles and tendons of the hip. **a** Schematic drawing of an anterior view through the hip with **b** transverse T1-weighted MR image correlation illustrates the relationships of the pectineus (*Pt*), adductor longus (*1*), adductor brevis (*2*), adductor magnus (*3*) and gracilis (*Gr*) muscles to each other. Observe the layered disposition of the adductor muscles, with the longus being the most superficial and the magnus the deepest. *ObtE*, obturator externus

12.2.3.3 Lateral Hip

The muscles of the lateral hip include the anterior portion of the gluteus maximus, the gluteus medius and the gluteus minimus. The arrangement of the lateral muscles consists of two layers: superficial and deep (Fig. 12.5). From posterior to anterior, the first layer is formed by the anterior portion of the gluteus maximus, the fasciae latae and the tensor fasciae latae muscle. The most superficial fibers of the gluteus maximus attach to the posterior portion of the fasciae latae, whereas the tensor fasciae latae muscle inserts into its anterior portion. This arrangement is referred in the French literature to as the "deltoid of Farabeuf", due to some analogies with the deltoid muscle in the shoulder which lies over the rotator cuff tendons. The most cranial portion of the fasciae latae is thickened and forms the "bandellette of Massiat", a strong fibrous band that inserts into the iliac crest. Distally, the fasciae latae descends along the lateral aspect of the thigh to insert into Gerdy's tubercle at the anterolateral aspect of the proximal tibial epiphysis. The deep layer of lateral hip muscles is composed of the gluteus minimus and the gluteus medius. The gluteus minimus takes its origin from the anterior third of the lateral aspect of the iliac wing, whereas the gluteus medius has a broader attachment to the posterior two thirds of the iliac wing. Compared with the gluteus medius, the gluteus minimus is anterior and deep. The two muscles form a continuum – the so-called abductor tendon cuff of the hip – and insert into the greater trochanter acting as powerful abductors of the thigh, somewhat similarly to the rotator cuff tendons in the shoulder; the posterior gluteus medius plays a secondary role as a extensor of the lower limb, whereas the gluteus minimus also acts as an flexor. The gluteus minimus tendon inserts onto the anterior facet of the trochanter (Fig. 12.6a). The anterior and middle portions of the gluteus medius continue down into a thin strap-like band that inserts, together with some muscle fibers, into the inferior aspect of the lateral facet (Fig. 12.6b), whereas its posterior portion gives rise to a strong tendon that inserts into the posterosuperior facet of the greater trochanter (Fig. 12.6c).

The anatomic relationship among the lateral hip muscles and tendons in the transverse plane is shown in Figure 12.7.

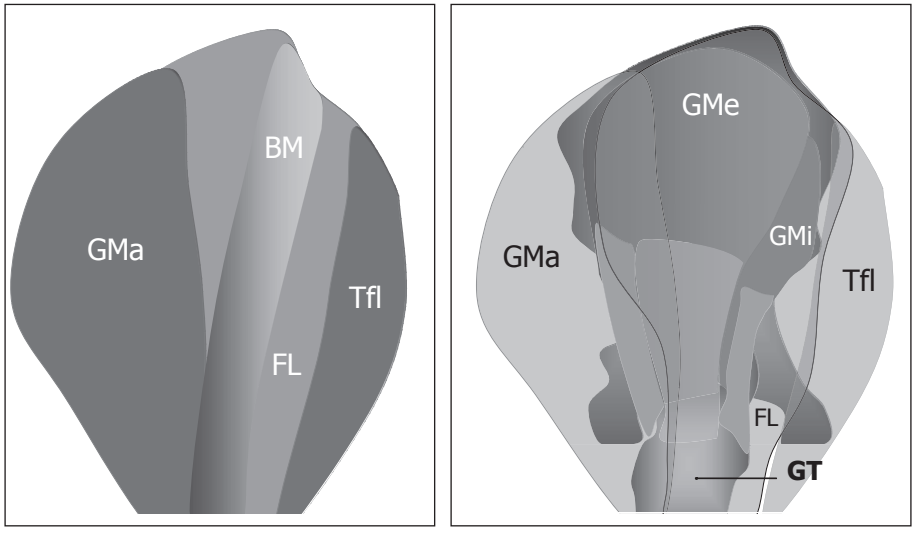

a b

Fig. 12.5a,b. Para-articular anatomy of the lateral aspect of the hip. **a** Schematic drawing of a lateral view through the hip showing the superficial layer of muscles and the fasciae latae. The "deltoid of Farabeuf" complex is composed of the large posterior gluteus maximus muscle (*GMa*), the anterior tensor fasciae latae muscle (*Tfl*) and the fasciae latae (*FL*) intervening in between these muscles. Observe the "bandellette of Massiat" (*BM*), which represents a focal thickening of the fasciae latae inserting onto the anterior portion of the iliac crest. **b** Schematic drawing of a lateral view through the hip showing the deep layer of muscles. The superficial structures depicted in **a** are here reported in a semitransparent rendering. Observe the relationships between the gluteus medius (*GMe*) and gluteus minimus (*GMi*) muscles located just deep to the fasciae latae and the anterior part of the gluteus maximus. The gluteus minimus is located anteriorly and deep relative to the gluteus medius. Both insert into the greater trochanter (*GT*)

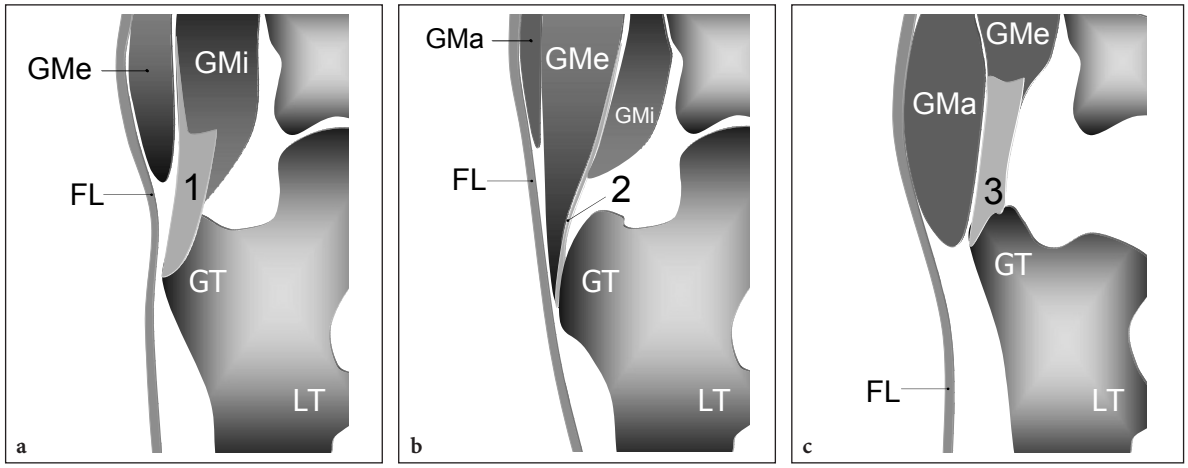

Fig. 12.6a–c. Anatomy of the lateral group (abductors) of muscles and tendons of the hip. Schematic drawings of a coronal view through the hip obtained from anterior (**a**) to posterior (**c**) illustrate the relationships of the gluteus maximus (*GMa*), medius (*GMe*) and minimus (*GMi*) muscles, the fasciae latae (*FL*), the gluteus minimus tendon (*1*), the anterior gluteus medius tendon (*2*) and the posterior gluteus medius tendon (*3*) to each other. The gluteus minimus is the smallest, deepest and most anterior muscle. The gluteus medius is located laterally and posteriorly to the gluteus minimus. The gluteus maximus is the largest, most superficial and posterior muscle. With respect to these muscles, the fasciae latae is the most superficial structure. *GT*, greater trochanter; *LT*, lesser trochanter

12.2.3.4 Posterior Hip

The posterior aspect of the hip includes a superficial and deep layer of muscles. The superficial layer is made of the largest muscle of the body, the gluteus maximus, which takes its origin from the iliac crest and the dorsal aspect of the sacrum to span laterally and inferiorly and insert into the posterior aspect of the proximal femoral metaphysis. Its most superficial fibers attach to the posterior aspect of the fasciae latae to form the posterior portion of the deltoid of Farabeuf. The deep layer of posterior hip muscles includes the piriformis, the oblique muscles and the quadratus femoris. All these muscles insert into the posterior trochanteric fossa that is located between the greater and lesser trochanter. More caudally, three ischiocrural muscles – the long head of the biceps femoris, the semitendinosus and the semimembranosus – are found (Fig. 12.8). These muscles arise from the ischial tuberosity and descend inferiorly to insert into the leg. All are flexors of the leg and weak extensors of the thigh. The long head of biceps femoris and the semitendinosus derive from a conjoined tendon which takes its origin from the lateral aspect of the ischial tuberosity. The muscle belly of the semitendinosus arises more cranially from the medial aspect of the tendon, whereas the muscle fibers of the long head of the biceps femoris originate more caudally from the lateral face of the tendon. The semimembranosus tendon takes its origin from the inferior aspect of the ischial tuberosity, in a more medial position compared with the conjoined tendon of the long head of the biceps femoris and semitendinosus, and continues downward in a large aponeurosis located deep to the semitendinosus. The semimembranosus muscle arises from the medial aspect of the aponeurosis and expands between the semitendinosus, located on its lateral side, and the vastus medialis and gracilis, located on its medial side.

The anatomic relationship among the posterior hip muscles and tendons in the transverse plane is shown in Figure 12.9.

12.2.4 Neurovascular Structures

Caudally to the inguinal ligament, the femoral triangle is a connective tissue space delimited by the medial edge of the adductor longus medially and the medial edge of the sartorius muscle laterally (Fig. 12.10a). It contains the common femoral artery and vein enveloped by a fascial sheath (femoral sheath), the femoral nerve and some inguinal lymph nodes. The common femoral artery enters the femoral triangle lateral to the femoral vein, crossing the "lacuna vasorum" (Fig. 12.10b). Over the hip joint, the artery is separated from the head of the femur by

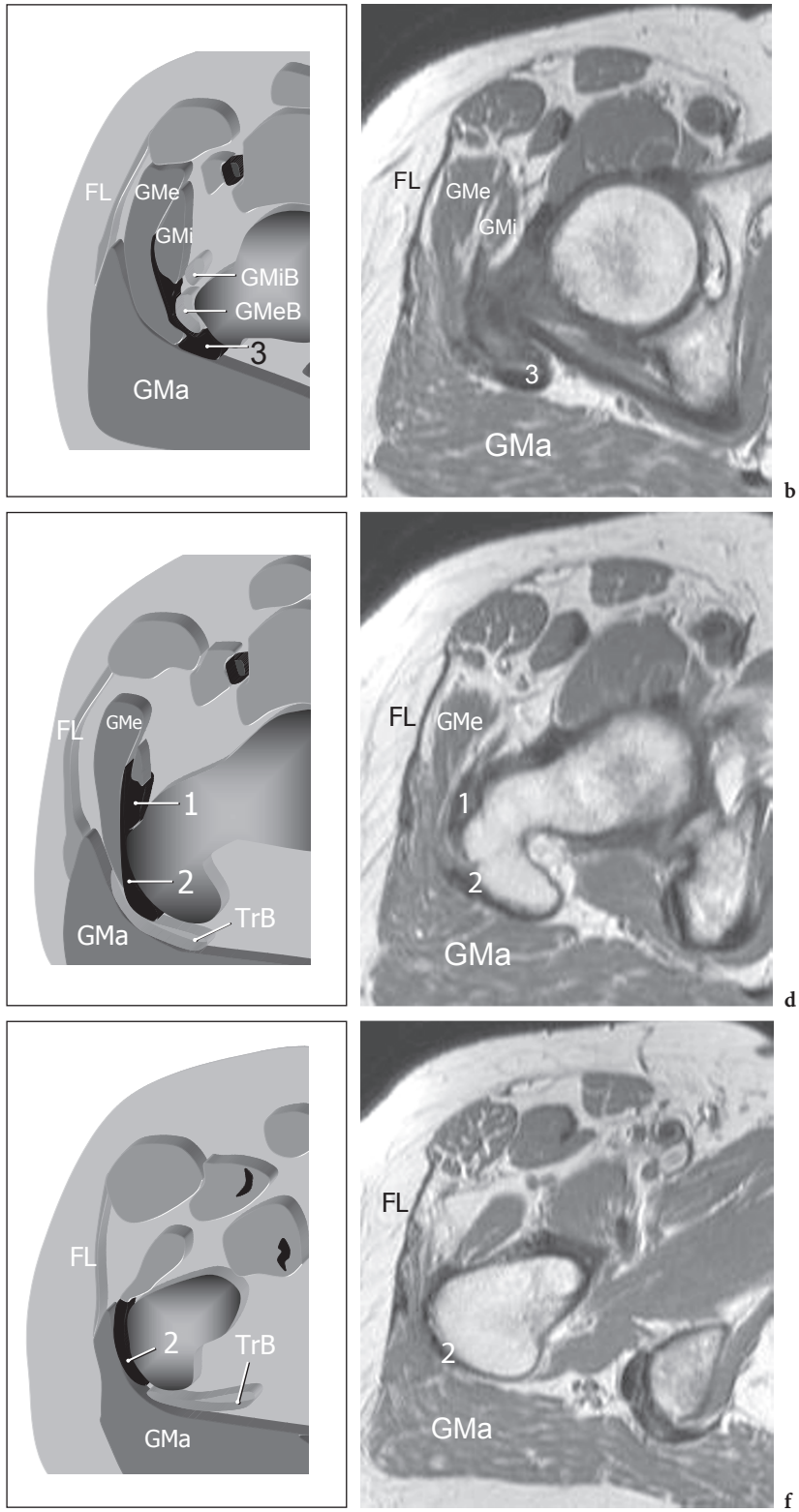

Fig. 12.7a–f. Anatomy of the lateral group (abductors) of muscles, tendons and gluteal bursae of the hip. Series of schematic drawings (**a,c,e**) and corresponding T1-weighted MR images (**b,d,f**) illustrate the relationship among the gluteus maximus (*GMa*), medius (*GMe*) and minimus (*GMi*) muscles and the respective tendons (*1*, *2*, *3*) in transverse planes obtained from proximal to distal. Observe the fasciae latae (*FL*) which covers them and the disposition of the gluteal synovial bursae–the subgluteus minimus bursa (*GMiB*), the subgluteus medius bursa (*GMeB*) and the trochanteric bursa (*TrB*)–relative to the greater trochanter and the tendons of the gluteus muscles

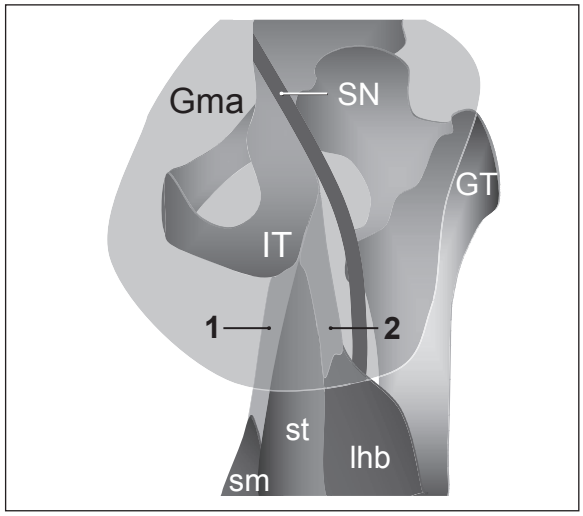

Fig. 12.8. Anatomy of the posterior (ischiocrural) muscles and tendons of the hip. Schematic drawing of a posterior view through the hip illustrates the insertion of the posterior muscles onto the ischial tuberosity (*IT*). The gluteus maximus (*Gma*) is shown in a semitransparent rendering over the ischiocrural muscles. Beneath it, observe the semimembranosus (*sm*), semitendinosus (*st*) and long head of the biceps femoris (*lhb*) muscles. The semimembranosus has a separate tendon (*1*), whereas the semitendinosus and the long head of the biceps arise from the lateral aspect of the ischial tuberosity (*IT*) through a common tendon (*2*). Note the relationships between these muscles and the sciatic nerve (*SN*). *GT*, greater trochanter

the iliopsoas tendon and the iliopsoas bursa. More distally, the femoral artery bisects the femoral triangle sending the deep femoral artery from which the medial circumflex artery arises. This latter branch is clinically important as it provides most of the blood supply to the head and neck of the femur.

The femoral nerve arises from the L2–L4 spinal nerve roots of the lumbar plexus and descends the abdomen within the substance of the psoas muscle (Stener et al. 1991). In the pelvis, it emerges from the lateral border of the psoas muscle and passes in a groove formed by the underlying lateral iliacus and medial psoas muscles. Then, it proceeds deep to the midpoint of the inguinal ligament lying on the lateral side of the common femoral vessels (Fig. 12.10b). The femoral nerve courses in the most medial portion of the "lacuna musculorum", separated from these vessels. It is covered by the fascia of the iliacus muscle on the lateral aspect of the femoral sheath. Moving to the distal portion of the femoral triangle, the femoral nerve splits into several branches which provide sensory innervation for the skin and the hip joint and motor supply for the anterior femoral muscles (quadriceps femoris and sartorius) and terminates as the saphenous nerve.

The lateral femoral cutaneous nerve courses more lateral relative to the femoral nerve. It arises from the L2 and L3 spinal nerve roots, emerges from the lateral border of the psoas muscle and crosses the iliacus muscle passing through a tunnel formed by a small split in the lateral end of the inguinal ligament in close proximity with the anterior superior iliac spine (Fig. 12.10b). This nerve is purely sensory and supplies the skin of the anterior and lateral aspects of the thigh.

On the posterior hip, the sciatic nerve exits the pelvis passing through the greater sciatic foramen and enters the gluteal region coursing deep to the inferior margin of the piriformis. This nerve is the largest nerve of the body, arises from the ventral branches of the L4 through S3 spinal nerves and, soon after its origin, assumes a flattened shape because it consists of medial and lateral trunks which split more distally to form the medial tibial nerve and the lateral common peroneal nerve at the apex of the popliteal fossa. While running deep to the gluteus maximus, the sciatic nerve courses midway between the greater trochanter and the ischial tuberosity and superficial to the obturator internus, quadratus femoris and adductor magnus muscles (Figs. 12.8, 12.9). It supplies the hamstring muscles by means of branches arising from its medial trunk with the exception of the short head of the biceps femoris which is supplied by a branch arising from the lateral trunk.

12.2.5 Bursae

There are several bursae about the hip joint, with variable extent and prevalence (Pfirrmann et al. 2001). The most important are the iliopsoas bursa on the anterior aspect of the hip, the complex of peritrochanteric bursae in relation to the abductor mechanism and the posterior ischiogluteal bursa.

The iliopsoas bursa is a large synovial-lined bursa which lies between the posterior aspect of the iliopsoas muscle and tendon and the anterior capsule of the hip joint. It measures approximately 5–7 cm in length and 2–4 cm in width and communicates with the hip joint in 10–15% of cases through a foramen 1–2 mm to 3 cm wide located between the pubofemoral and iliofemoral ligaments. In normal states, the

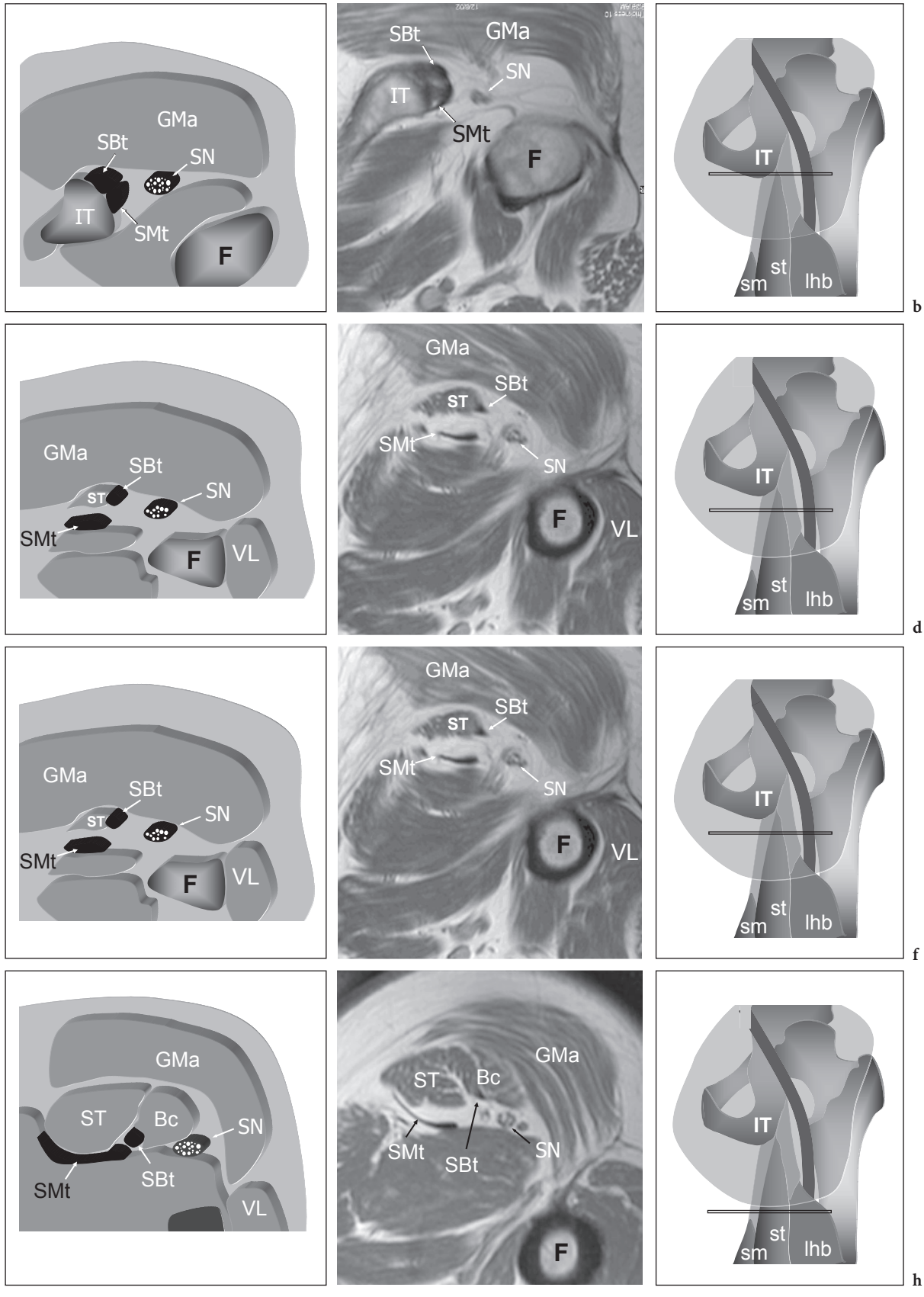
GMa
SBt
SN
IT
SMt
F
SBt
GMa
SN
IT
SMt
F
IT
st
sm
lhb
a
b
GMa
SBt
ST
SN
SMt
F
VL
GMa
SBt
ST
SMt
SN
F
VL
IT
st
sm
lhb
c
d
GMa
SBt
ST
SN
SMt
F
VL
GMa
SBt
ST
SMt
SN
F
VL
IT
st
sm
lhb
e
f
GMa
ST
Bc
SN
SMt
SBt
VL
GMa
ST
Bc
SMt
SBt
SN
F
IT
st
sm
lhb
g
h

Fig. 12.9a–h. Anatomy of the posterior group (ischiocrural) of muscles and tendons of the hip. Series of schematic drawings (**a,c,e,g**) and corresponding T1-weighted MR images (**b,d,f,h**) illustrate the relationship among the gluteus maximus muscle (*GMa*), the common tendon (*SBt*) of the semitendinosus (*ST*) and biceps muscle (*Bc*), and the semimembranosus tendon (*SMt*) in transverse planes obtained from proximal to distal. Note the sciatic nerve (*SN*), which courses on the lateral side of these structures. *IT*, ischial tuberosity; *F*, femur; *VL*, vastus lateralis muscle. The drawings in the right-hand column of the figure indicate the cross-sectional planes of reference. *sm*, semimembranosus muscle; *st*, semitendinosus muscle; *lhb*, long head of the biceps femoris muscle

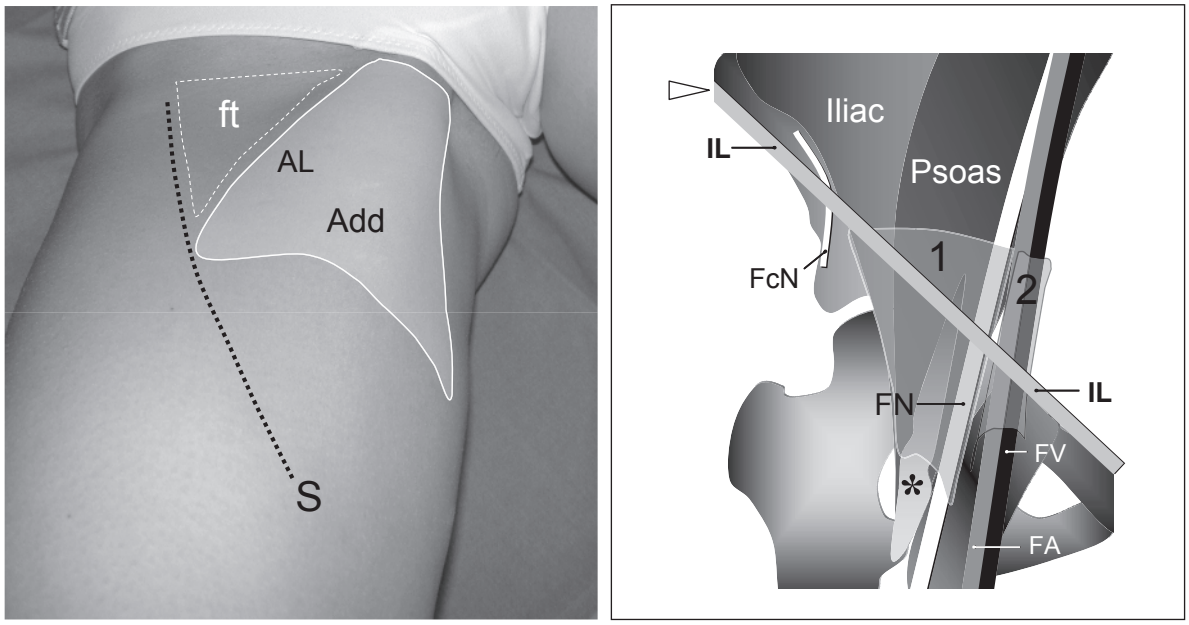

a b

Fig. 12.10a,b. Anatomy of the femoral triangle. **a** Photograph of the right thigh obtained during resisted adduction and internal rotation. The femoral triangle (*ft*) can be seen as a shallow concavity located distally to the inguinal ligament, which forms its base. The other boundaries of this triangle can be appreciated on the skin of slender individuals by the prominence of the sartorius muscle (*S*) laterally and the adductor longus muscle (*AL*) medially, this latter muscle being the most superficial and lateral of the adductor (*Add*) group. **b** Schematic drawing of an anterior view through the hip shows the inguinal ligament (*IL*) joining the anterior superior superior iliac spine (*arrowhead*) with the pubis. The space between the ligament and the anterior aspect of the iliopubic branch is divided into two compartments by the iliopectineal ligament. The former compartment, which is also referred to as the "lacuna musculorum", contains the iliopsoas muscle and the femoral nerve (*FN*) covered by the iliac fascia (*1*). The latter, the "lacuna vasorum", houses the common femoral artery (*FA*), which is contiguous laterally with the femoral vein (*FV*). The femoral vessels are enveloped by a femoral sheath (*2*). Note the lateral femoral cutaneous (*FcN*) nerve as it courses deep to the inguinal ligament in close proximity with the anterior superior iliac spine. *Asterisk*, iliopsoas tendon

bursa is collapsed and contains only a small amount of fluid. Its main function is to reduce the attrition between the iliopsoas tendon and the anterior aspect of the hip joint during muscle activation and joint movements (Ginesty et al. 1998). A direct communication between the iliopsoas bursa and the joint cavity can be encountered in approximately 15% of healthy subjects. It may be congenital or acquired in nature. In this respect, the iliopsoas bursa is somewhat similar to the bursa of the semimembranosus-gastrocnemius of the knee. In fact, both structures are located close to the joint capsule and have a close relationship with para-articular tendons. In both cases, the communication between the bursa and the joint cavity is more frequently observed in adults and, when large joint effusions are present, the passage of fluid within the bursal cavity leads to a decrease in the intra-articular pressure.

Several synovial bursae are located around the greater trochanter allowing a smooth gliding of the tendons and fasciae latae against the bone. The most important are the trochanteric bursa and the bursae

of the gluteus medius and minimus. The trochanteric bursa is the largest and the most constantly present bursa around the greater trochanter (Fig. 12.11a). It separates the undersurface of the gluteus maximus and the fasciae latae from the tendon of the gluteus medius and the lateral aspect of the greater trochanter. More distally, the subgluteus maximus bursa lies between the distal attachment of the gluteus maximus muscle and the dorsal aspect of the femur. The bursa of the gluteus medius, which is commonly referred to as the subgluteus medius bursa, is located between the anterosuperior part of the lateral facet of the greater trochanter and the gluteus medius tendon, whereas the gluteus minimus bursa, also named the subgluteus minimus bursa, is found anteromedially to the insertion of the gluteus minimus (Fig. 12.11b,c).

The posterior ischiogluteal bursa is located between the ischial tuberosity and the deep surface of the gluteus maximus. It does not communicate with the hip joint and allows a smooth gliding of the gluteus maximus over the ischial tuberosity. As the bursa lies in close contact with the sciatic and the posterior femoral cutaneous nerves, ischiogluteal bursitis may produce symptoms mimicking a radiculopathy.

12.3 Essentials of Clinical History and Physical Examination

Before starting to examine the patient's hip with US, two main steps should be considered. First, the examiner should be aware of the essentials of the clinical history and physical examination to best focus the US analysis on the appropriate structures of the hip. This usually takes no more than a couple of minutes and can be performed with the patient lying supine on the examination bed. The clinical history should be focused on the duration of symptoms, characteristics of the pain (i.e., inflammatory or mechanical) and associated conditions. In inflammatory arthritis, the patient complains of hip pain typically at night or at rest, whereas in degenerative conditions the pain is worsened with weight-bearing or during walking. In some para-articular abnormalities, such as in patients with tendinitis or bursitis involving the lateral hip structures, night pain may be a common complaint, especially when the patient sleeps on the affected side. This recalls the distribution of pain found in some shoulder pathology, such as the rotator cuff disease. An audible snap or a palpable click

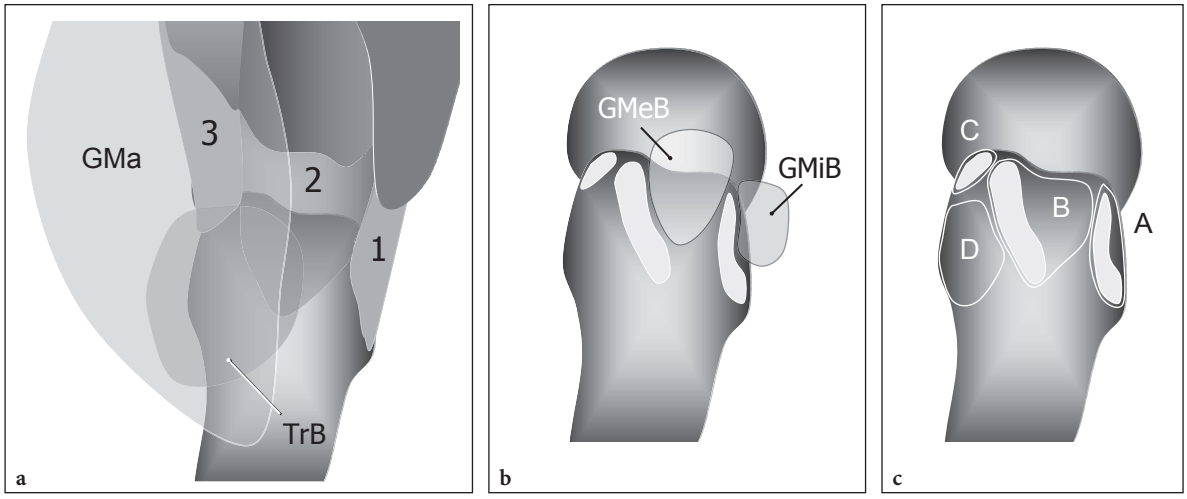

Fig. 12.11a–c. Synovial bursae around the greater trochanter. Schematic drawings of a lateral view through the greater trochanter obtained from superficial (**a**) to deep (**c**) illustrate the gluteus minimus tendon (*1*) and the anterior (*2*) and posterior (*3*) tendons of the gluteus medius which insert into the anterior (*A*), lateral (*B*) and posterosuperior (*C*) facets of the greater trochanter respectively. Three main synovial bursae are found in the trochanteric region. The largest trochanteric bursa (*TrB*) is located between the deep aspect of the gluteus maximus muscle (*GMa*) and the tendons of the gluteus medius and the inferolateral facet (*D*) of the greater trochanter. The subgluteus medius bursa (*GMeB*) lies between the anterior part of the lateral facet (*B*) and the undersurface of the anterior tendon of the gluteus medius, whereas the subgluteus minimus bursa (*GMiB*) is found anteriorly to the gluteus minimus tendon

is reported by patients who suffer from instability of either the iliopsoas tendon (internal snapping) or the fasciae latae (external snapping) against the deep bone structures. The precise location of the snapping sensation along with knowledge of the movements that reproduce it can be a useful aid to focus the US examination appropriately. In these cases, efforts should be made to perform the US examination in the same conditions that reproduce the click clinically. Due to its deep location, physical examination of the hip joint is difficult. In general, a rough differentiation between para-articular and articular disorders can be obtained by considering the limitation of the articular range of motion which occurs in joint disorders. Palpation can be useful in the assessment of anterior (iliopsoas bursitis, ganglion cysts, common femoral artery pseudoaneurysms, etc.) or lateral (hypertrophy of the tensor fasciae latae muscle) space-occupying lesions. Local tenderness over the greater trochanter can be appreciated in abductor tendinitis or lateral bursitis. During the physical assessment, specific maneuvers can be performed if a definite diagnosis is suspected on clinical grounds (e.g., a resisted abduction of the lower extremity with the knee extended which leads to pain in the trochanteric region can reinforce the suspicion that a gluteus medius tendinopathy is present). After that, a careful review of all previous imaging studies of the hip should be done. The availability of a recent plain film of the pelvis including oblique views of the affected hip is an essential prerequisite for a correct US examination. Plain films give a detailed depiction of the hip bones, coxofemoral, sacroiliac and symphysis pubis joints, as well as para-articular calcifications.

12.4 Normal US Findings and Scanning Technique

Similar to other joints, the routine scanning technique for US examination should consider the anterior, medial, lateral and posterior aspects of the hip as separate quadrants. At least for beginners, a systematic approach to each quadrant aids the and understanding of both US anatomy and scanning technique. To best examine the hip, the patient lies on the examination table with the aspect of the hip to be evaluated adequately exposed. We usually start routine hip scanning with the evaluation of the anterior region while keeping the patient supine; the lateral region is examined with the patient lying in a lateral position on the opposite side; then, the posterior hip structures are best investigated with the patient prone on the examination bed.

12.4.1 Anterior Hip

The hip joint is best evaluated in both longitudinal and transverse oblique planes obtained over the femoral neck. Longitudinal US images are well suited to demonstrating the anterior synovial recess, in which even small intra-articular effusions may collect. The US appearance of this recess has been extensively described in the literature and correlates well with both anatomic and histologic features (Robben et al. 1999). It lies between the deep fascia of the iliopsoas and the femoral neck and is composed of an anterior and a posterior hyperechoic layer (Fig. 12.12). The two layers correspond to the anterior joint capsule which, after leaving the anterior border of the acetabulum, extends inferolaterally to reach the intertrochanteric line. At this level, the most superficial fibers of the joint capsule are in continuity with the periosteum, whereas the deep ones reflect and travel upward to insert into the junction between the femoral head and neck, at the distal edge of the articular cartilage. Each layer is composed of thick outer fibrous envelope and a thin inner synovial membrane; the fibrous component, which is histologically composed of collagen fibers, appears as a 2-4 mm thick hyperechoic band, whereas the normal synovial lining is too thin to be revealed with US. The anterior fibrous layer of the joint recess is thicker than the posterior one, probably because the anterior capsule is reinforced at this level by the iliofemoral ligament. In the absence of an intra-articular effusion, the two layers are shrunk and separated by a hyperechoic line representing the collapsed synovial recess. This sign is commonly referred to as the "stripe sign" (Robben et al. 1999). Nevertheless, it should be noted that US differentiation of the two layers is more feasible in infants using high-frequency probes (Weybright et al. 2003). When examining this recess with US, care should be taken not to confuse the anterior and posterior layers of the joint capsule with an effusion, because the capsule may appear artifactually hypoechoic when imaging is not perpendicular to the US beam. In addition, these structures are more difficult to visualize in obese patients due to the deep position of the joint. In these patients, lower-frequency transducers (center frequency of approxi-

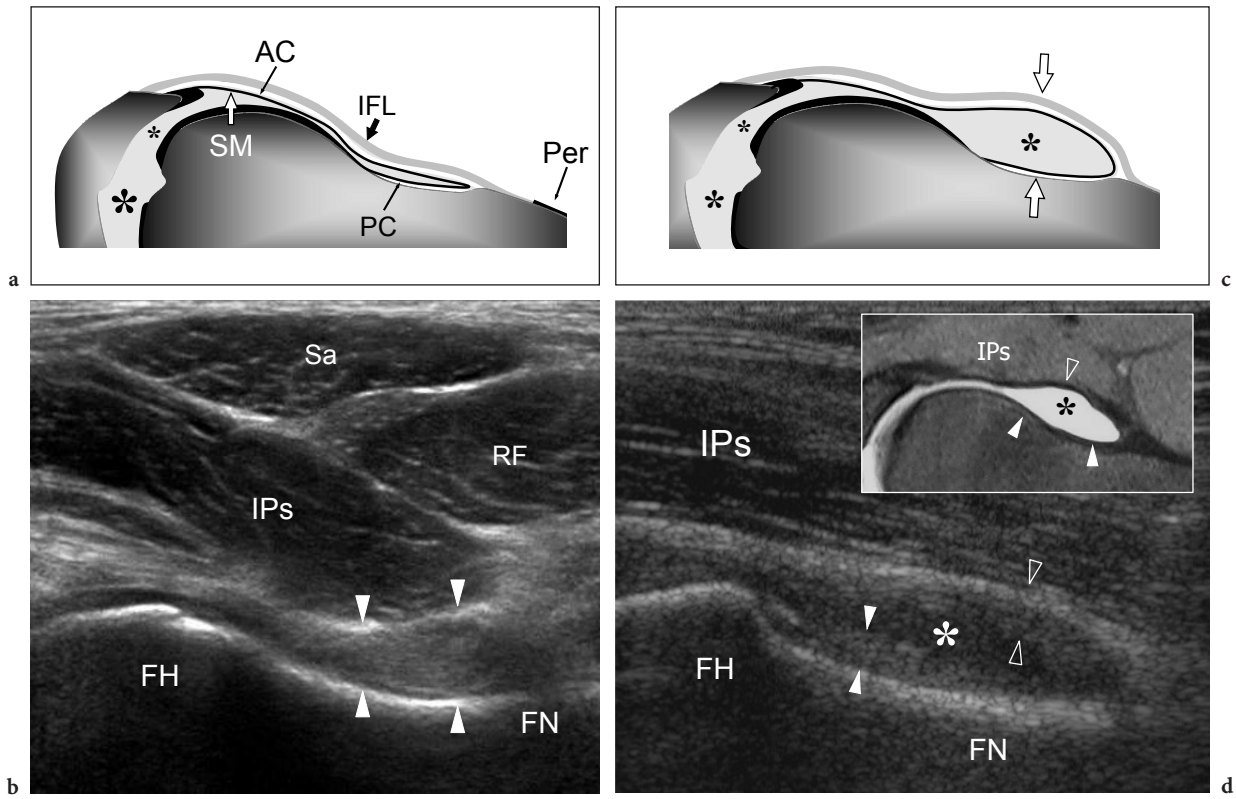

Fig. 12.12a-d. Anterior recess of the hip joint. **a,b** Transverse oblique 12–5 MHz US images with **c,d** schematic drawing correlation obtained over the hip joint in a healthy subject (**a,c**) and in a patient with intra-articular effusion (**b,d**) . In **a,c** the hypoechoic band of tissue (*arrowheads*) found between the anterior bony cortex of the femoral neck (*FN*) and the deep boundary of the iliopsoas muscle (*IPs*) is related to the sum of the iliofemoral ligament (*IFL*), the anterior (*AC*) and posterior (*PC*) joint capsule and the synovial membrane (*SM*). *Per*, periosteum. **b,d** An intra-articular effusion (*asterisk*) distends the anterior synovial recess and allows differentiation of two distinct capsular layers (*arrowheads*). Note that the anterior layer (*open arrowheads*) is thicker than the deep one (*white arrowheads*) because of the presence of the iliofemoral ligament. *RF*, rectus femoris; *Sa*, sartorius; *IPs*, iliopsoas; *FH*, femoral head. In the insert shown in **d**, an axial oblique fat-suppressed T1-weighted MR-arthrographic image demonstrates the capsular layers (*arrowheads*) as hypointense linear bands separated by the joint recess (*asterisk*) filled with gadolinium contrast

mately 5 MHz) can help the examination. Cranial to the anterior recess, the fibrocartilaginous labrum of the acetabulum can be detected as a homogeneously hyperechoic triangular structure which has the same appearance as the glenoid labrum or the knee meniscus (Fig. 12.13a). In some individuals, the iliofemoral ligament can occasionally be appreciated superficial to the anterosuperior labrum as a flat fibrillar structure joining the anterior inferior iliac spine and the acetabular rim with the intertrochanteric line (Fig. 12.13b). In adults, the assessment of the anterior capsuloligamentous structures requires accurate positioning of the focal zone and, possibly, low frequencies.

US can accurately image the muscles located superficially to the hip joint. They are best depicted by means of transverse planes, whereas longitudinal US planes have only a lesser importance. The use of wide-array linear probes or extended field-of-view techniques may help to obtain a panoramic view of them.

The anterior muscles detected at the articular level are, from lateral to medial: the tensor fasciae latae, the rectus femoris, the sartorius, the iliopsoas and the pectineus. Over the joint space, the iliopsoas muscle is the first to be identified in a lateral position relative to the femoral neurovascular bundle. Its tendon lies in an eccentric position within the posterior part of the muscle belly and can be detected as a hyperechoic anisotropic fibrillar structure (Fig. 12.14). The tendon is in close relationship with the anterior hip capsule and the two structures can usually be distinguished

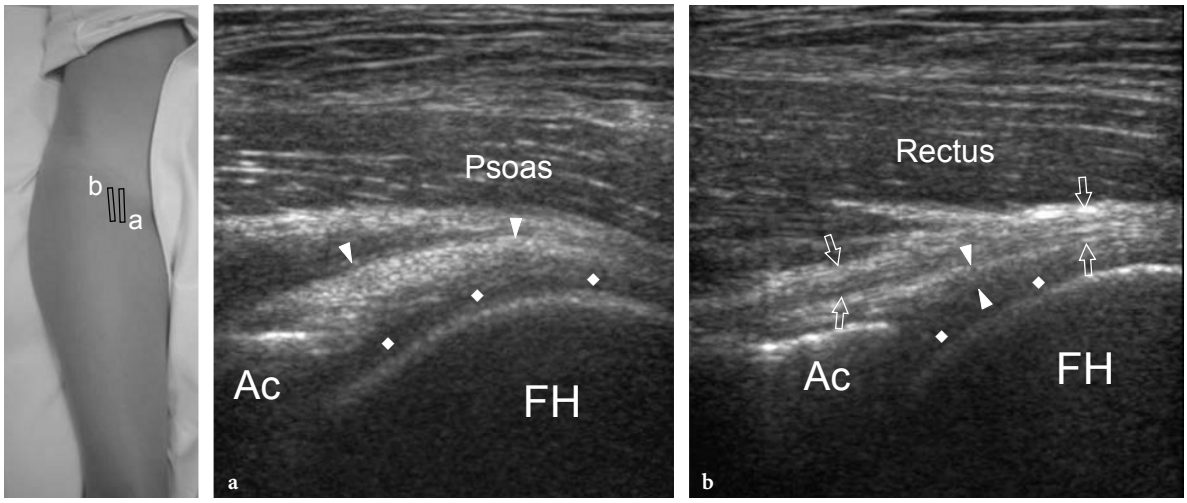

Fig. 12.13a,b. Hip labrum and iliofemoral ligament. **a** Sagittal 12–5 MHz US image over the anterior aspect of the hip, just lateral to the iliopsoas tendon, identifies the anterior fibrocartilaginous labrum (*arrowheads*) as a homogeneously hyperechoic triangular structure arising from the rim of the acetabulum (*Ac*). Observe the labrum, which covers the articular cartilage (*rhombi*) of the femoral head (*FH*). **b** Sagittal 12–5 MHz US image obtained approximately 1 cm external to the scanning plane shown in **a** demonstrates a thinner labrum (*arrowheads*) overlaid by a cord-like fibrillar structure (*arrows*) representing the iliofemoral ligament. The photograph at the left side of the figure indicates probe positioning

with US. A synovial bursa, the iliopsoas bursa, intervenes between the tendon and the anterior capsule. The main function of the bursa is reduction of tendon friction over the hip joint during muscle activation and joint movements (Ginesty et al. 1998). Similar to most other synovial bursae in the body, the iliopsoas bursa is collapsed in normal states and, therefore, cannot be detected with US.

To examine the other anterior hip muscles, US scanning should begin over the anterior superior iliac spine to image the cranial insertions of the sartorius medially and the tensor fasciae latae laterally. The short tendons of these muscles are best visualized with US in the sagittal plane as hyperechoic fibrillar structures inserting into the bright cortical echo of the anterior superior iliac spine (Fig. 12.15). In a group of 40 healthy subjects, the mean thickness of the tendon of the tensor fasciae latae muscle was found to measure approximately 2.1 mm with no significant side differences (Bass and Connel 1992). During US examination of the hip in sportsmen, this tendon should be routinely assessed because it can be affected by tendinopathy leading to unexplained anterior groin pain (Bass and Connel 1992). Both sartorius and tensor fasciae latae are muscles located in a very superficial position, just under the fascia. Soon after their origin, the sartorius courses medially to reach the internal aspect of the thigh overlying the rectus femoris muscle. On the other hand, the muscle belly of the tensor fasciae latae proceeds laterally and caudally to insert onto the anterior border of the fasciae latae. Due to a large amount of fatty tissue among the fascicles, this latter muscle has a more echogenic appearance than the sartorius (Bass and Connel 1992). Its distal insertion is best evaluated in longitudinal planes and somewhat resembles the distal insertions of the rectus femoris and the medial head of the gastrocnemius. In fact, in normal conditions, it exhibits a pointed appearance due to a progressive distal tapering of the muscle toward the fascia, superficially to the vastus lateralis.

Just medial to the anterior superior iliac spine, the lateral femoral cutaneous nerve can occasionally be seen as a small tubular structure passing through a tunnel formed by a split in the lateral end of the inguinal ligament (Fig. 12.16). In alternative, this nerve may cross the inguinal ligament passing superficial or deep to it. Then, transverse US images reveal the intrapelvic portion of the psoas and the iliacus muscle which lies over the inner face of the iliac wing (Fig. 12.17). In slender subjects, US can detect the hyperechoic intramuscular tendon surrounded by hypoechoic muscle fibers. The soft-tissue structures adjacent to the pelvic portion of the iliopsoas muscle should be carefully analyzed in case of effusion in the iliopsoas bursa, because this bursa can extend inside the pelvis, thus mimicking a pelvis mass (Bianchi et al. 2002b).

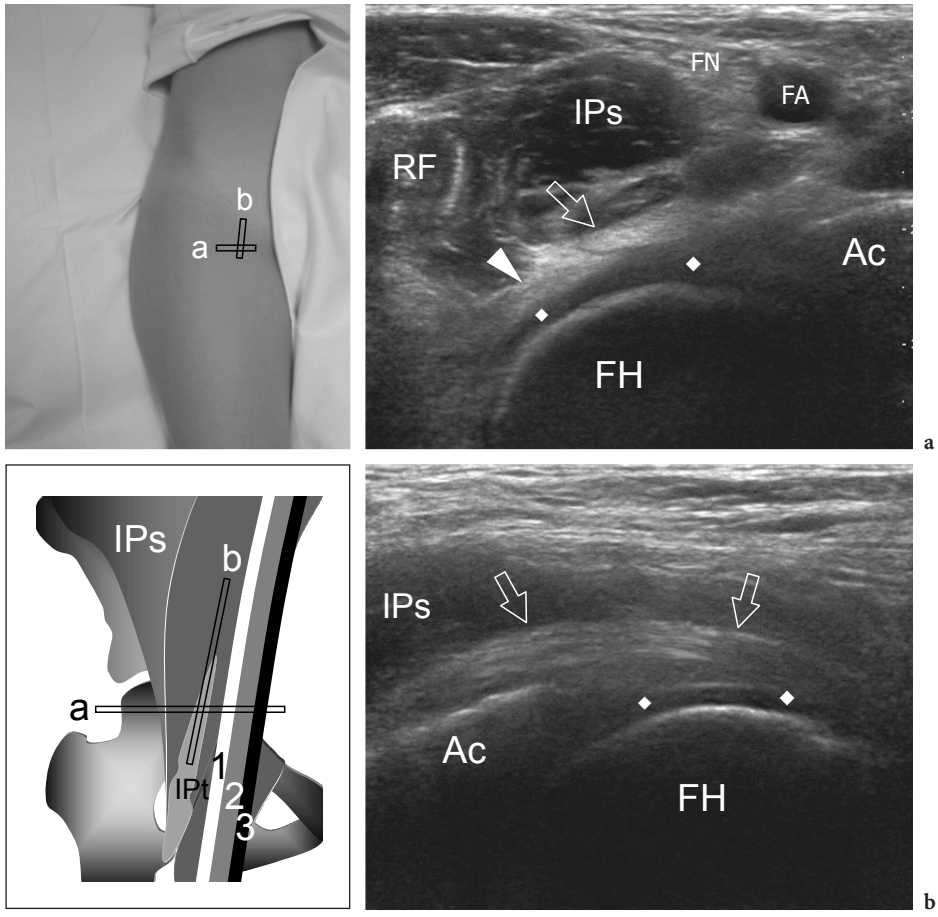

Fig. 12.14a,b. Iliopsoas muscle and tendon. **a** Transverse and **b** sagittal 12–5 MHz US images obtained over the anterior aspect of the hip joint in a healthy subject demonstrate the iliopsoas muscle (*IPs*) and tendon (*arrow*), which are located between the rectus femoris (*RF*) and the neurovascular bundle, superficial to the anterior capsular plane (*white arrowhead*) and the articular cartilage (*rhombi*) of the femoral head (*FH*). *FN*, femoral nerve; *FA*, common femoral artery; *Ac*, acetabulum. The photograph and the schematic drawing at the left side of the figure indicate probe positioning

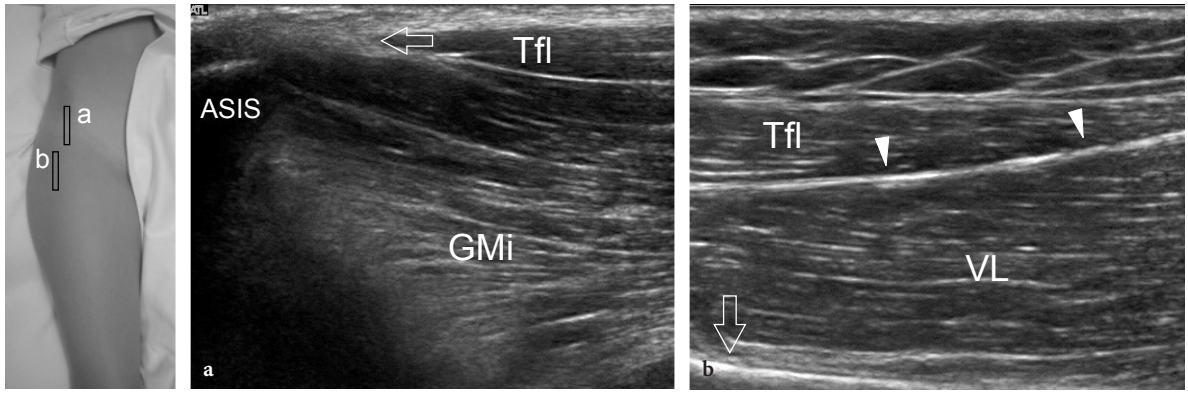

Fig. 12.15a,b. Tensor fasciae latae muscle. Sagittal 12–5 MHz US images obtained in a healthy subject over the proximal (**a**) and distal (**b**) insertion of the tensor fasciae latae muscle (*Tfl*). **a** The proximal tendon (*arrow*) of the tensor fasciae latae muscle can be appreciated as it inserts into the anterior superior iliac spine (*ASIS*). In the same plane, the belly of the gluteus minimus (*GMi*) is seen deeply to the tensor fasciae latae muscle. In **b**, the distal myotendinous junction of the tensor fasciae latae muscle (*Tfl*) exhibits a typical pointed appearance as a result of the convergence of its muscle fibers into the fasciae latae (*arrowheads*). At this level, the muscle belly of the vastus lateralis (*VL*) is found between the tensor fasciae latae muscle and the femur (*arrow*). The photograph at the left side of the figure indicates probe positioning

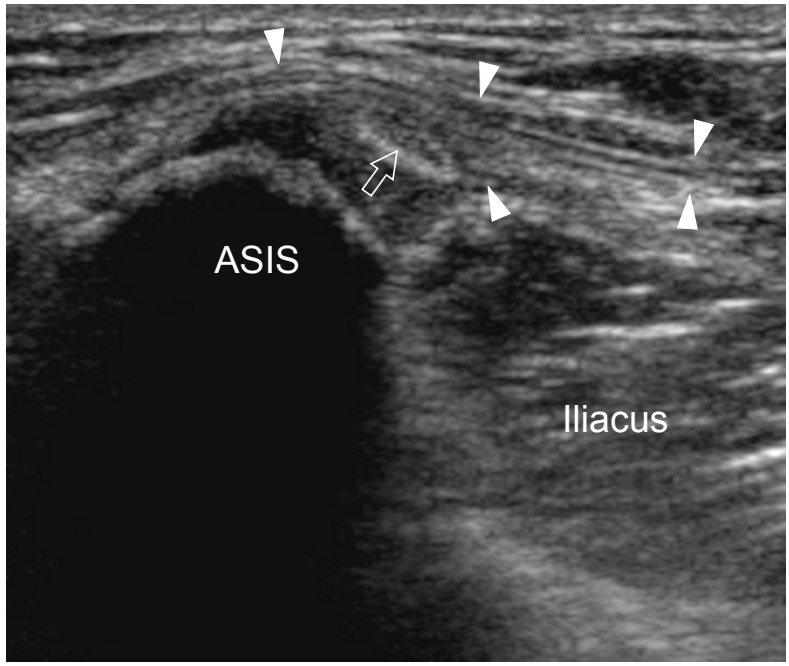

Fig. 12.16. Lateral femoral cutaneous nerve. Transverse 12–5 MHz US image obtained over the anterior superior iliac spine (*ASIS*) in a healthy subject depicts the nerve (*arrow*) as it passes through the tunnel formed by a split in the lateral end of the inguinal ligament (*arrowheads*)

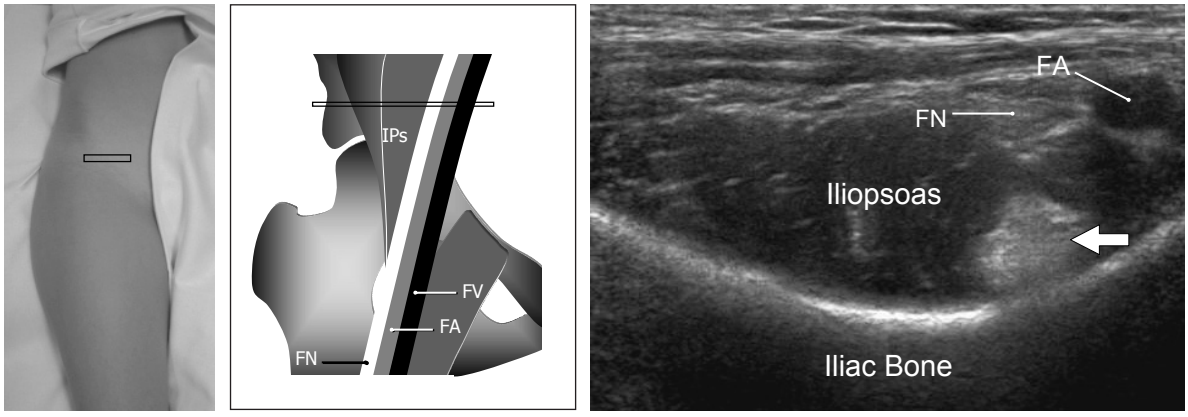

Fig. 12.17. Intrapelvic portion of the iliopsoas muscle. Transverse 12–5 MHz US image obtained over the intrapelvic portion of the iliopsoas (*IPs*) muscle in a healthy subject. The muscle is seen lying over the anterior surface of the iliac bone. Its tendon (*arrow*) is located in an anterior and medial position. It appears as a well-defined oval hyperechoic structure embedded within the hypoechoic muscle belly. The femoral nerve (*FN*) is found in a superficial location, just laterally to the common femoral artery (*FA*). *FV*, femoral vein. The photograph and the schematic drawing at the left side of the figure indicate probe positioning

After that, the probe should be positioned around the anterior inferior iliac spine. This apophysis can easily be identified as a linear bright structure with posterior acoustic shadowing, located in a more caudal and deep position relative to the anterior superior iliac spine. The direct tendon of the rectus femoris takes its origin from the anterior inferior iliac spine. A careful scanning technique based on short-axis and long-axis planes may be useful to reveal the indirect tendon that joins the lateral aspect of the direct tendon. Its demonstration may be problematic in obese patients. In normal subjects, the strong direct tendon may display a posterior acoustic shadowing that should not be misinterpreted as an intratendinous or soft-tissue calcification (Fig. 12.18). The correct explanation for this phenomenon is

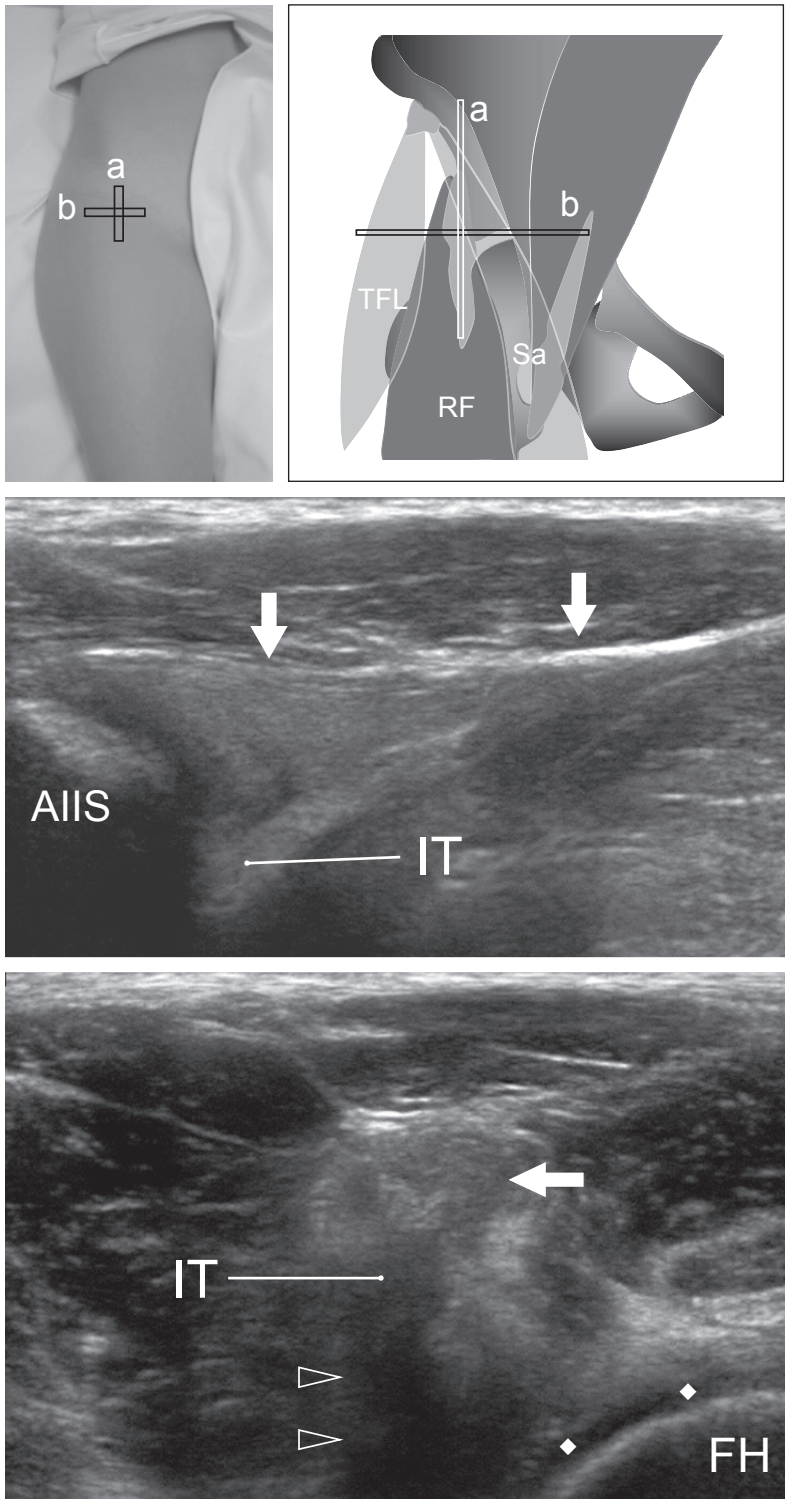

Fig. 12.18a,b. Rectus femoris tendon. **a** Long- and **b** short-axis 12–5 MHz US images obtained over the anterior hip in a healthy subject. In **a**, the direct tendon of the rectus femoris appears as a straight hyperechoic fibrillar structure (*arrows*) arising from the anterior inferior iliac spine (*AIIS*). In close apposition with the direct tendon, the indirect tendon (*IT*) of the rectus femoris assumes a curvilinear shape directed deeply. In **b**, the indirect tendon (*IT*) can be appreciated on the lateral side of the direct tendon (*arrow*) showing a typical posterior acoustic shadowing (*arrowheads*). Note the medial femoral head (*FH*) covered by the hypoechoic layer of articular cartilage (*rhombi*). The photograph and the schematic drawing at the top of the figure indicate probe positioning. *SA*, sartorius; *TFL*, tensor fasciae latae; *RF*, rectus femoris muscle

unknown although we believe it can be, at least in part, related to changes in orientation of fibers at the union of the direct and indirect tendons of the rectus femoris. More distally, transverse US images can demonstrate the myotendinous junction of the rectus femoris with the muscle fibers that arise from the lateral aspect of the tendon. Moving the transducer further downwards, the muscle belly can be seen progressively enlarging between the tensor fasciae latae and the sartorius (Fig. 12.19). Within the proximal rectus femoris muscle, the central aponeurosis represents the distal continuity of the indirect tendon, whereas the superficial aponeurosis arises from the direct tendon (Hasselman et al. 1995; Bianchi et al. 2002a).

12.4.2 Medial Hip

Medially to the iliopsoas muscle and tendon, US is able to image the femoral neurovascular bundle (Fig. 12.20). The femoral nerve, the common femoral artery and vein are imaged in sequence from lateral to medial. The femoral nerve exhibits the characteristic fascicular pattern of peripheral nerves and can be seen splitting into two or three distal branches in the inguinal region. In the supra-inguinal region, the nerve may exhibit an oval or triangular cross-sectional shape. In normal subjects, its mean diameters are 9.8±2.1 mm (mediolateral) and 3.1±0.8 mm (anteroposterior) with an average cross-sectional area of 21.7 mm2 (Gruber et al. 2002). Due to their small size, the divisional branches of the femoral nerve are difficult to examine with US soon after their origin. The femoral vein has a greater cross-section than the artery and is easily compressible with the probe. Venous compression test, color Doppler imaging and spectral analysis should be part of the hip examination in cases of suspected thrombosis of the femoral vessels. In elderly subjects, calcified plaques scattered along the arterial wall can be considered signs of peripheral vascular disease.

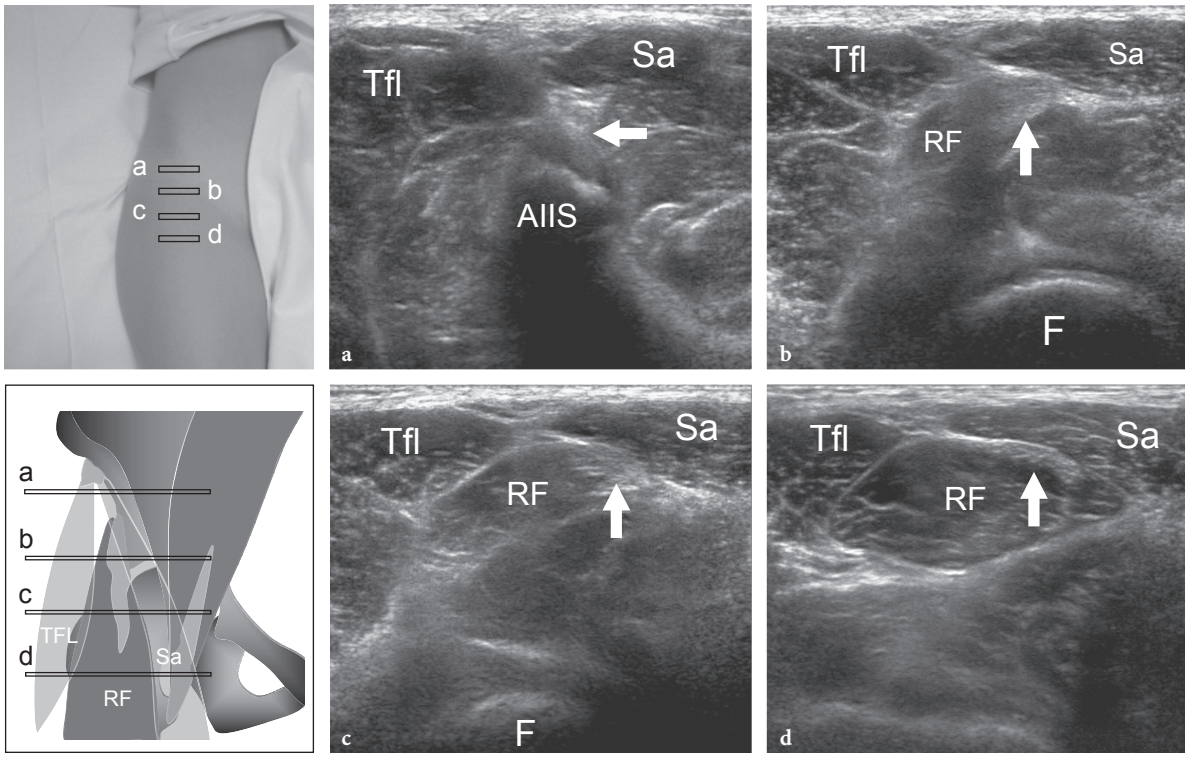

Fig. 12.19a–d. Anterior hip muscles. Series of transverse 12–5 MHz US images over the anterior hip in a healthy subject obtained from proximal (**a**) to distal (**d**). **a** Just distally to the anterior inferior iliac spine (*AIIS*), the rectus femoris tendon (*arrow*) is located between the medial sartorius muscle (*Sa*) and the lateral tensor fasciae latae muscle (*Tfl*). **b** The most cranial fibers (*RF*) of the rectus femoris muscle are seen arising from the lateral aspect of the tendon (*arrow*). **c, d** Proceeding downwards, the muscle belly of the rectus femoris progressively enlarges and becomes more superficial. *F*, femur. The photograph and the schematic drawing at the left side of the figure indicate probe positioning

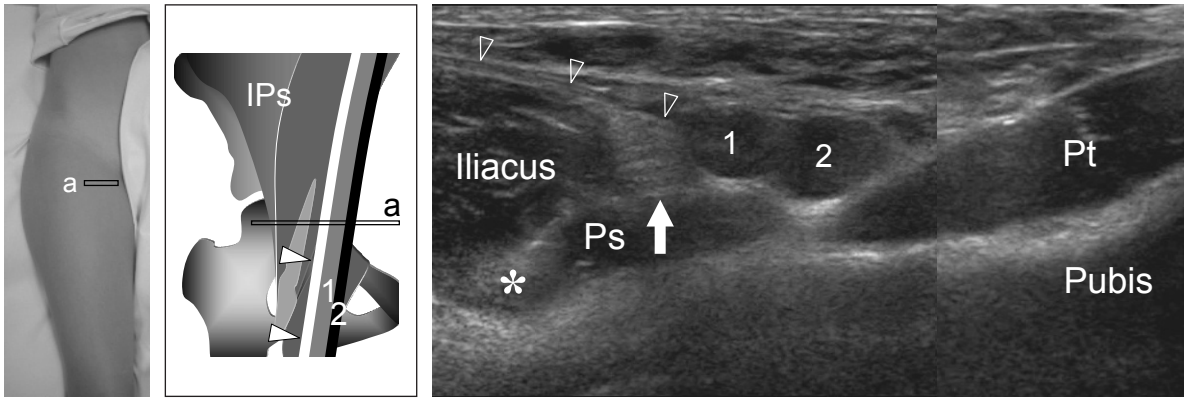

Fig. 12.20. Femoral neurovascular bundle. Transverse 12–5 MHz US image obtained just inferior to the inguinal ligament in a healthy subject. The common femoral artery (*1*) and vein (*2*) and the femoral nerve (*arrow*) are located between the pectineus (*Pt*) and the iliopsoas muscle. Observe that the femoral nerve courses in a groove formed by the two components of the iliopsoas - the iliacus and the psoas (*Ps*) - covered by the iliac fascia (*arrowheads*). The nerve exhibits the typical fascicular pattern and is located superficial and medial to the iliopsoas tendon (*asterisk*). As regards the vessels, the vein has a larger cross-section than the artery. The photograph and the schematic drawing at the left side of the figure indicate probe positioning. In the schematic drawing *arrowheads* indicate the femoral nerve. *IPs*, iliopsoas

The pelvic insertion of the adductor muscles should be evaluated in transverse planes starting from the muscle bellies while the patient keeps the thigh abducted and externally rotated with the knee bent. Three muscle layers are recognized in these planes (Fig. 12.21). The most superficial is referred to the lateral adductor longus and the medial gracilis, the intermediate to the adductor brevis and the deep to the adductor magnus. Deepening the field-of-view of the US image may be required to recognize the deepest of these muscle layers. US scanning should proceed upward, following the myotendinous insertions of these muscles and their tendons up to the pubis. Short-axis US planes are essential in order not to skip minor tears at the proximal myotendinous junction of these muscles. Then, long-axis US planes should be obtained over the tendon insertions to the pubis. These latter planes are particularly useful to assess the most superficial tendon of the adductor longus, to evaluate tendon retraction in cases of avulsion injuries (excluding a simultaneous involvement of the adductor brevis), as well as to best recognize avulsed flecks of bone.

12.4.3 Lateral Hip

The US examination of the lateral hip quadrant is best performed by asking the patient to lie on the opposite hip assuming an oblique lateral or true lateral position. Transverse and longitudinal US images obtained cranially to the greater trochanter show the superficial gluteus medius and the deep gluteus minimus muscles. It must be noted that the anterior margins of these muscles blend together and that a definite demarcation between them may be feasible with US only at the level of their middle and posterior portions. To best recognize them, the examiner should first identify the tensor fasciae latae: shifting the transducer posterior to it, the anterior margin of both muscles appears. Similarly, one could first obtain posterior US images over the anterior portion of the gluteus maximus as a landmark: moving the transducer anterior to this muscle, the posterior margin of the gluteus medius can be appreciated. In a more superficial position, the fasciae latae appears as a linear hyperechoic band joining the anterior edge of the gluteus maximus and the posterior portion of the tensor fasciae latae muscle. The fascia lies over the lateral aspect of the gluteus medius and the greater trochanter.

Once these muscle bellies have been evaluated, the probe is moved down to reach the greater trochanter. Due to a different orientation of the fibers of regional muscles and tendons, the optimal assessment of these structures can best be obtained by evaluating each individual structure in sequence. The gluteus minimus tendon is detected anteriorly as a hyperechoic structure that arises from the deep aspect of the muscle to insert into the anterior facet of the greater trochanter (Fig. 12.22). Transverse US images obtained over the lateral facet of the greater trochanter demonstrate the anterior tendon

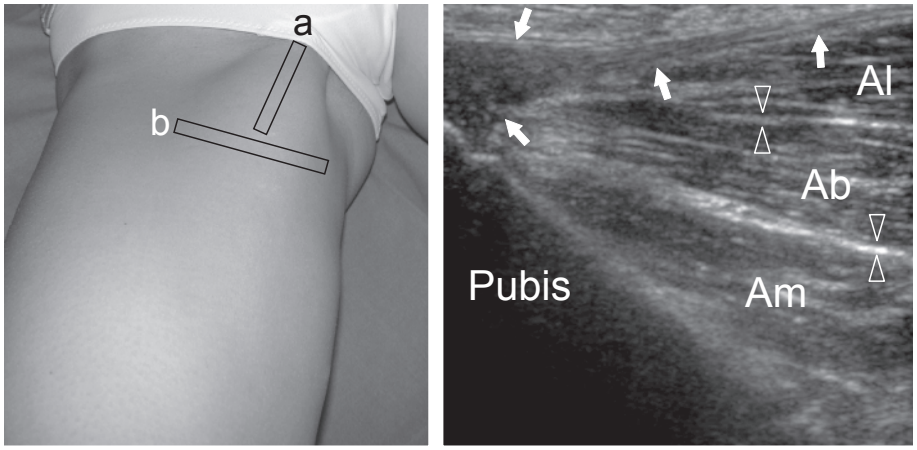

a

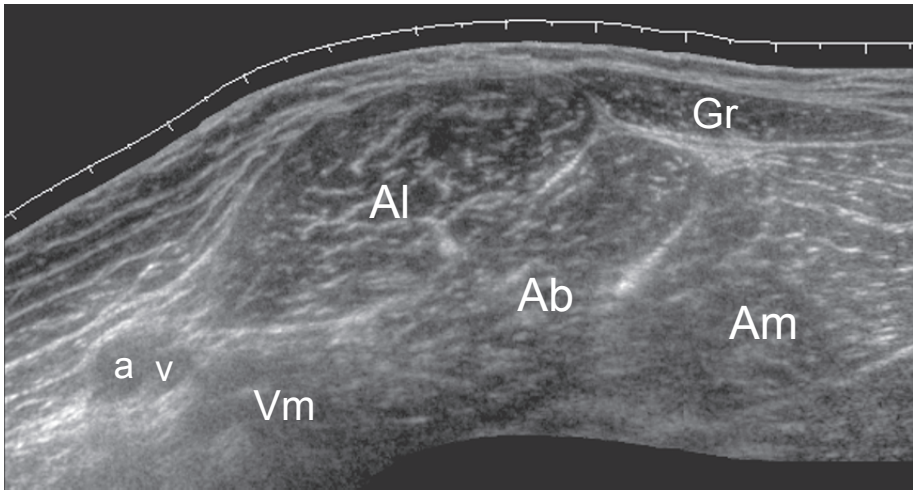

b

Fig. 12.21a,b. Adductor hip muscles. **a** Long-axis 12–5 MHz US image of the adductor longus tendon insertion. The proximal tendon of the adductor longus (*arrows*) is seen arising eccentrically from the muscle belly (*Al*) and inserting on the pubis superficial to the adductor brevis (*Ab*) and the adductor magnus (*Am*). The hyperechoic fascial planes (*arrowheads*) intervening between these muscles may help to separate them. **b** Transverse extended field-of-view 12–5 MHz US image over the upper medial thigh demonstrates the relationship of the adductor longus (*Al*), adductor brevis (*Ab*), adductor magnus (*Am*), gracilis (*Gr*) and vastus medialis (*Vm*) to each other. Note that these muscles lie medially to the femoral artery (*a*) and vein (*v*). The photograph at the upper left side of the figure indicates probe positioning

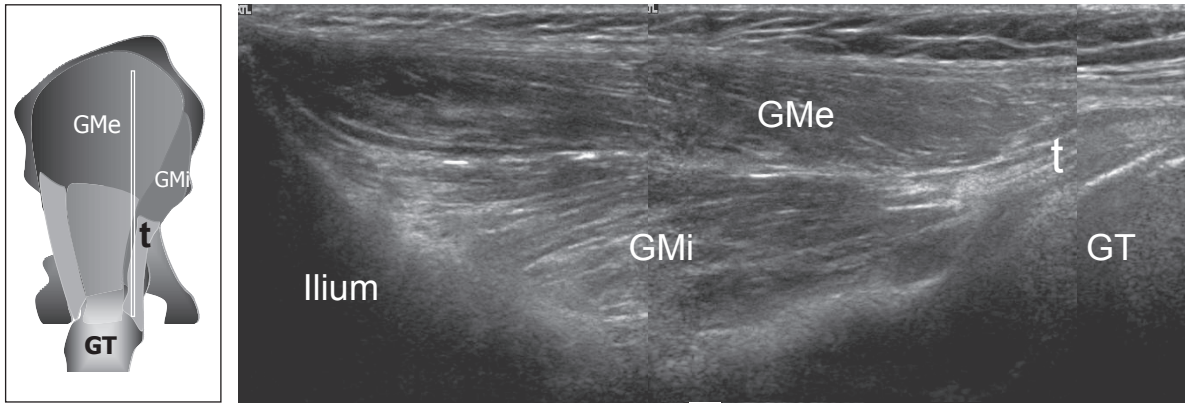

Fig. 12.22. Gluteus minimus muscle. Coronal split-screen 12–5 MHz US image obtained over the muscle (*GMi*) and tendon (*t*) of the gluteus minimus. Note the gluteus medius muscle (*GMe*), which overlies the gluteus minimus. The tendon of the gluteus minimus is seen inserting onto the anterior facet of the greater trochanter (*GT*). The schematic drawing at the left side of the figure indicates probe positioning

of the gluteus medius tendon as a curvilinear band (Fig. 12.23). Shifting the probe more posteriorly, the anterior portion of the gluteus maximus can be seen covering the posterior part of the tendon of the gluteus medius. Coronal US images are then obtained in the supratrochanteric and peritrochanteric area (Fig. 12.24). While the tendons of the gluteus muscles are located superficially and, therefore, can be evaluated without difficulty, an adequate adjustment of the focal zone (depending on the variable thickness of subcutaneous fat) is necessary to properly assess the muscle bellies. Moving the probe from anterior to posterior, the gluteus minimus and the gluteus medius are respectively assessed. Lateral hip tendons are best imaged by tilting the probe parallel to their long axis in order to avoid anisotropic effects. Knowledge of their bony attachments into the different facets of the greater trochanter may help to identify them (Fig. 12.23). Due to too small a fluid content, the bursae around the greater trochanter are not visible with US in normal conditions. Coronal planes are the best to demonstrate the fasciae latae, which appears as a homogeneous hyperechoic band with smooth margins that, from cranial to caudal, overlies the gluteus medius muscle, the anterior gluteus medius tendon and the greater trochanter (Fig. 12.24).

12.4.4 Posterior Hip

The posterior hip quadrant is examined infrequently because it is less commonly involved by pathologic changes. To image this quadrant with US, the patient is asked to lie prone with the feet hanging over the

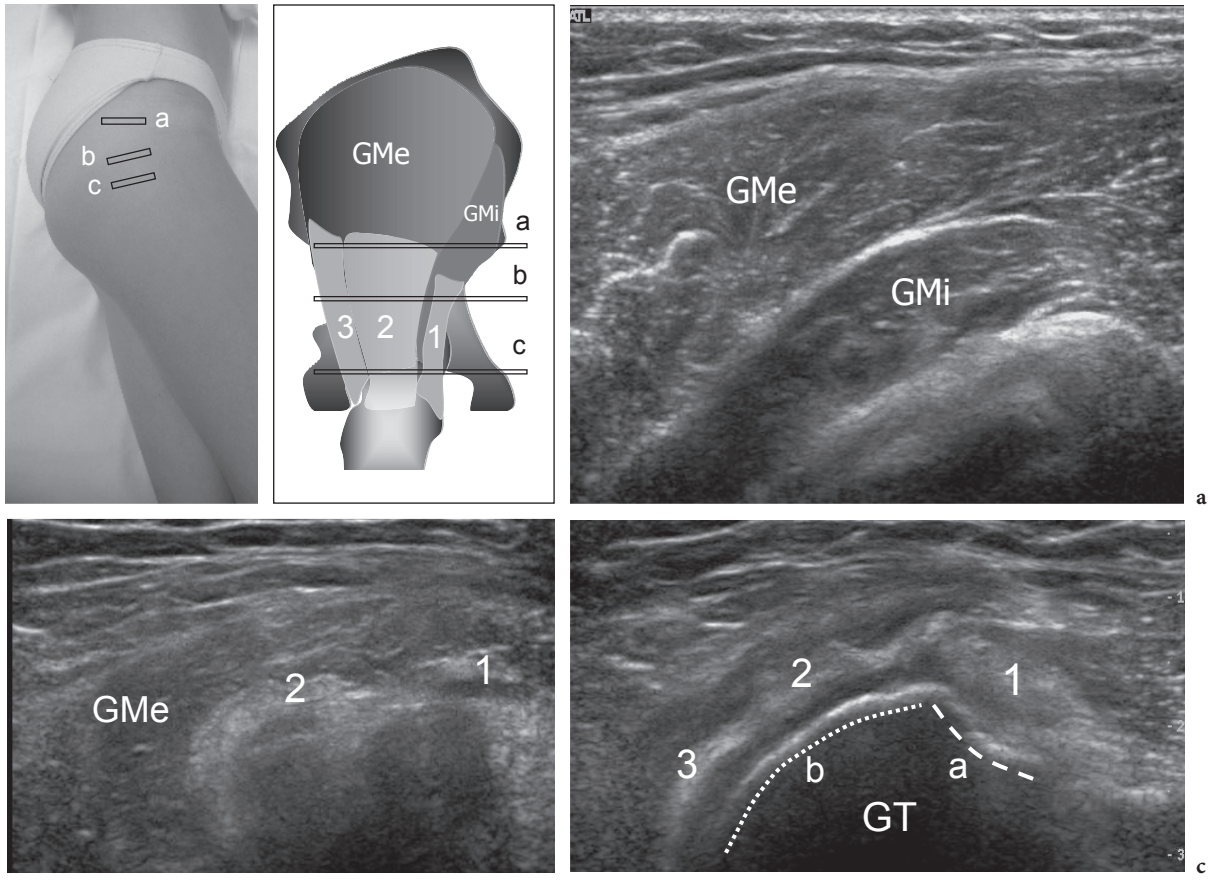

Fig. 12.23a–c. Gluteus medius and minimus tendons. Transverse 12–5 MHz US images obtained over the lateral hip from proximal (**a**) to distal (**c**). In **a**, the gluteus minimus muscle (*GMi*) is located anteriorly and deep to the gluteus medius (*GMe*) muscle. **b,c** More distally, the tendon of the gluteus minimus (*1*) and the anterior (*2*) and posterior (*3*) tendons of the gluteus medius are progressively appreciated as separate hyperechoic structures. The former tendon inserts onto the anterior facet (*a*, *dashed line*) of the greater trochanter (*GT*), whereas the two latter tendons are seen inserting into its posterior aspect (*b*, *pointed line*). The photograph and the schematic drawing at the upper left side of the figure indicate probe positioning

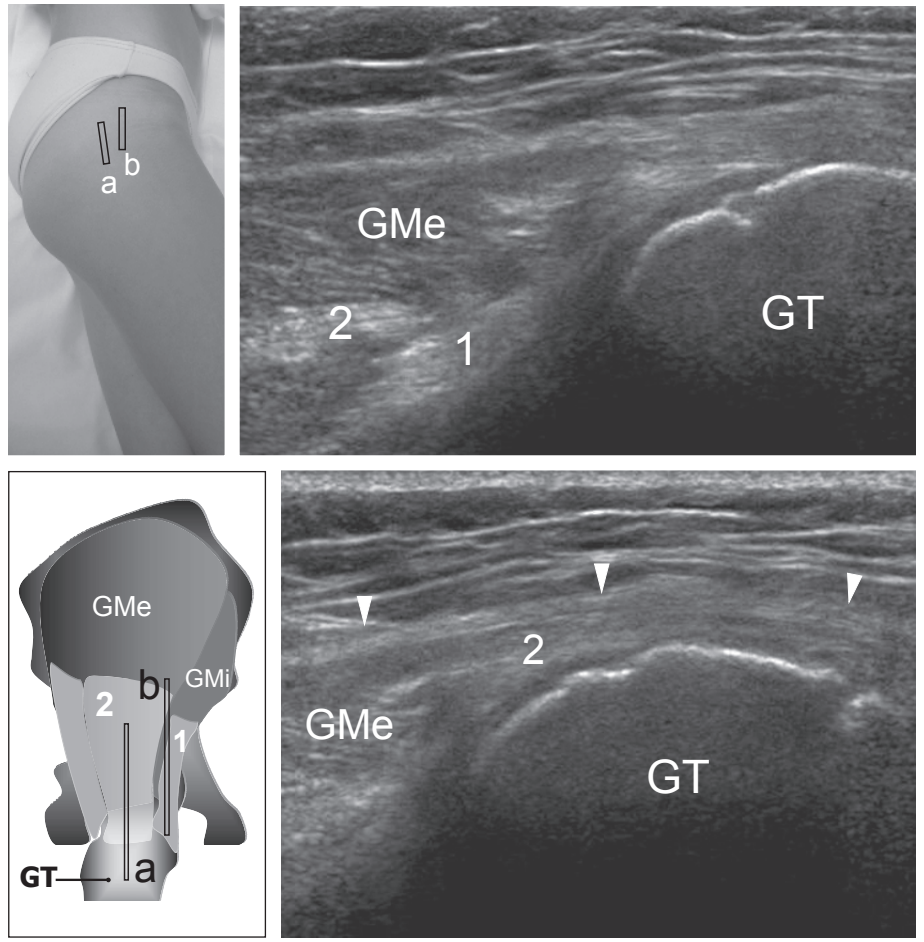

Fig. 12.24a,b. Gluteus medius and minimus tendons. **a** Coronal 12–5 MHz US image obtained over the gluteus medius muscle (*GMe*) and tendon (*2*). Note the tendon (*1*) of the gluteus minimus located just deep to the gluteus medius. *GT*, greater trochanter. **b** The gluteus medius continues down into its distal tendon (*2*), which inserts into the lateral aspect of the greater trochanter (*GT*). The fasciae latae (*arrowheads*) is located superficially to the gluteus medius tendon. The photograph and the schematic drawing at the left side of the figure indicate probe positioning

edge of the examination bed. In adults with thick thighs, an appropriate study can require the use of low frequencies due to the bulk of subcutaneous tissue and gluteus maximus muscle in this area. The gluteus maximus muscle is best evaluated on transverse and coronal oblique planes oriented according to its long- and short-axis. The whole muscle can be imaged from its medial origin to its lateral insertion into the femur. The US assessment of the deeper structures is more difficult and less than accurate. In most cases, we believe the cranial muscles inserting onto the posterior trochanteric fossa, such as the piriformis, the oblique muscles and the quadratus femoris, cannot be reliably assessed with US. MR imaging is the most appropriate imaging modality for their evaluation. On the other hand, the ischiocrural muscles can be reliably distinguished with US (Cohen 2002). Transverse US planes are the most useful for recognizing these muscles as individual structures. The ischial tuberosity is the main landmark, because it is readily apparent due to the posterior acoustic shadowing of bone and allows an appropriate localization of the surrounding anatomic structures. Once detected, the most cranial portion of the ischiocrural tendons can be demonstrated as they insert on its lateral aspect (Fig. 12.25). At this level, the semimembranosus tendon and the conjoined tendon of the semitendinosus and the long head of the biceps femoris cannot be separated. Lateral to them, the sciatic nerve can be seen

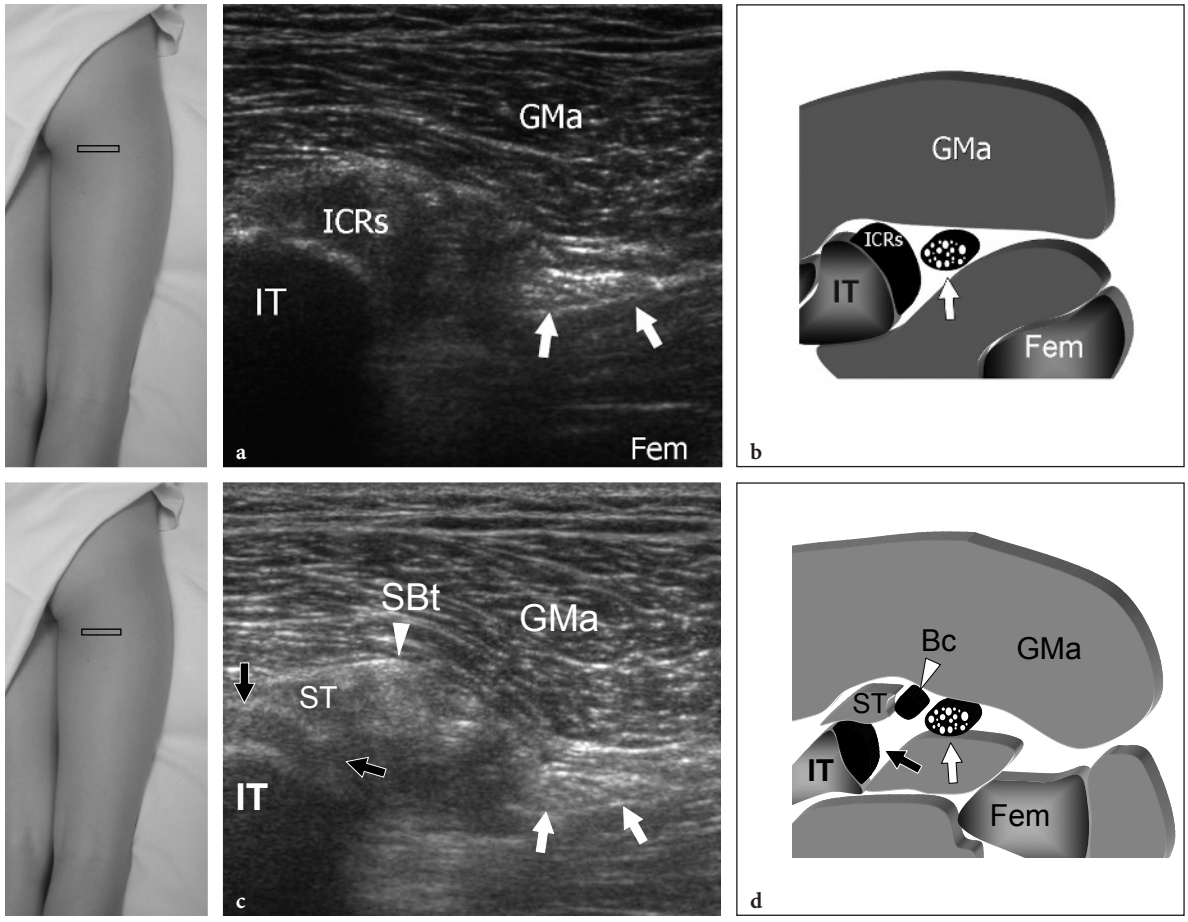

Fig. 12.25a–d. Ischiocrural muscles and tendons. **a,c** Transverse 12–5 MHz US images with corresponding **b,d** schematic drawings over the posterior group of hip muscles in a healthy subject obtained from proximal (**a,b**) to distal (**c,d**). In **a,b**, the ischiocrural tendons (*ICRs*) are not separated and appear as a single hyperechoic band arising from the ischial tuberosity (*IT*). The sciatic nerve (*arrows*) courses just laterally to the tendon complex and deep to the gluteus maximus muscle (*GMa*). *Fem*, femur. In **c,d**, the proximal fibers of the semitendinosus muscle (*ST*) are seen arising from the internal aspect of the conjoined tendon of the semitendinosus and long head of the biceps femoris (*SBt*; in **c**; *Bc* in **d**). At the same level, the semimembranosus tendon (*black arrows*) originates from the ischial tuberosity. *White arrows* indicate the sciatic nerve. The photographs at the left side of the figure indicate probe positioning

as a flattened structure with fascicular echotexture surrounded by hyperechoic fat (Fig. 12.25). At this site, low-frequency scanheads may be helpful to best delineate the deep-lying nerve in patients with large body habitus. The nerve can be followed downwards from the greater sciatic foramen (Graif et al. 1991). In some individuals, the inferior gluteal artery can be appreciated on the medial side of the nerve with color Doppler imaging.

More distally, the conjoined tendon of semitendinosus and biceps femoris can be distinguished from the tendon of semimembranosus owing to its more superficial and lateral position (Fig. 12.26). At this level, the two hyperechoic tendons and the sciatic nerve form the boundaries of a hyperechoic triangle (Cohen 2002). The detection of this triangle is very helpful because it allows prompt recognition of the main local anatomic structures. The conjoined tendon of the semitendinosus and biceps femoris appears as a sagittal comma-shaped structure located between the medial semitendinosus and the lateral biceps muscles (Fig. 12.26). In this respect, one should remember that the muscle belly of the semitendinosus arises from the tendon in a more cranial position compared with the biceps muscle. On the other hand, the semimembranosus continues in a large coronal aponeurosis which arises from the internal side of the tendon and runs medial to it (Fig. 12.26). There are no muscle fibers of the semimembranosus at this level. More caudal transverse

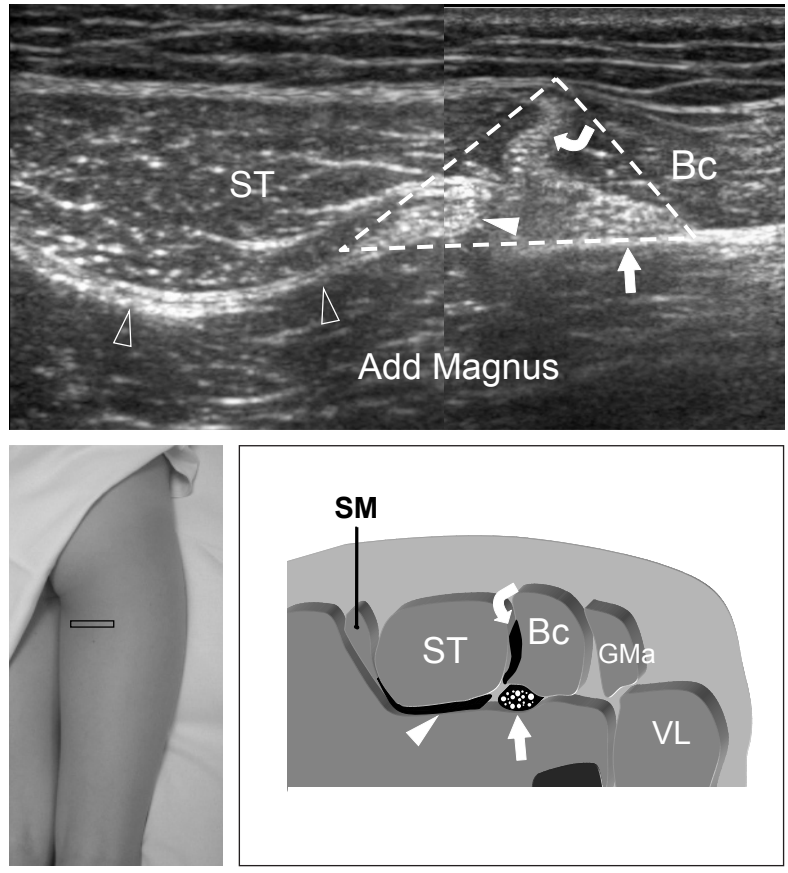

Fig. 12.26a,b. Ischiocrural muscles and tendons. **a** Transverse 12–5 MHz US image with **b** schematic drawing correlation obtained over the posterior group of hip muscles just caudally to the level described in Figure 12.25c,d. Note that the two hyperechoic tendons of the semitendinosus-biceps (*curved arrow*) and semimembranosus (*white arrowhead*) and the sciatic nerve (*straight arrow*) form the boundaries of a hyperechoic triangle (*dashed line*). A thin comma-shaped hyperechoic lamina (*open arrowheads*) arises from the medial aspect of the semimembranosus tendon. This lamina separates the semitendinosus muscle (*ST*), which is located superficially, from the deep adductor magnus. On the same level, the vertically oriented conjoined tendon of the semitendinosus-biceps separates the bellies of the lateral long head of the biceps (*Bc*) from the medial semitendinosus muscle. *GMa*, gluteus maximus; *VL*, vastus lateralis. The photograph at the lower left side of the figure indicates probe positioning

scans demonstrate the semimembranosus muscle arising from the medial end of the aponeurosis. The semitendinosus and biceps femoris muscles lie laterally. The sciatic nerve is easily detected in the midline, just anterior to the biceps femoris muscle.

In summary, one should remember that the semitendinosus and the biceps femoris muscles arise from a common tendon located over the semimembranosus tendon. This conjoined tendon inserts into the lateral aspect of the ischial tuberosity rather than into its inferior face. Shifting the transducer downwards on transverse planes, the first muscle which appears is the semitendinosus, followed by the lateral biceps femoris and, more distally, by the medial semimembranosus. The sciatic nerve is always located on the lateral side of the ischiocrural tendons. More distally, it can be detected just deep to the biceps muscle.

12.5 Hip Pathology

12.5.1 Anterior and Medial Hip Pathology

Several muscles attached onto the pelvic bones are subjected to considerable tensile forces, often related to eccentric muscle contractions. Injury

to these muscles at their hip insertion is common among participants in organized sports, and especially among adolescents and school-aged athletes as a result of either overuse and microtrauma or extreme unbalanced contractions during sport or recreational activities: the adductor longus, tensor fasciae latae and rectus femoris are the most frequently involved and may be cause of groin pain and disability. Especially in adolescents, a high prevalence of apophyseal avulsions is observed in acute injuries (see Chapter 19). Therefore, care should always be taken to check the bony insertions of these muscles when examining hip tendons with US in the pediatric age group. Chronic tears with muscle retraction may appear equivocal at physical examination, assuming an aggressive appearance possibly resembling a neoplastic or infectious process. US can help the diagnosis in clinically doubtful cases although minimal disruptive trauma in the acute phase may go unnoticed with this technique. MR imaging is best suited to the evaluation of these minor traumas, especially in professional athletes involved in agonistic activity, to establish whether and when they can return to their sport. In addition to avulsion injuries, the iliopsoas tendon is typically involved by instability in the hip region producing a painful snapping sensation during hip motion. In the absence of a history of a specific traumatic event, metabolic diseases such as amyloid deposition disease may also affect hip tendons. In these cases, the tendons may appear diffusely thickened and hypoechoic without calcifications (Fig. 12.27). In addition, iliopsoas bursitis and paralabral ganglion cysts are common findings in patients with osteoarthritic features and synovitis of the hip joint and may often mimic a space-occupying lesion in the soft tissues around the hip.

12.5.1.1 Tensor Fasciae Latae Tendinopathy

Overuse tendinopathies of the hip affect mostly the tendon of the tensor fasciae latae (Bass and Connel 2002) and the rectus femoris tendon. Patients complain of localized anterior hip pain which comes on after or, in more severe disease, during sport activities. This condition typically involves sprinters and is secondary to a forceful extension of the hip. Physical examination reveals tenderness over the anterior superior and anterior inferior iliac spines. Contraction of the muscle against resistance can increase the local pain. Clinically, the diagnosis of tensor fasciae latae tendinopathy can be suspected when a young sportsman complains of pain just below the most anterior aspect of the iliac crest. US shows degenerative involvement of the tendon, which appears thickened and heterogeneous in structure. Just posterior to this tendon, the insertion of the fasciae latae can be involved as well (Fig. 12.28). In a series of 12 patients with tensor fasciae latae tendinopathy, the tendon appeared significantly thickened (mean anteroposterior size 4.7 mm) compared with asymptomatic volunteers (mean anteroposterior size 2.1 mm) (Bass and Connel 2002). Echotextural abnormalities include a hypoechoic cone-shaped area located in the deep portion of the tendon, an appearance resembling the more common jumper's knee. Pressure with the probe over the tendon insertion can reproduce the patient's symptoms. With simple restriction of activity, such injuries usually heal quickly and without consequences.

12.5.1.2 Rectus Femoris Tendon Tear

When tendinopathy affects the rectus femoris tendon, the US features are the same as described for the tensor fasciae latae. Tears of anterior tendons are rare and mostly affect the rectus femoris in sportsmen with a previous history of rectus femoris tendinopathy. The trauma mechanism involves a forceful contraction of the muscle against resistance, such as when kicking a ball with the hip extended. Therefore, this condition occurs more often in sports such as soccer, martial arts and sprinting. Clinically, the patient presents with groin pain and loss of extension. In the rectus femoris, proximal tears occur less frequently than tears in the midsubstance of the muscle belly involving the central aponeurosis (see Chapter 13) or at the level of the distal myotendinous junction (see Chapter 14). From the pathophysiologic point of view, the rectus femoris tendon ruptures either at its insertion into bone with detachment of a bone fragment or at the proximal myotendinous junction involving its direct head. Partial tendon tears are more common than complete detachments. US depicts the tear as a focal gap in the tendon fibers associated with local hematoma (Fig. 12.29). In complete ruptures, tendon retraction occurs and may mimic a soft-tissue mass in the upper medial thigh. Healing can be followed by fibrous encasement of the injured tendon, calcifications and ossification of the hematoma, which appears as a well-delimited hyperechoic area with posterior acoustic

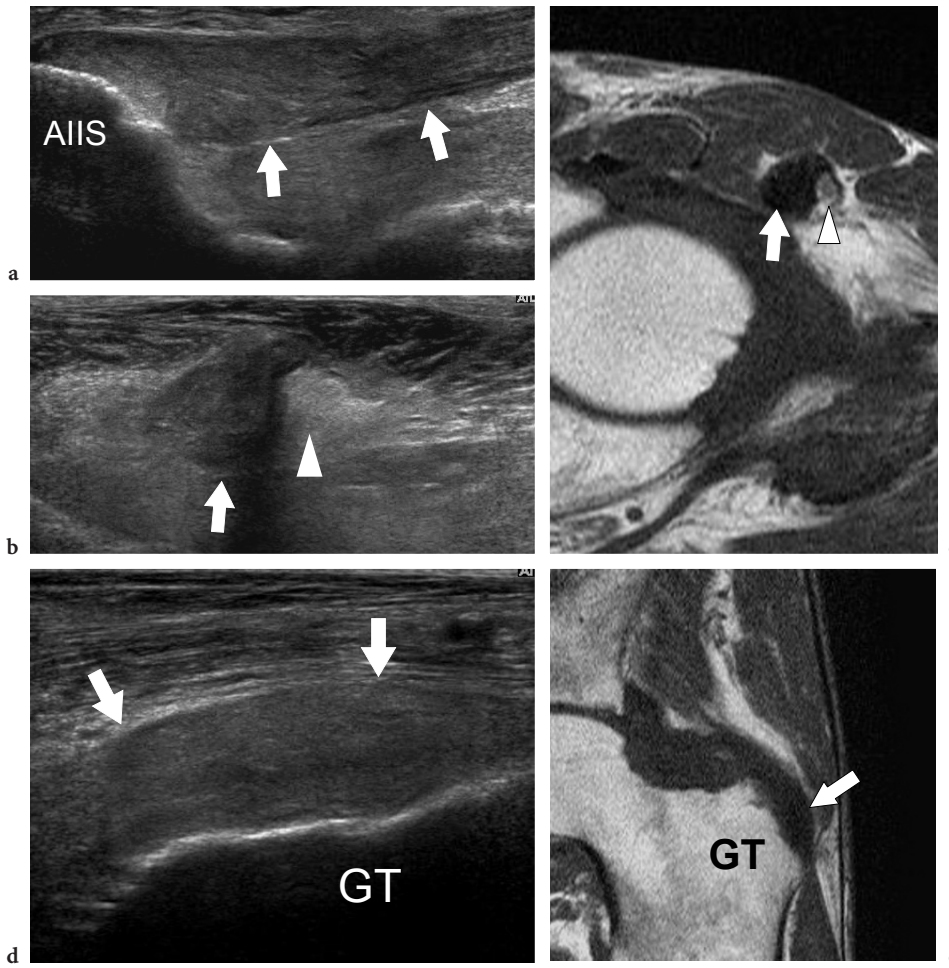

Fig. 12.27a–e. Intratendinous amyloid deposits in a patient affected by chronic renal failure. **a** Long- and **b** short-axis 12–5 MHz US images obtained over the anterior hip with **c** transverse T1-weighted MR imaging correlation demonstrate a diffusely swollen and hypoechoic direct tendon of the rectus femoris (*arrows*). On the side of the direct tendon, observe the indirect tendon (*arrowhead*), which retains a normal appearance. *AIIS*, anterior inferior iliac spine. **d,e** More distally, **d** coronal 12–5 MHz US image over the lateral hip with **e** T1-weighted MR imaging correlation shows a markedly enlarged and hypoechoic anterior tendon of the gluteus medius (*arrow*) owing to amyloid infiltration. *GT*, greater trochanter

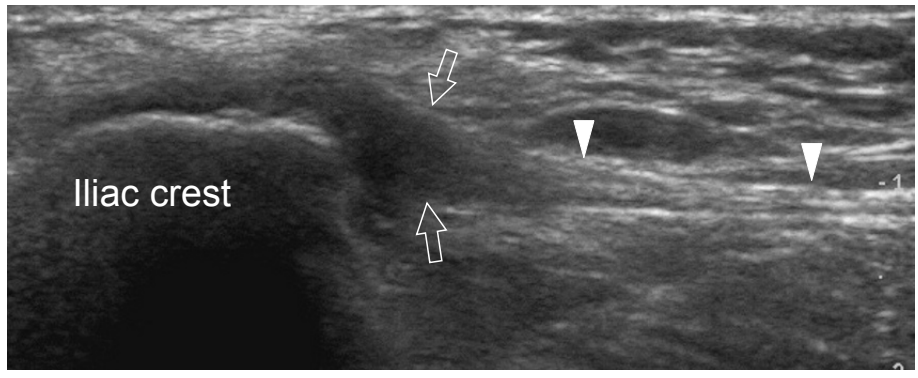

Fig. 12.28. Fasciae latae insertional tendinopathy in a patient presenting with focal tenderness and pain over the right iliac crest. Coronal 12–5 MHz US image obtained at the level of insertion of the bandellette of Massiat into the iliac crest demonstrates proximal swelling and a hypoechoic appearance of the preinsertional portion of the fasciae latae reflecting focal tendinopathy (*arrows*). Observe the normal thickness and hyperechoic appearance of the distal part of the band (*arrowheads*)

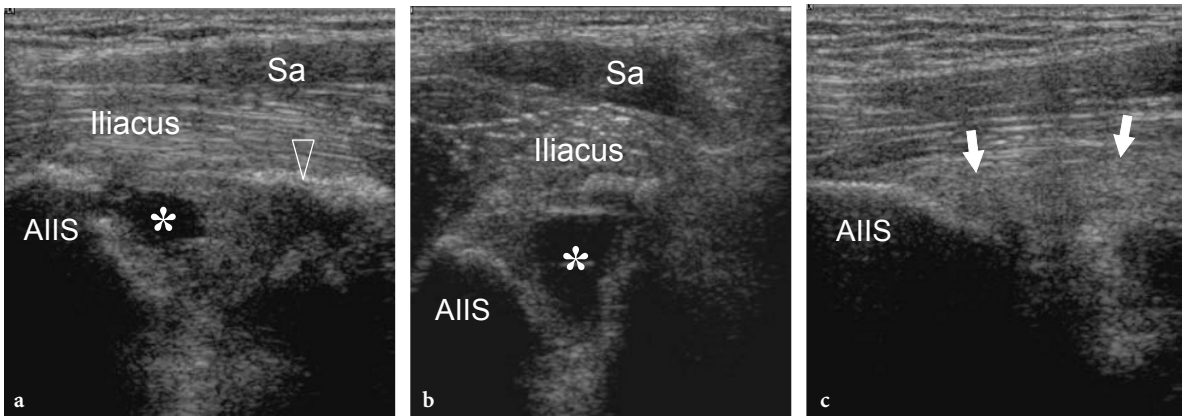

Fig. 12.29a–c. Rectus femoris tendon tear. **a** Long- and **b** short-axis 12–5 MHz US images obtained over the insertion of the proximal tendon of the rectus femoris on the anterior inferior iliac spine (*AIIS*) reveals a complete tear of the direct rectus femoris tendon (*arrowhead*) which appears retracted downward. A hypoechoic collection reflecting the hematoma (*asterisk*) is seen between the retracted tendon and the iliac spine. Superficial to the ruptured tendon, the iliacus and the sartorius (*Sa*) muscles can be appreciated. **c** Corresponding long-axis 12–5 MHz US image on the contralateral side demonstrates the intact rectus femoris tendon (*arrows*) which inserts into the anterior inferior iliac spine

shadowing (Fig. 12.30a–c). Although uncommon, calcifications in the rectus femoris tendon may also reflect calcifying tendinitis (Fig. 12.30d–f). In these cases, standard anteroposterior radiographs should always be obtained to confirm the diagnosis after US examination.

12.5.1.3 Hip Adductor Injuries

The symphysis pubis and the inferior branch of the pubis are the origin for the adductor longus, adductor brevis and gracilis muscles. Hip adductor injuries are common sporting injuries following overuse or/and acute trauma in which there is a combination of hyperabduction of the hip and hyperextension of the abdominal wall, occasionally with forced external rotation of the leg (Rizio et al. 2004). Soccer and rugby are the most commonly involved sports. These injuries are often described in relation to a single muscle, the superficial adductor longus and the gracilis being the most commonly affected (Robinson et al. 2004). In the acute phase, it may be difficult to distinguish between injuries of the individual muscles, because pain and tenderness is diffuse over the groin. The main differential diagnoses of adductor dysfunction include osteitis pubis and prehernia complex (Robinson et al. 2004). Plain films are not so helpful as in other sites in the pelvis because discrete avulsed fragments are not seen in these injuries. In partial tears, US demonstrates an irregular, hypoechoic and ill-defined adductor origin over the symphysis pubis, whereas a complete separation of the adductor longus from the pubis is seen in complete rupture. In acute traumas of the adductor longus tendon, the area closer to the pubis may exhibit a mixed appearance due to the hematoma, debris and possibly damage of the fibrocartilage enthesis. In the subacute and chronic phases, the retracted tendon may appear as a blunted hypoechoic mass with posterior attenuation of the US beam, which must not be confused with a neoplasm (Fig. 12.31). In significant traumas, a tear of the adductor longus may also extend to the superficial fibers of the underlying adductor brevis. In these cases, distinguishing a simple adductor longus tear from a combined avulsion of

Fig. 12.31a–c. Acute avulsion injury of the adductor longus tendon. **a** Long-axis 12–5 MHz US image obtained over the insertion of the adductor longus tendon on the proximal medial thigh. The adductor longus muscle (*Add Lg*) appears retracted from the pubis (*asterisk*) and surrounded by a large heterogeneous collection reflecting a post-traumatic hematoma (*H*). Observe the short hyperechoic tendon (*arrowhead*) of the adductor longus. Coronal **b** T2-weighted **c** and Gd-enhanced T1-weighted MR images confirm the complete avulsion of the adductor longus tendon (*arrowhead*) from the pubis (*asterisk*). In **b**, the large hematoma (*H*) is characterized by a high signal intensity, whereas in **c** it appears hypointense and surrounded by a thick high-signal rim as a result of peripheral organization

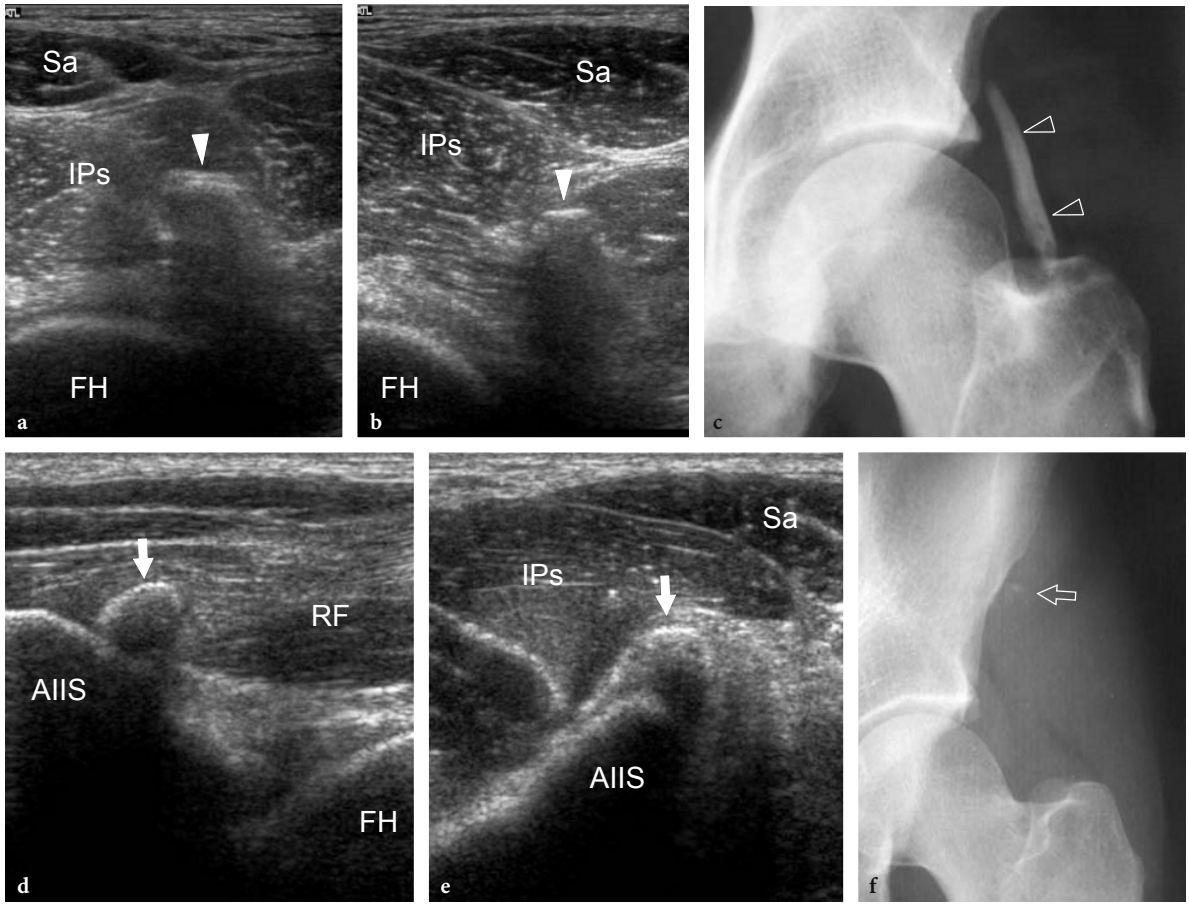

Fig. 12.30a–f. Calcifications in the rectus femoris tendon. Two different cases. **a–c** Patient with previous partial tear of rectus femoris tendon. **a,b** Transverse 12–5 MHz US images obtained along the length of the rectus femoris tendon demonstrate a hyperechoic structure with posterior acoustic shadowing representing a calcified direct tendon of the rectus femoris (*arrowhead*). *FH*, femoral head; *Sa*, sartorius muscle; *IPs*, iliopsoas muscle. **c** Anteroposterior radiograph confirms the US findings. **d–f** Elite athlete with hydroxyapatite crystal deposition disease complaining of pain in the anterior hip region during exercise. **d** Long- and **e** short-axis 12–5 MHz US images obtained over the proximal tendon of the rectus femoris with **f** anteroposterior radiographic correlation reveals a well-defined calcification (*arrow*) within the rectus femoris tendon. Note the relationships of the rectus femoris tendon with the iliopsoas (*IPs*) and sartorius (*Sa*) muscles. *FH*, femoral head

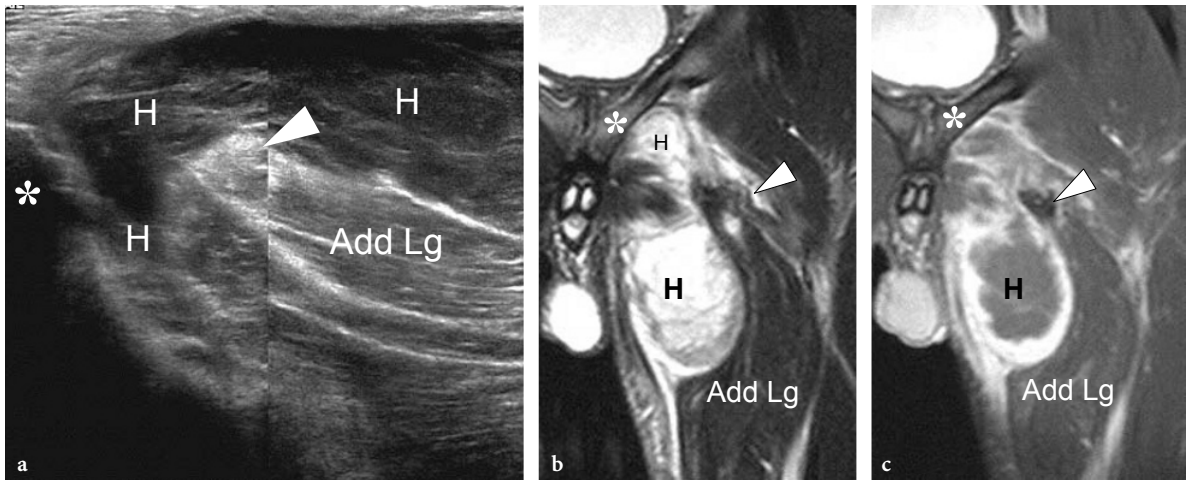

the adductor longus and partial tear of the adductor brevis may be problematic with US. Transverse US planes may be helpful for this purpose. On the other hand, the diagnosis of complete detachment of both muscles from their insertions is straightforward (Fig. 12.32). In low-grade injuries and adductor tendinopathy causing resistant chronic groin pain, US has demonstrated a low sensitivity for detecting chronic myotendinous strain or tenoperiosteal disease. In these cases, gadolinium-enhanced MR imaging is a more reliable indicator of the disease process (Robinson et al. 2004).

The prognosis for hip adductor traumas depends mainly on the complexity of the tear and the site of injury. In general, injuries to the adductor longus occurring at the level of the myotendinous junction are less serious and a prompt recovery can be expected within 1 or 2 weeks. In contrast, avulsion or proximal lesions may require 1–3 months before a return to normal activity. Treatment is conservative and includes rest, anti-inflammatory drugs and decreased weight-bearing for several weeks followed by gradual return to exercise, and stretching and strengthening to restore the normal range of motion.

12.5.1.4 Snapping Iliopsoas Tendon

The snapping hip has been defined as hip pain accompanied by an audible or palpable clicking or snapping during joint motion or walking. This syndrome can derive from a variety of intra- or extra-articular pathologic conditions (Anda et al. 1986; Janzen et al. 1996; Pelsser et al. 2001). The intra-articular snapping hip is most often related to abnormalities of the joint itself, presence of intra-articular loose bodies, synovial osteochondromatosis and labrum tears. In these cases, osteochondral or fibrocartilaginous fragments impinge between the acetabular cavity and the femoral head causing the snapping sensation. Intra-articular causes are demonstrated on standard radiographs, CT scan and MR-arthrography that can best detect the occurrence of intra-articular loose bodies and labrum tears. Although the US findings in osteochondromatosis have been described in the literature (Pai and van Holsbeeck 1995), we believe that this technique has intrinsic limitations in this field because it is not able to provide a complete assessment of the hip cavity. Deep loose fragments located in proximity to the teres ligament, for instance, cannot be visualized. This is an important drawback because the surgeon is obliged to dislocate the hip for their removal. On the other hand, the extra-articular causes of snapping hip may be divided into internal and external. Internal snapping hip is essentially caused by snapping of the iliopsoas tendon and muscle over the iliopectineal eminence. External causes are discussed later, in Sect. 12.5.2.2. Snapping may be painful and can limit occupational or recreational activities (Wahl et al. 2004). Because this syndrome can be caused by a variety of conditions that require different treatments (conservative or surgical), a precise diagnosis

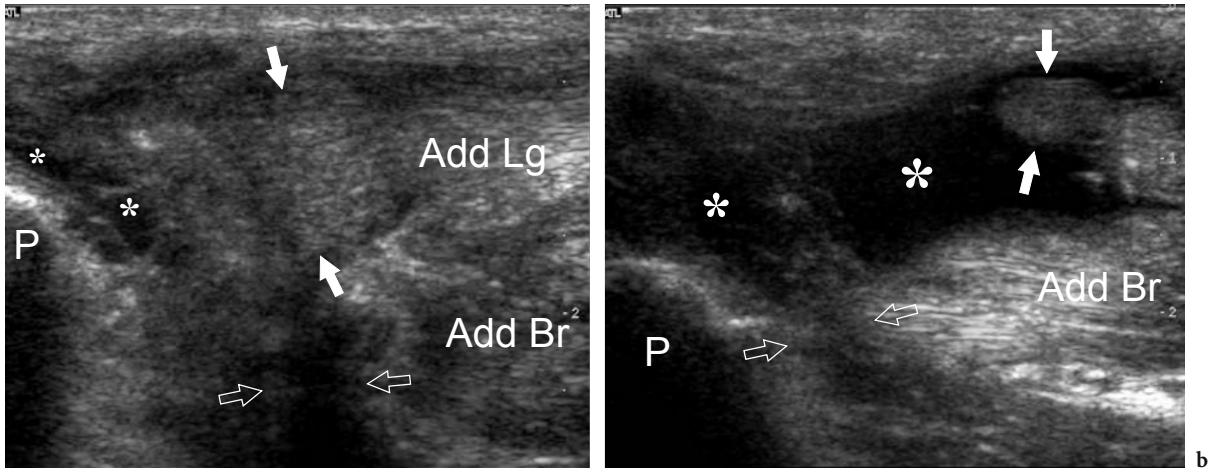

a b

Fig. 12.32a,b. Combined acute avulsion injury of the adductor longus and brevis. Long-axis 12–5 MHz US images obtained over the insertion of the adductor muscles on the pubis (*P*) reveals discontinuity with "bell-clapper" retraction of the proximal tendon (*white arrows*) of the adductor longus muscle (*Add Lg*). The torn tendon end is separated from the pubis by a hypoechoic hematoma (*asterisks*). On a deeper plane, note a hypoechoic cleft (*open arrows*) at the insertion of the adductor brevis (*Add Br*) indicating a combined tear of both muscles

of the involved structure is required to increase the potential for successful treatment.

Because of its anatomic position, the iliopsoas tendon lies in close relationship with the bone surface of the iliopectineal eminence and shifts laterally when the hip is flexed, abducted and externally rotated. When the hip comes back in an extended, adducted and internally rotated position, the tendon first impinges on the iliopectineal eminence and then moves abruptly in a medial direction causing the snap (Fig. 12.33) (Pelsser et al. 2001). Iliopsoas bursography can detect snapping of the iliopsoas tendon but this technique is invasive and difficult to perform in the absence of a bursal effusion. Because of its dynamic capabilities, US has proven to be a quick, inexpensive and readily available technique for assessment of snapping hip. US examination is performed with the patient supine on the examination bed. Oblique transverse US images oriented along the short-axis of the tendon are obtained over the iliopectineal eminence while the patient is asked to place the hip in the frog leg position and then to return it to the normal anatomic position. As an alternative, the patient is simply asked to generate the hip movement that produces the snapping sensation (Hashimoto et al. 1997; Pelsser et al. 2001). In normal conditions, the iliopsoas tendon can be seen gliding smoothly over the ilium during hip movements. In cases of iliopsoas instability, an abrupt sudden medial-to-lateral or lateral-to-medial motion of the tendon is apparent. It is essential to correlate the timing of tendon snapping visible at US with the snapping sensation and, even more importantly, with the referred pain. In fact, snapping can occur in the absence of any clinical effect and its relationship with hip pain should always be demonstrated before starting treatment. The examination is completed with static scanning to rule out tendon thickening or effusion inside the iliopsoas bursa. However, these signs are associated in a minority of cases (Pelsser et al. 2001). Comparison with the unaffected contralateral side has been suggested in doubtful cases (Janzen et al. 1996). For painful snapping iliopsoas tendon, treatment includes rest, stretching exercises and anti-inflammatory medication, reserving surgery (tendon lengthening) for refractory cases (Wahl et al. 2004).

Overall, in patients with clinical symptoms suggesting internal snapping hip, we believe that a standard radiograph of the pelvis must be obtained initially, to evaluate the hip bones and the joint spaces, as well as to rule out the presence of calcified intra-articular loose bodies. Dynamic US scanning should be obtained if the patient is symptomatic, to reveal a snapping iliopsoas tendon and correlate it directly with the patient's symptoms. A negative US examination should be followed by MR imaging, CT or MR-arthrography to exclude intra-articular disorders (Janzen et al. 1996).

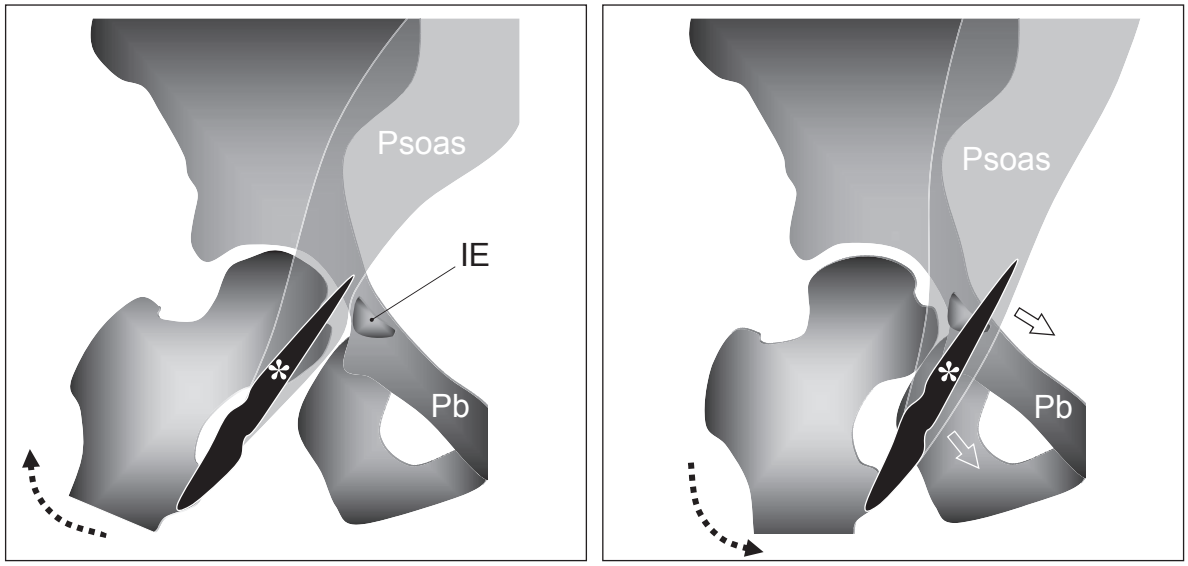

a b

Fig. 12.33a,b. Snapping iliopsoas tendon. Schematic drawings illustrate the mechanism of the snapping iliopsoas tendon. **a** When the hip is flexed, externally rotated and abducted, the iliopsoas tendon (*asterisk*) shifts laterally relative to the iliopectineal eminence (*IE*). **b** When the hip returns to an extended position, the iliopsoas tendon (*asterisk*) impinges against the iliopectineal eminence until snapping over it and moving suddenly medially. *Pb*, pubis

12.5.1.5 Iliopsoas Bursitis

In normal conditions, the iliopsoas bursa cannot be visualized with US because its cavity contains only a thin film of synovial fluid. When communicating with the joint cavity, hip joint fluid can enter the bursa (Fig. 12.34a). In cases of abundant joint effusions, the bursa acts primarily as a reservoir thus limiting the damage to the intra-articular structures related to a high intra-articular pressure. Intra-articular fluid, synovial fronding and loose bodies arising from the joint cavity can be found inside the bursa and are easily demonstrated with US. Serous effusion within the bursa appears as an anechoic fluid collection without apparent walls (Fig. 12.34b-d). On transverse US images, the iliopsoas bursa is located between the medial femoral vessels and the lateral iliopsoas muscle. The close relationship between the iliopsoas bursa and the adjacent neurovascular bundle explains why compression of the femoral vein and entrapment of the femoral nerve is not

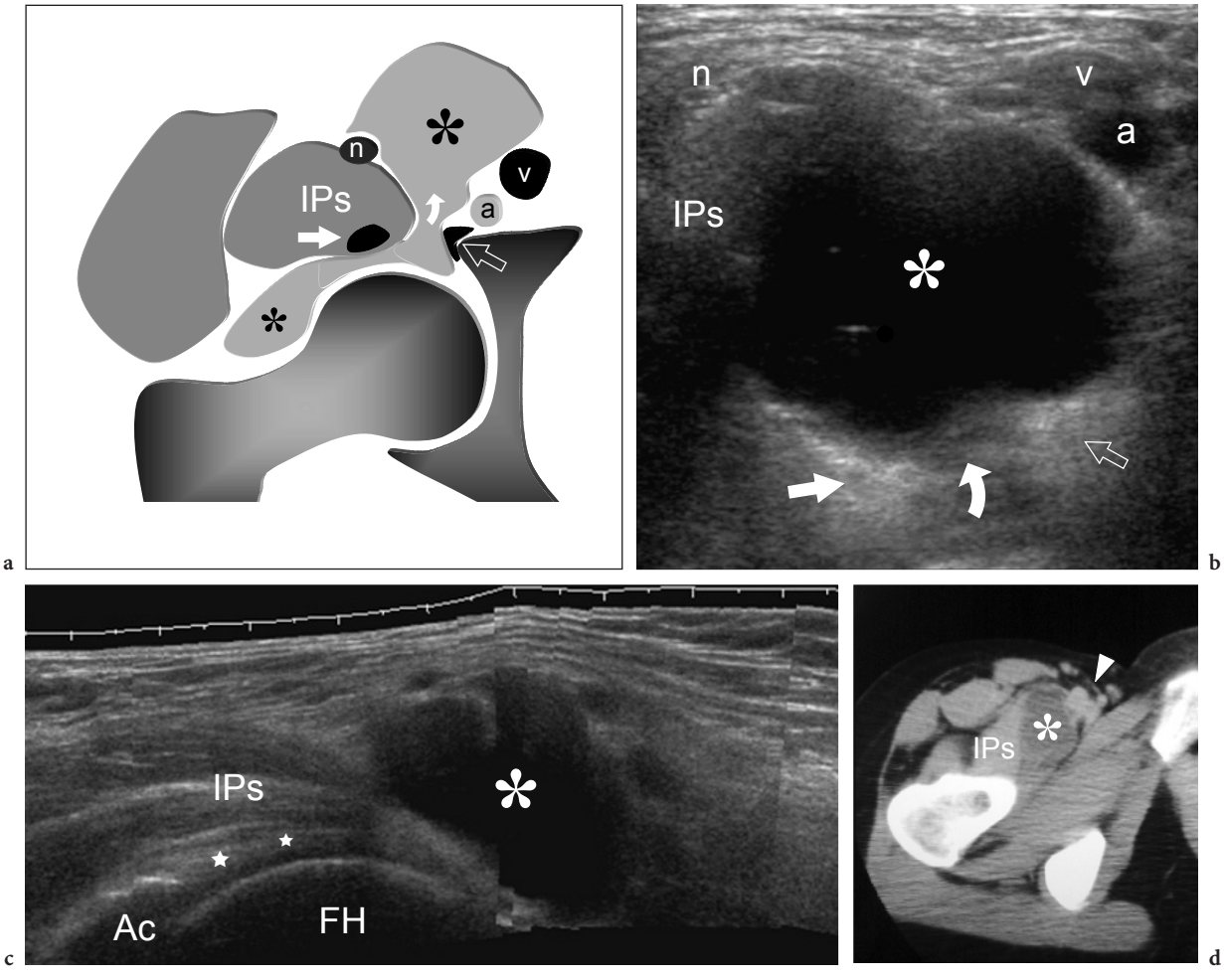

Fig. 12.34a–d. Iliopsoas bursitis. **a** Schematic drawing of a transverse view through the hip illustrates an effusion located inside the iliopsoas synovial bursa (*large asterisk*). The joint cavity communicates with the bursa through a thin pedicle (*curved arrow*). Note the anterior recess filled with fluid (*small asterisk*), the iliopsoas muscle (*IPs*) and tendon (*white straight arrow*). The anterosuperior labrum (*open arrow*) appears normal. Filling the bursa with intra-articular fluid decreases the pressure inside the hip joint and may help to prevent intra-articular lesions. **b** Transverse oblique and **c** sagittal 12–5 MHz US images obtained over the anterior hip demonstrate the enlarged iliopsoas bursa (*asterisk*) filled with anechoic synovial fluid. A discrete pedicle (*curved arrow*) can be appreciated in **b** between the iliopsoas (*IPs*) tendon (*white straight arrow*) and the labrum (*open arrow*). Observe the displaced but otherwise normal-appearing common femoral artery (*a*) and vein (*v*) and femoral nerve (*n*). In **c**, the relationships of the distended bursa (*asterisk*) with the normal iliopsoas muscle (*IPs*), the labrum (*stars*), the femoral head (*FH*) and the acetabulum (*Ac*) are depicted on sagittal view. **d** CT scan identifies the bursa (*asterisk*) between the iliopsoas (*IPs*) and the femoral vessels (*arrowhead*)

infrequent in patients with large bursal distention (Pellman et al. 1986; Yoon et al. 2000). When the bursa is filled with synovial pannus, such as in longstanding rheumatoid arthritis, it appears as a para-articular mass with internal echogenic solid components and can have a large size because of the slow progression of the disease process (Fig. 12.35) (Bianchi et al. 2002b). Larger cysts can develop inside the pelvis between the iliac bone and the iliopsoas muscle (Fig. 12.36). These "giant" cysts can be responsible of a mass effect on the pelvic structures (Salmeron et al. 1999; Ginesty et al. 1998; Janus and Hermann 1982) and might be biopsied to rule out a tumor if the possibility of intrapelvic extension of a distended bursa is not kept in mind. US-guided aspiration of bursal fluid is best performed with a large-bore needle (Fig. 12.36).

12.5.1.6 Paralabral Ganglion Cysts

Ganglion cysts can be encountered along the anterior aspect of the hip. They arise from the acetabular labrum as a result of labral fissure and subsequent mucoid degeneration with formation of a cyst filled with mucoid material (Fig. 12.37a). The pathogenesis of hip ganglia is somewhat similar to that of glenoid ganglia of the shoulder or parameniscal cysts in the knee. Hip ganglia present clinically as well-circumscribed groin masses that are usually painless or slightly painful at deep palpation or extreme movements of the hip. The clinical detection of these cysts is difficult and the diagnosis relies mainly on imaging findings. At US examination, paralabral ganglion cysts appear as lobulated, hypoechoic cystic lesions with well-defined borders

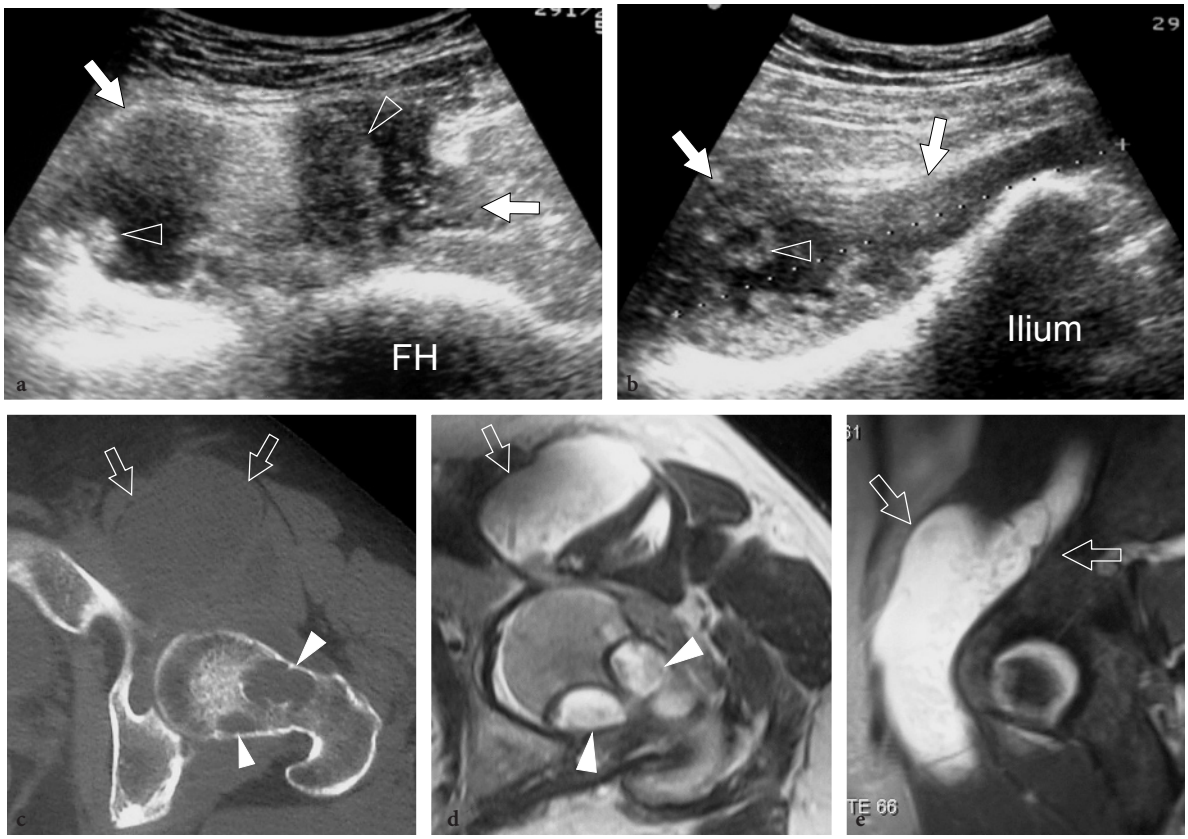

Fig. 12.35a–e. Iliopsoas bursitis in patient with advanced rheumatoid arthritis. **a,b** Transverse oblique 3.5 MHz US images obtained **a** at the level of the femoral head (*FH*) and **b** over the ilium. The iliopsoas bursa (*arrows*) appears markedly swollen and contains anechoic effusion and echogenic synovial folds (*arrowheads*) representing rheumatoid pannus. **c** Corresponding transverse CT image confirms bursal distention by its hypodense content. Large marginal erosions (*arrowheads*) can be appreciated as associated findings in the femur. **d** Transverse T2-weighted and **e** sagittal fast-STIR MR images confirm the US findings. In **e**, observe the bursa extending within the pelvis (*arrows*)

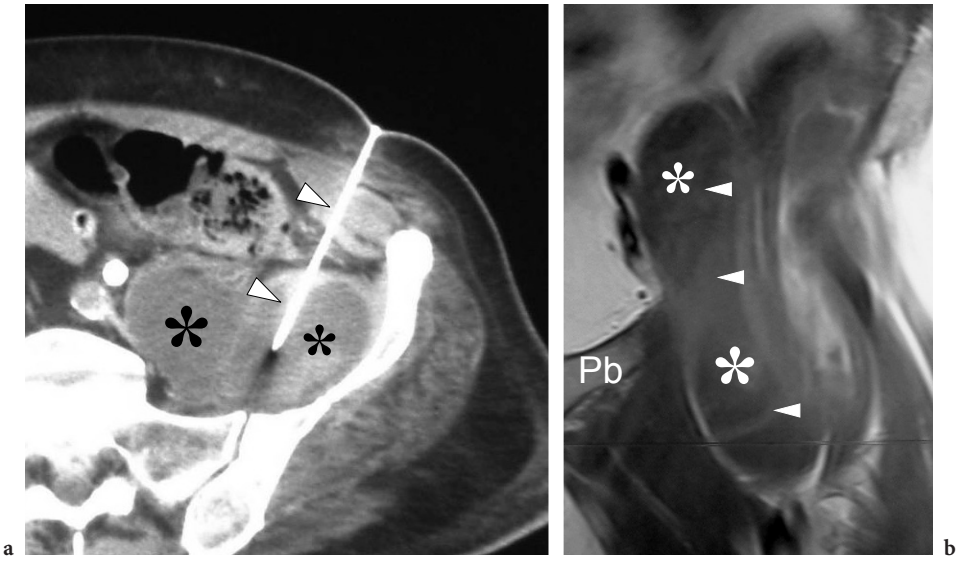

a b

Fig. 12.36a,b. Extension of iliopsoas bursitis within the pelvis. **a** Axial CT scan demonstrates a large mass (*asterisks*) filled with hypodense fluid in the left pelvic fossa, close to the ilium. Observe the needle (*arrowheads*) guided within the mass for percutaneous biopsy. **b** Coronal Gd-enhanced T1-weighted MR image reveals an enlarged bursa located, in part, within the pelvic cavity (*asterisks*) and contrast material uptake by its walls and septa (*arrowheads*). *Pb*, pubis

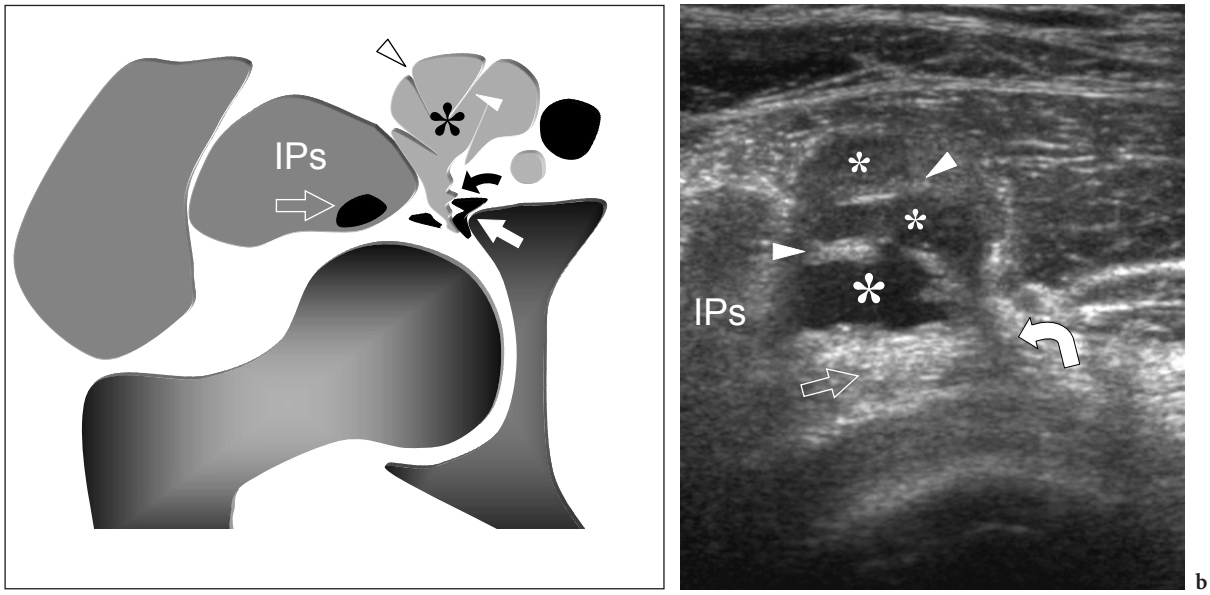

a b

Fig. 12.37a,b. Anterior ganglion cyst. **a** Schematic drawing of a transverse view through the hip and **b** corresponding transverse 12–5 MHz US image illustrate a ganglion cyst (*asterisks*) arising from the anterior aspect of the hip joint. The cyst communicates with the torn anterosuperior labrum (*white straight arrow*) through a short pedicle (*curved arrow*). Internal septations can be appreciated (*arrowheads*). Note the iliopsoas muscle (*IPs*) and tendon (*open arrow*)

and internal septations (Figs. 12.37b, 12.38). They are usually smaller than the iliopsoas bursitis and, because of their thickened wall and mucoid content, do not show any significant change in shape when compressed with the probe. In some instances, the enlarging ganglion cyst can dissect proximally underneath the iliopsoas muscle and expand inside the pelvic cavity (Fig. 12.39). Large acetabular paralabral cysts may result in compression of the femoral vessels and nerve.

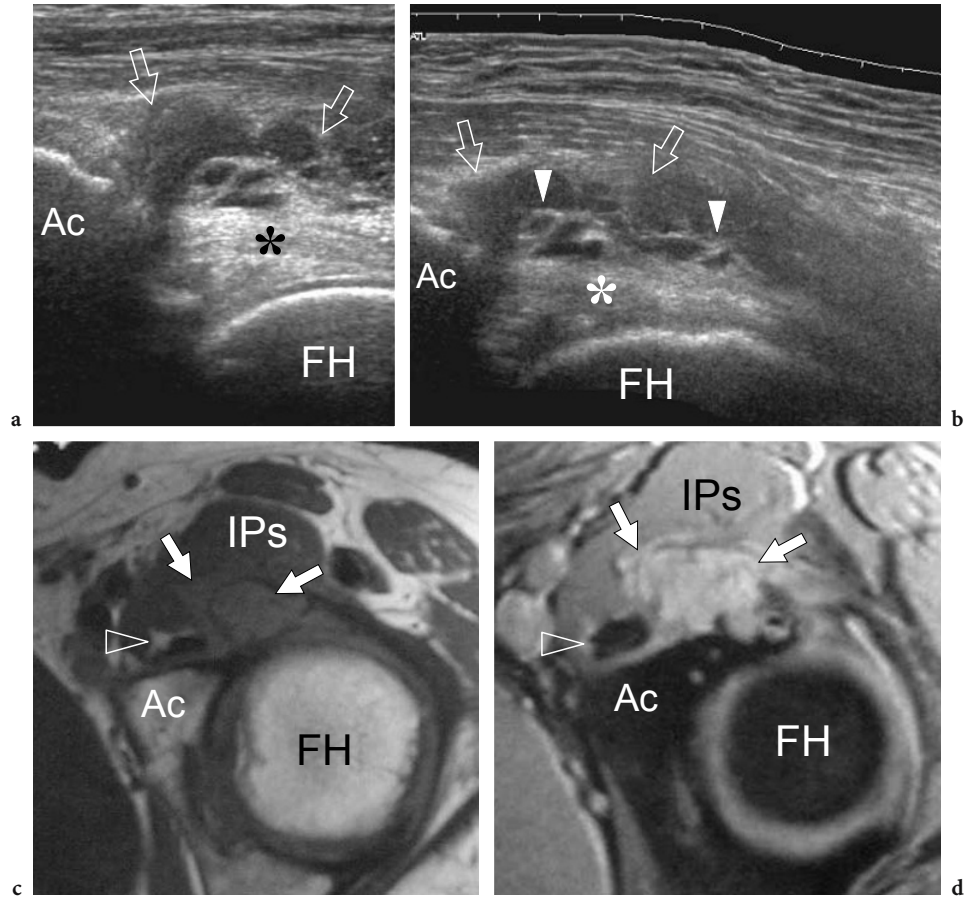

Fig. 12.38a–d. Anterior ganglion cyst. **a** Transverse and **b** sagittal extended field-of-view 12–5 MHz US images obtained over the anterior aspect of the hip demonstrate a ganglion cyst (*arrows*) which appears as a complex mass with fluid-filled cavities and prominent echogenic septations (*arrowheads*). Note the close relationship between the cyst and the anterosuperior labrum (*asterisk*). *Ac*, acetabulum; *FH*, femoral head. **c** Transverse T1-weighted and **d** fat-suppressed T2-weighted MR images. In **c**, the ganglion (*arrows*) appears isointense relative to the iliopsoas muscle (*IPs*) and tendon (*arrowhead*), whereas in **d** it exhibits hyperintense signal. Internal septations are barely visible

12.5.1.7 Inguinal Lymphadenopathies

Differential diagnosis of labrum ganglia includes other firm anterior groin masses, such as inguinal lymphadenopathies. Pathologically enlarged lymph nodes may be difficult to distinguish from ganglion cysts based on physical examination. In contrast, US allows rapid and easy differentiation between these two conditions, which require different treatment and carry a different prognosis. In general, groin nodes tend to be slightly larger than lymph nodes in the neck. Adenopathies appear as oval or rounded solid hypoechoic masses with a central hyperechoic hilum. Accumulation of fatty tissue in the hilum with atrophy of the surrounding hypoechoic cortex, an appearance quite similar to that of superficial lipomas, is a common finding in normal groin nodes (Fig. 12.40a). Detection of a thin hypoechoic peripheral rim and a hilar distribution of vasculature at color Doppler imaging together with the multiplicity of nodes with a similar appearance in the groin space may help to avoid this confusion. A less defined differentiation between the hypoechoic cortex and the hyperechoic hilum can be encountered in highly inflammatory states, lymphomas or neoplastic conditions, when the hilum becomes hypoechoic as a result of infiltrative processes (Fig. 12.40b,c). The main criteria for malignancy include node enlargement, rounded shape and heterogeneous echotexture; however, reliable histopathologic differentiation cannot be obtained with US. In nodal abscesses, disruption of the normal nodal architecture and echo-poor areas within the adjacent subcutaneous

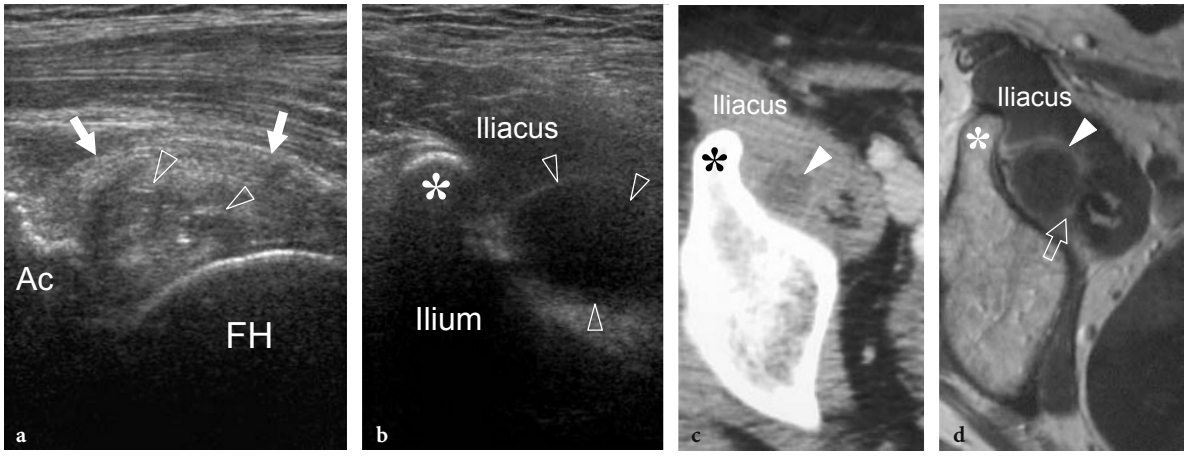

Fig. 12.39a–d. Anterior ganglion cyst in a patient with chronic hip pain and symptoms related to femoral neuropathy. **a** Sagittal 12–5 MHz US image obtained over the femoral head (*FH*) and **b** transverse 12–5 MHz US image obtained over the anterior inferior iliac spine (*asterisk*) reveals the ganglion cyst (*arrowheads*) arising from a degenerated and heterogeneous anterosuperior labrum (*arrows*) and expanding between the deep boundary of the iliacus muscle and the anterior aspect of the ilium. At this level, the ganglion appears as an anechoic cystic structure. *Ac*, acetabulum. **c,d** Transverse **c** CT scan and **d** Gd-enhanced T1-weighted MR image obtained at the same level as **b** confirm the US findings. In **d,** observe a rim of contrast enhancement (*arrow*) depicting the cystic wall. In this particular case, the mass effect of the ganglion cyst led to an indirect compression of the femoral nerve which courses under the fascia of the iliacus muscle. Surgical removal of the ganglion caused relief of the symptoms

tissue, as an expression of intense edema and abscess formation, can be seen with US (Fig. 12.40d). When the benign appearance of an inguinal lymph node is uncertain at US examination, clinical correlation is essential and percutaneous needle biopsy or surgical removal of the abnormal node is indicated.

12.5.1.8 Arterial Pseudoaneurysms

US and Doppler techniques are accurate means to diagnose injuries to the femoral vessels in the groin. These usually occur as a result of iatrogenic procedures (arterial catheterization), but may also be involved in displaced fractures of the pubis and the femoral neck, crush injuries, blunt trauma and so forth. The most common site for arterial injuries is the common and proximal superficial femoral artery. The main complication is a pseudoaneurysm. Other less frequent complications include thrombosis, arteriovenous fistula, dissection, intimal flaps and perivascular hematoma. Pseudoaneurysms of the femoral artery follow a tear of the vessel wall followed by leakage of blood from the artery into the adjacent tissue and usually appear as pulsatile well-defined anechoic masses located closely to the artery (Fig. 12.41). Mural thrombus is often present and partially fills the pseudoaneurysm sac. Blood flow inside the pseudoaneurysm is typically swirling with alternating red and blue colors (Fig. 12.41b). In most cases, color Doppler imaging allows depiction of the direct communication, the neck, intervening between the artery and the sac. At Doppler spectral analysis, blood in this tract exhibits bidirectional high velocities entering the cavity from the damaged artery in systole and exiting from it in diastole, the so-called to-and-fro signal (Fig. 12.41c). Clinically, a pulsatile lump in the groin may be mimicked by soft-tissue masses, such as lymphadenopathies, located superficial to the artery which may enhance transmission of systolic pulses on the skin, as well as by underlying structures displacing the artery toward the surface. In both cases, US is a reliable technique to exclude a pseudoaneurysm. US is also useful to assist with compression closure of the pseudoaneurysm, with a success rate of 75–80% of cases (Fellmeth et al. 1991). Once the neck of the pseudoaneurysm has been identified with US, pressure is applied over it with the transducer with color Doppler imaging switched on until flow signal ceases to be seen within the sac. The optimum length of time for compression has been reported as ranging from 15 to 60 min (Coley et al. 1995). After the compression procedure, the patency of the femoral artery should be assessed and the occlusion of the pseudoaneurysm confirmed 24 h after closure with color Doppler US. A recently reported alternative to compression is the injection of thrombin under US guidance directly into the pseudoaneurysm flow lumen (Kang et al. 1998; Paulson et al. 2000). This procedure has

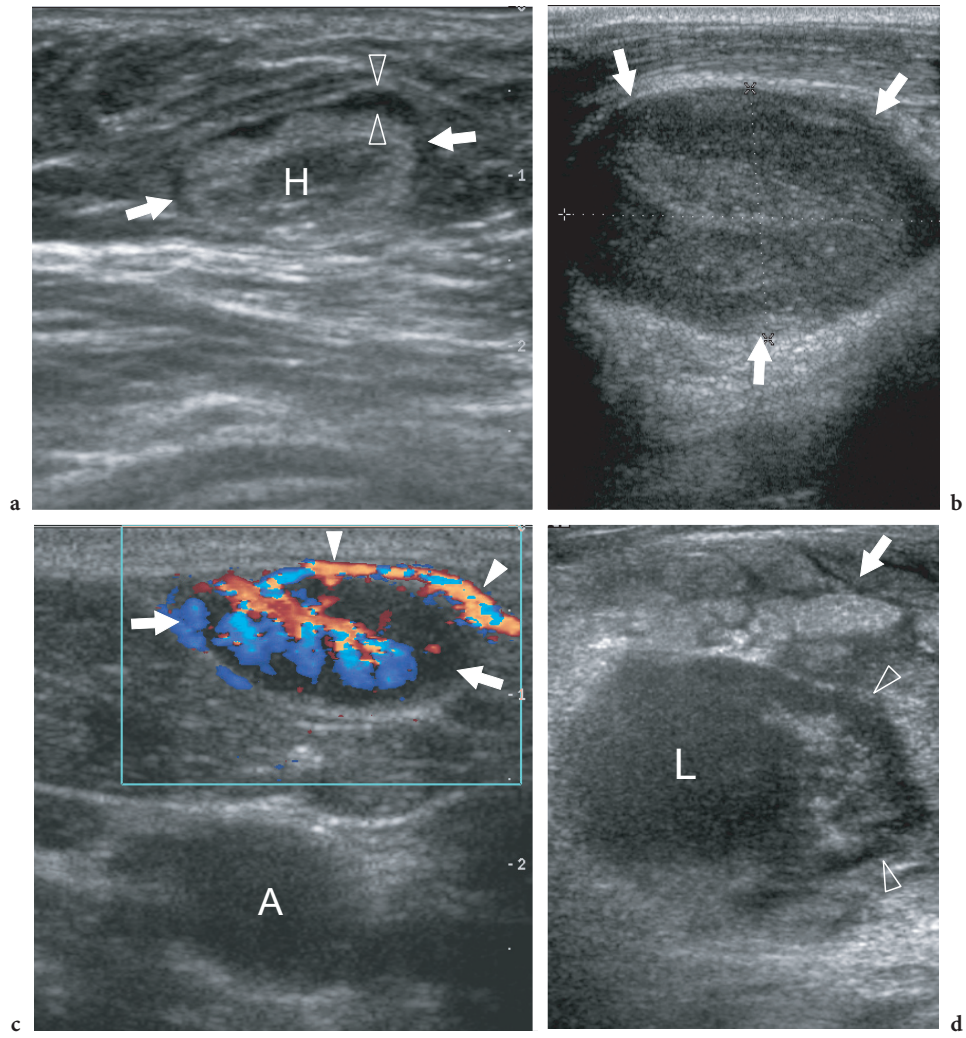

Fig. 12.40a–d. Groin lymphadenopathies. Spectrum of US findings in four different cases. **a** Long-axis 12–5 MHz US image of a normal lymph node (*arrows*) with atrophic hypoechoic cortex (*arrowheads*) and a thickened hilum (*H*) due to abundant fat deposition. **b** Long-axis 12–5 MHz US image of a metastatic node from adenocarcinoma. Observe the considerable enlargement and rounding of the lymph node (*arrows*). The central hilar area is no longer demonstrated. **c** Long-axis 12–5 MHz color Doppler US image of a reactive lymph node (*arrows*) shows a single vascular pole (*arrowheads*) branching with a root-like pattern within the hilum. *A*, common femoral artery. **d** Nodal abscess. Transverse 12–5 MHz US image of the inguinal region in a patient with groin infection reveals a hypoechoic fluid collection (*arrowheads*) in the subcutaneous tissue spreading from a node (*L*) and infiltrating among the adjacent fat lobules (*arrow*)

proved to be superior to compression repair and has the advantage of being able to treat even those pseudoaneurysms that are not amenable to compression, including those in which it is not possible to arrest flow in the neck, those arising cranially to the inguinal ligament and those associated with marked groin tenderness. Using a appropriate technique, thrombin injection has proved to be safe without significant complications or risk of downstream embolization (Paulson et al. 2001). In most cases, this procedure leads to pseudoaneurysm thrombosis in a few seconds (Paulson et al. 2000).

12.5.1.9 Femoral and Lateral Femoral Cutaneous Neuropathies

Entrapment of the femoral nerve is a rare condition resulting from a variety of space-occupying processes in the iliacus compartments, such as hematoma, iliacus abscess, iliopsoas bursitis or iatrogenic complications after vessel cannulation, during fracture fixation with metallic plates or inguinal hernia repair. In severe neuropathy, wasting and weakness of the quadriceps muscle, a reduced knee reflex and

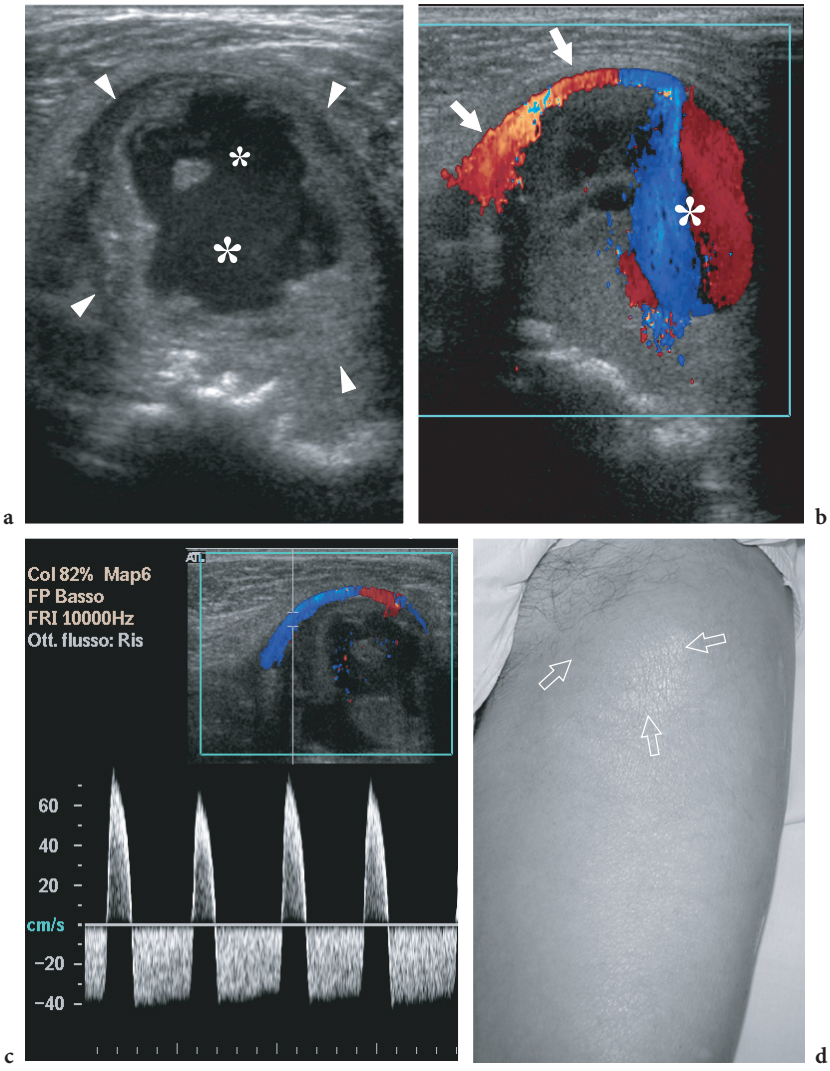

Fig. 12.41a–d. Pseudoaneurysm of the femoral artery following common femoral artery puncture in a patient presenting with a pulsatile lump in the groin. **a** Sagittal oblique gray-scale and **b** color Doppler 12–5 MHz US images over the inguinal region reveal a large complex mass (*arrowheads*) with thickened walls and an irregularly-shaped central cavity (*asterisks*). Color Doppler US demonstrates whirling flow within the mass in continuity with a displaced femoral artery (*arrows*) by means of a thin neck. **c** Spectral Doppler analysis obtained in the communicating tract displays bidirectional velocities as the forward flow in systole is ejected in diastole. **d** Photograph shows the soft-tissue lump (*arrows*) in the femoral triangle related to the pseudoaneurysm

sensory impairment over the anteromedial thigh can be observed clinically. The onset of clinical symptoms may be gradual or sudden with back, hip and thigh pain mimicking radiculopathy. High-resolution US may be useful to identify the cause of nerve compression in the suprainguinal, inguinal and infrainguinal regions, in most cases appearing as a kinking or fibrous encasement of the nerve bundle beneath the inguinal ligament (Gruber et al. 2002). In negative cases, other imaging modalities should be indicated to exclude a more proximal level of nerve involvement, such as disk disease producing lumbar spinal nerve compression or retroperitoneal and intrapelvic lesions.

Lateral cutaneous nerve compression occurs more commonly in the obese and pregnant women, especially when the abdomen bulges over the inguinal ligament and compresses the nerve as it enters the thigh deep to the lateral end of the inguinal ligament. Symptoms may be worsened by walking or with prolonged standing and typically disappear with weight loss, exercises for the abdominal muscles or delivery. Lateral femoral neuropathy causes the syndrome of "meralgia paresthetica", which typically presents

with numbness and paresthesias in the anterolateral region of the thigh, the area of distribution of this nerve. The skin may be exquisitely hypersensitive to touch. The value of US in this syndrome is actually limited. Even using high-frequency transducers, US is most often unable to detect abnormalities along the course of this nerve. Only in a few cases a fusiform thickening of nerve can be appreciated at the lateral end of the inguinal ligament as an indicator of nerve compression (Fig. 12.42).

12.5.2 Lateral Hip Pathology

Lateral hip pain is a common clinical challenge that may be secondary to a variety of either intra-articular or periarticular pathology, including trauma, avascular necrosis, infection, stress fractures of the femoral neck, irradiated pain from the spine, entrapment neuropathies, trochanteric bursitis and tendinopathies of the gluteus medius and minimus muscles. Around the greater trochanter, US is able to provide clinically useful information to distinguish gluteus tendinopathy from trochanteric bursitis, assess snapping hip due to instability of the iliotibial band and differentiate the Morel-Lavallée lesion from a mass.

12.5.2.1 Greater Trochanteric Pain Syndrome

Tendinopathy or bursitis around the trochanteric region are the main indications for US examination of the lateral hip. Because these conditions cannot be distinguished on the basis of the clinical findings, they are conventionally grouped in the greater trochanteric pain syndrome (Karpinski and Piggott 1985). Middle-aged to elderly women are the most commonly affected. Patients typically complain of a pinpoint pain over the lateral and posterior aspect of the greater trochanter associated with tenderness at deep pressure. There is no limitation of hip motion and the patient reports pain when sleeping on the affected side or under weight-bearing. The pathogenesis of greater trochanteric pain syndrome is not completely understood, although rheumatologists and orthopaedic surgeons are becoming increasingly aware that local microtrauma leading to tears of the abductor tendons, as opposed to trochanteric bursitis, may be the leading cause of this syndrome (Connell et al. 2003; Cvitanic et al. 2004). Symptoms are typically unilateral although degenerative signs may often be observed bilaterally. Standard radiographs may reveal either intratendinous or bursal calcifications or calcific enthesopathy, although pathologic changes are not detectable in most patients.

In the greater trochanteric pain syndrome, US has been reported as a useful and accurate means to assess pathologic changes of the gluteus medius and minimus tendons, a condition referred to as "rotator cuff tear of the hip". Most patients with tendinopathy exhibit abnormalities in the anterior and posterior portion of the gluteus medius, while an effusion inside the trochanteric bursa can be an associated finding. Signs of tendinopathy include focal swelling of the affected tendon portion and heterogeneous tendon echotexture. These changes are the same as observed in other sites of the body, such as the patellar tendon at the knee and the common extensor tendon at

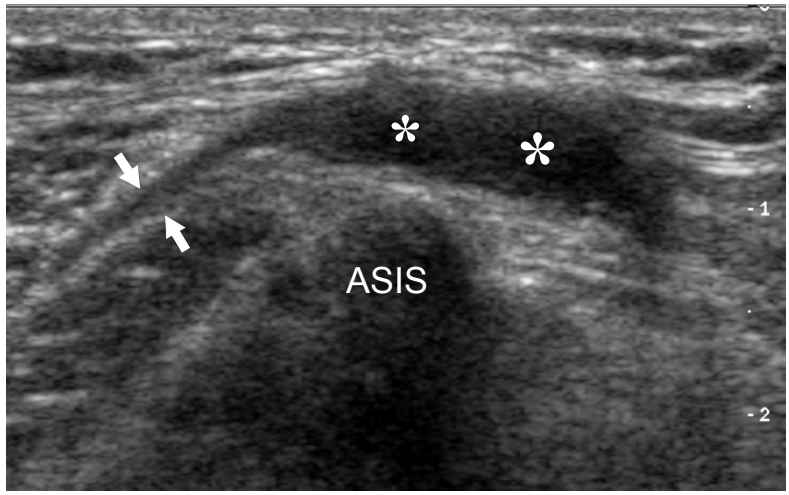

Fig. 12.42. Lateral femoral cutaneous neuropathy in a patient with chronic sensory symptoms irradiated over the anterolateral region of the thigh. Long-axis 12–5 MHz US image of the lateral femoral nerve (*arrows*) demonstrates a fusiform hypoechoic swelling (*asterisks*) of the nerve at the point where it crosses the anterior superior iliac spine (*ASIS*) below the inguinal ligament

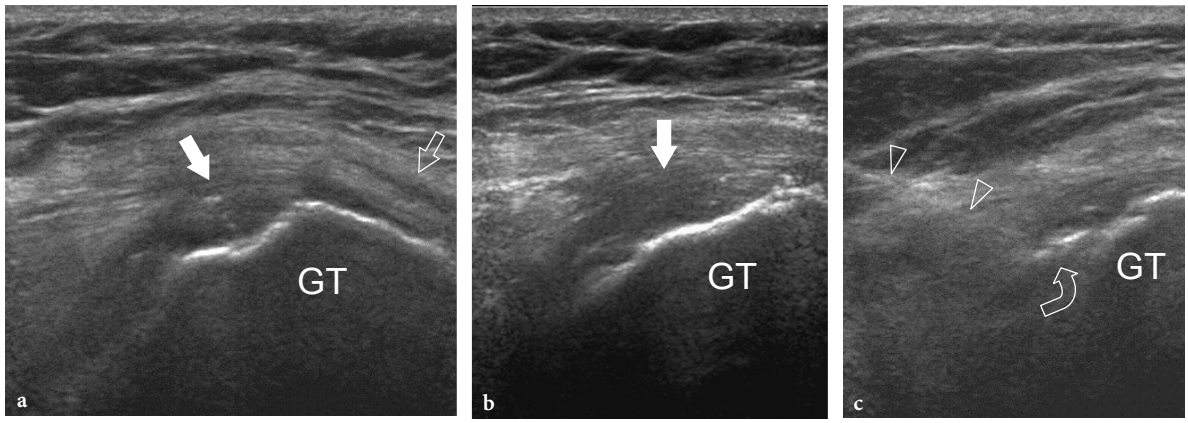

Fig. 12.43a–c. Gluteus minimus tendinopathy. **a** Long- and **b** short-axis 12–5 MHz US images reveal diffuse swelling and a heterogeneous hypoechoic appearance of the gluteus minimus tendon (*white arrow*). Observe the normal anterior tendon of the gluteus medius (*open arrow*). *GT*, greater trochanter. **c** Transverse 12–5 MHz US image obtained during US-guided steroid injection demonstrates the needle (*arrowheads*) and the injected steroids as hyperechoic spots (*curved arrow*) located at the deep aspect of the gluteus minimus tendon

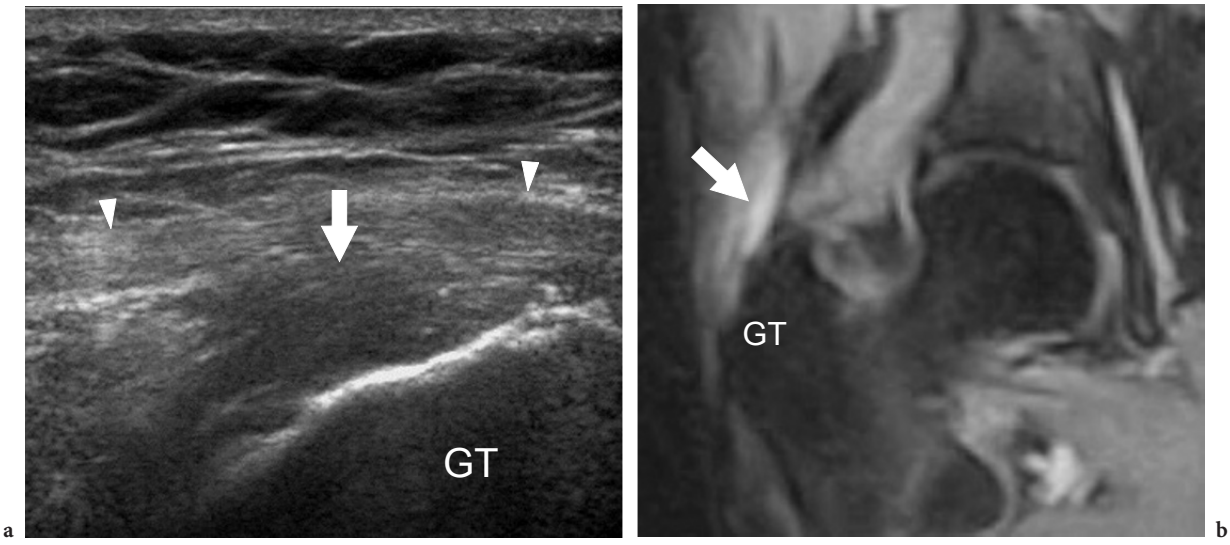

Fig. 12.44a,b. Tendinopathy of the anterior tendon of the gluteus medius. **a** Coronal 12–5 MHz US image over the greater trochanter (*GT*) shows swelling and a heterogeneous hypoechoic appearance of the anterior tendon (*arrow*) of the gluteus medius. Observe the fasciae latae (*arrowheads*), which appears slightly thickened but without signs of discontinuity. **b** Corresponding coronal fast-STIR MR image confirms the presence of a swollen and hyperintense tendon (*arrow*) owing to degenerative changes and edema. The greater trochanter (*GT*) displays normal intensity signal

the elbow, and reflect histopathologic changes with collagen degeneration and calcific metaplasia. The tendon of the gluteus minimus (Fig. 12.43), the anterior (Fig. 12.44) and posterior (Fig. 12.45) tendons of the gluteus medius can be involved alone or in association, and anterior portion of the gluteus medius being the most commonly affected whereas only a minority of patients show changes in the gluteus minimus (Connell et al. 2003). Hyperechoic spots related to calcifications may occasionally be found at the tendon insertion (Fig. 12.46). Partial-thickness tears usually involve the deep portion of the anterior gluteus medius tendon (Connell et al. 2003). In complete tears, the tendon appears retracted proximally and an echo-poor effusion related to the hematoma can be appreciated between it and the naked greater trochanter filling the trochanteric bursa (Fig. 12.47). From the pathophysiologic point of view, one could also hypothesize some analogies between abductor cuff tendinopathy and shoulder impingement

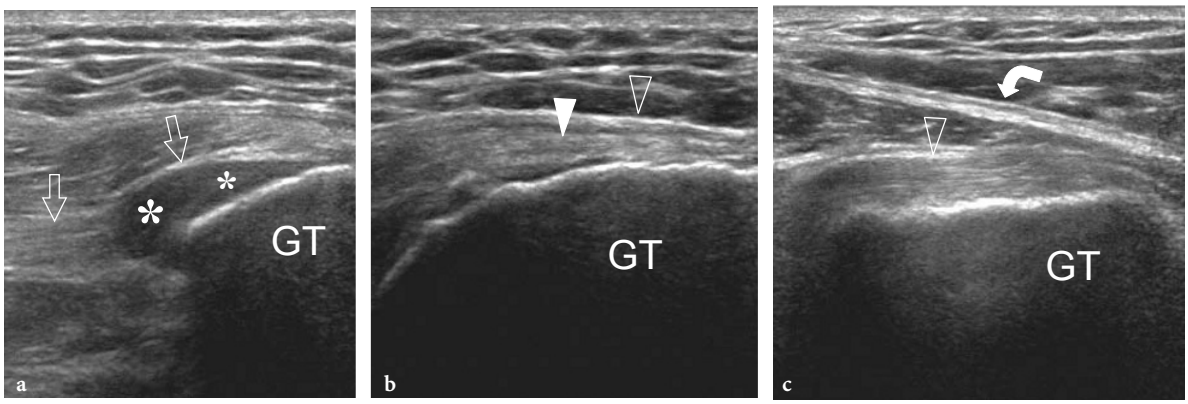

Fig. 12.45a–c. Tendinopathy of the posterior tendon of the gluteus medius. Coronal 12–5 MHz US images obtained over the posterior (**a**) and anterior (**b**) tendon of the gluteus medius and tendon of the gluteus minimus (**c**). In **a** tendinopathy appears asa swollen, hypoechoic and heterogeneous area (*asterisks*) located inside the distal part of the gluteus medius tendon (*arrows*). In **b** the anterior tendon of the gluteus medius (*white arrowhead*) presents a normal internal structure and a regular surface (*open arrowhead*). In **c** note the normal gluteus minimus tendon (*open arrowhead*) and fasciae latae (*curved arrow*). *GT*, greater trochanter

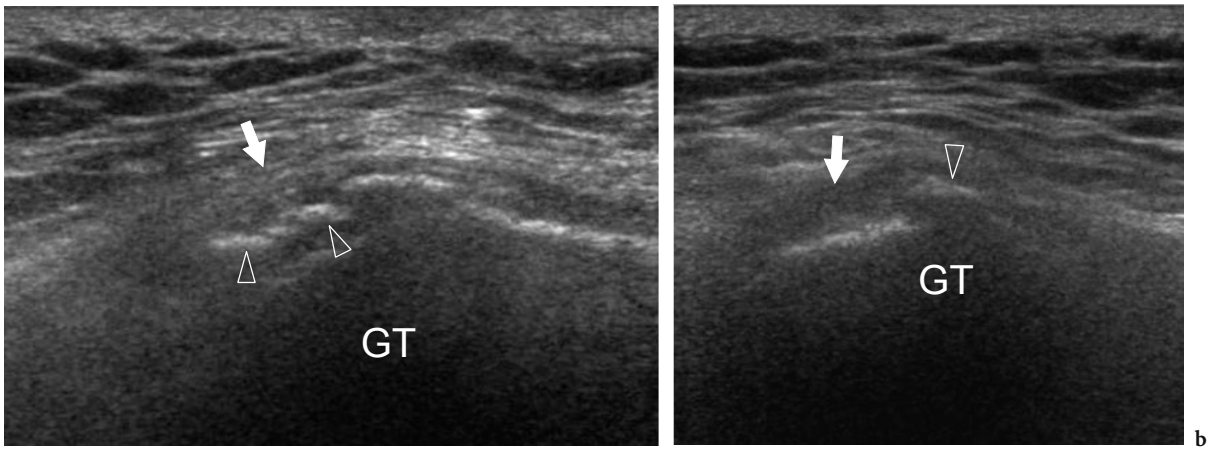

Fig. 12.46a,b. Calcific tendinopathy of the anterior tendon of the gluteus medius. **A** Coronal and **b** transverse 12–5 MHz US images demonstrate a swollen, hypoechoic and heterogeneous gluteus medius tendon (*arrow*). Intratendinous calcifications are depicted as hyperechoic spots (*arrowheads*) located within the tendon substance. *GT*, greater trochanter

syndrome by considering the attrition of the fasciae latae against the tendons of the gluteus medius and minimus and the trochanteric bursa similar to that of the acromion with the rotator cuff and the subacromial subdeltoid bursa. In hip abductor tendinopathy, US has a value in redirecting the diagnosis to tendon abnormalities rather than intra-articular disease as the cause of hip pain. When examining the gluteus medius and minimus, some difficulties can be encountered in obese patients because of an increased thickness of the subcutaneous tissue. In these cases, applying pressure with the probe on the skin or using a lower-frequency probe (5 MHz) are only partially effective. Also, due to the oblique course of the tendon insertion over the greater trochanter, careful scanning technique is needed to avoid misinterpreting artifacts related to anisotropy as focal tendinopathy or partial tears (Connell et al. 2003). Correlation with the contralateral side may be useful, particularly when the examiner has limited experience in this field. The first treatment of gluteus tendinopathy includes rest, physical therapy and local steroid injections (Fig. 12.43c). In refractory cases and avulsion injuries, surgery with debridement and tendon reattachment may be indicated.

Fluid distension of the trochanteric bursa appears as a well-circumscribed crescentic-shaped hypoechoic to anechoic collection located superficially to the posterior insertion of the gluteus medius and the lateral aspect of the greater trochan-

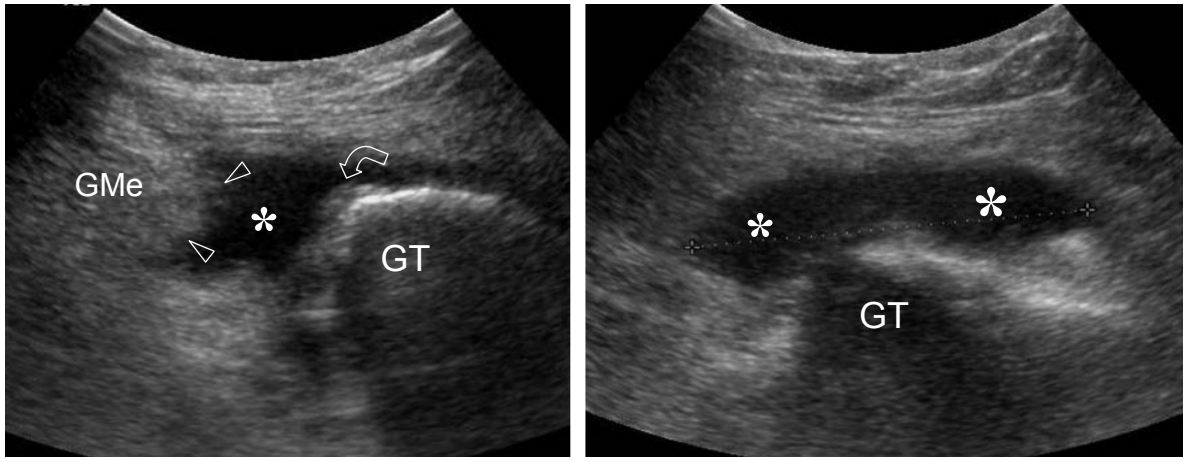

a b

Fig. 12.47a,b. Gluteus medius anterior tendon tear. **a** Coronal and **b** transverse 2–4 MHz US images reveal a complete tear of the gluteus medius tendon (*GMe*) which appears retracted proximally (*arrowheads*) from the insertion site (*curved arrow*). An anechoic effusion related to the hematoma (*asterisks*) is seen between it and the greater trochanter (*GT*), also expanding within the trochanteric bursa

ter and deep to the gluteus maximus (Fig. 12.48). Often, trochanteric bursitis is difficult to differentiate from an underlying tendinopathy and, in many instances, the two conditions can coexist (Fig. 12.49). From the pathophysiologic point of view, trochanteric bursitis could be interpreted as a true impingement syndrome (Heller 2003). When the hip abductor tendons tear, disuse atrophy of the involved muscles may lead to loss of containment of the femoral head, lateral subluxation and impingement of the greater trochanter on the fasciae latae, thus sustaining development of bursitis. Therefore, one could hypothesize detection of trochanteric bursitis with US would be an important marker of early mechanical failure of the joint and joint instability (Heller 2003). Treatment includes intrabursal injection of anesthetics and corticosteroids. US guidance can increase the efficacy of local therapy by allowing accurate insertion of the medication inside the affected bursa or near the degenerated tendon (Figs. 12.49, 12.50). For this purpose, the needle should be guided inside the bursa by approaching the greater trochanter from a posterolateral direction.

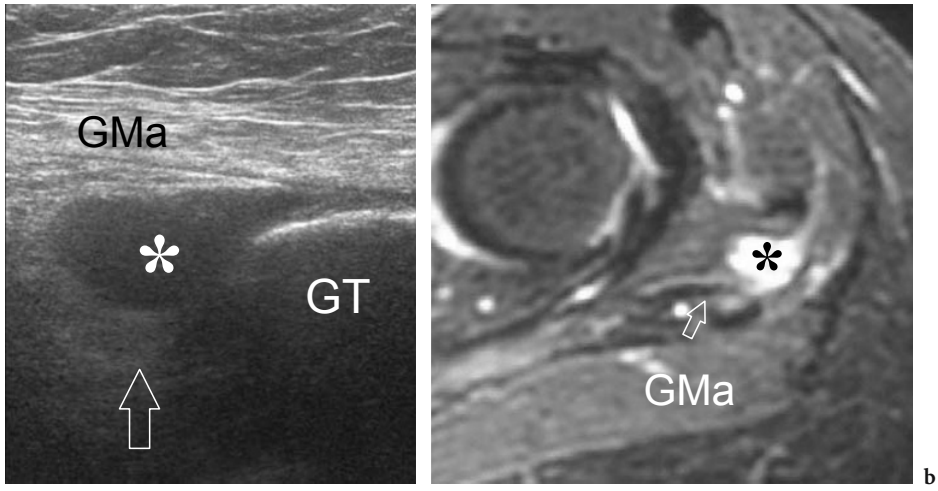

a b

Fig. 12.48a,b. Trochanteric bursitis. **a** Coronal 12–5 MHz US image shows a well-defined oval-shaped anechoic fluid collection (*asterisk*) located between the deep aspect of the gluteus maximus muscle (*GMa*), the posterosuperior aspect of the greater trochanter (*GT*) and the lateral aspect of the gluteus medius tendon (*void arrow*). **b** Transverse fast-STIR MR image confirms fluid distension of the bursa consistent with trochanteric bursitis.

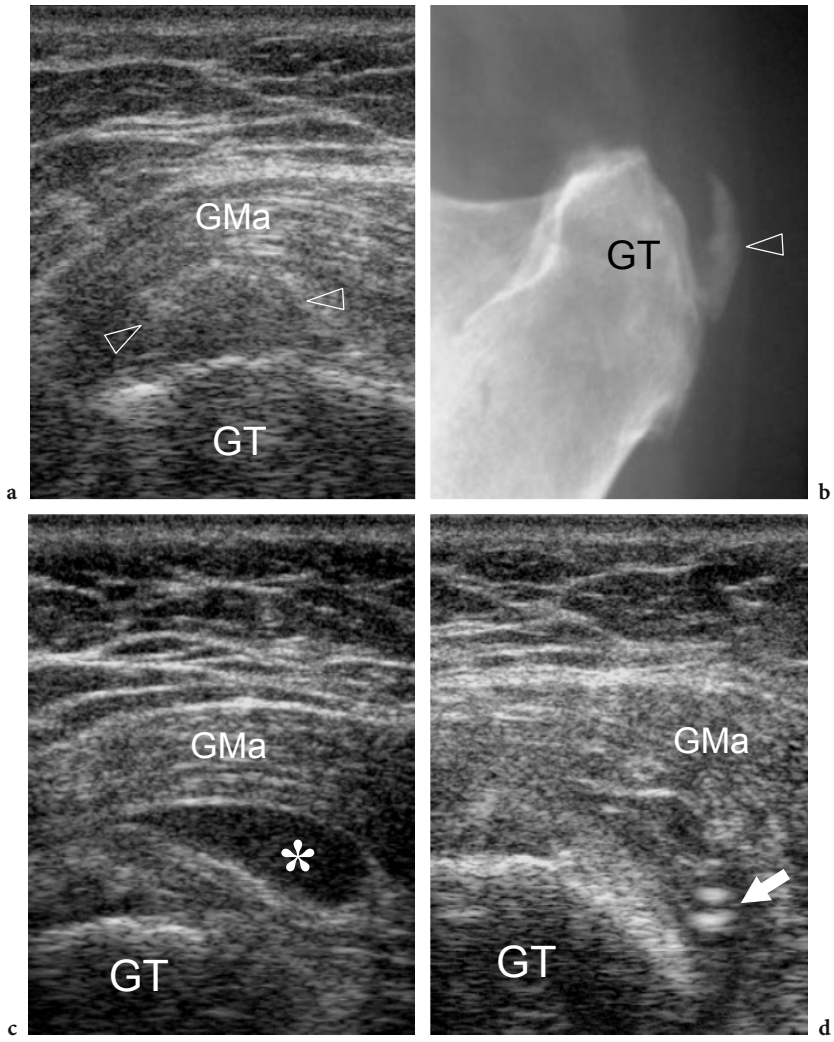

Fig. 12.49a–d. Trochanteric bursitis. **a** Transverse 12–5 MHz US image obtained over the greater trochanter (*GT*) shows an irregular calcification (*arrowheads*) with faint posterior acoustic shadowing located within the gluteus medius tendon and deep to the gluteus maximus muscle (*GMa*). **b** Anteroposterior radiograph confirms the occurrence of an arc-shaped calcification (*arrowhead*) over the greater trochanter (*GT*). **c** Transverse 12–5 MHz US image obtained in a more posterior position relative to **a** demonstrates distension of the trochanteric bursa by anechoic fluid (*asterisk*). **d** Same scanning plane shown in **c** during US-guided injection of corticosteroid. Note the reverberations of the needle tip (*arrow*) positioned at the center of the bursa under US guidance.

12.5.2.2 Snapping Iliotibial Band

At the lateral aspect of the hip, extra-articular snapping hip can be secondary to intermittent impingement of the posterior border of the fasciae latae or the anterior portion of the gluteus maximus over the osseous prominence of the greater trochanter. The clinical appearance is nearly similar to that already described for the snapping iliopsoas tendon but with the patient referring symptoms over the lateral aspect of the hip. This condition can be painful or completely asymptomatic. US can detect echotextural abnormalities of the fasciae latae, which may appear thickened and hypoechoic (Choi et al. 2002). Dynamic US scanning can easily disclose the abrupt, sudden displacement of the fasciae latae which mostly occurs when the adducted and extended hip is flexed or when the adducted and internally rotated hip is flexed and externally rotated with the knee bent (Choi et al. 2002). The patient should be placed in a lateral position with the contralateral hip lying on the examination table. In many cases, however, the patient is able to reproduce the hip snap only

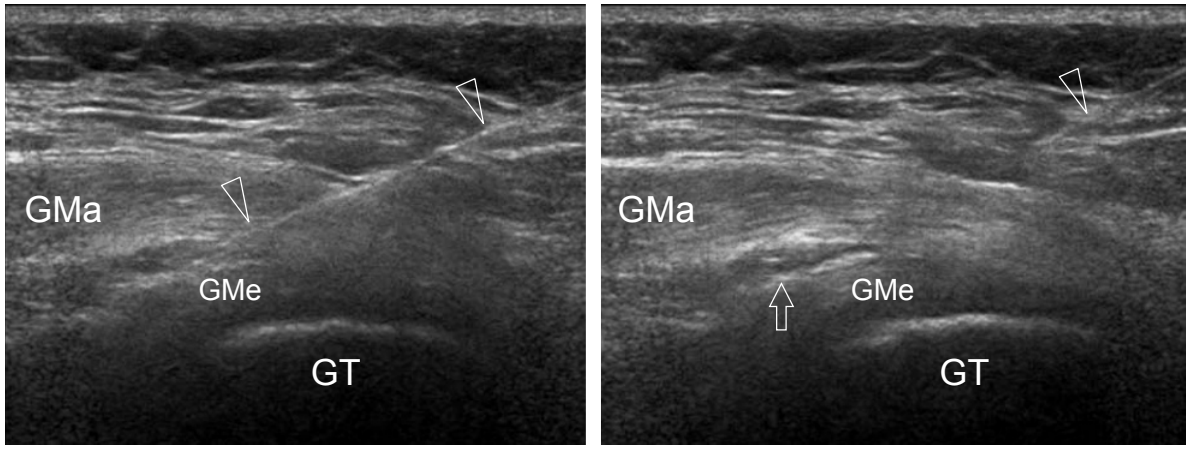

a b

Fig. 12.50a,b. US-guided injection of corticosteroid within the trochanteric bursa in a patient with tendinopathy of the anterior tendon of the gluteus medius. **a** Coronal 12–5 MHz US image showing positioning of the needle (*arrowheads*) between the gluteus maximus (*GMa*) and the gluteus medius (*GMe*). **b** After injection and withdrawal of the needle (*arrowhead*), the trochanteric bursa (*arrow*) appears distended with fluid. *GT*, greater tuberosity

when standing up. Transverse US images obtained over the lateral aspect of the greater trochanter are the most useful to depict this condition (Fig. 12.51) (Pelsser et al. 2001). Only slight pressure with the probe should be applied on the skin so as not to hinder the passage of the iliotibial band over the bone. Typically, the snap can be felt through the transducer by the examiner.

12.5.2.3 Morel-Lavallée Lesion

Morel-Lavallée lesion is a post-traumatic seroma which most commonly develops along the trochanteric region and the proximal thigh between the deep layer of the subcutaneous tissue and the fascia (Morel-Lavallée 1863). This lesion results from an injury with a shear strain mechanism causing a hemorrhage of the rich vascular plexus that pierces the fasciae latae. The extravasion of blood spreads along the perifascial plane dissecting the fat lobules of the subcutaneous tissue (Mellado et al. 2004). In longstanding lesions, a reactive pseudocapsule may develop around the collection and the process of organization of blood and debris may cause a heterogeneous appearance of the hematoma that may lead to a misdiagnosis of soft-tissue tumor. In chronic cases, the diagnosis can be difficult due to the slow growth rate of the mass, the local pain and the patient who does not relate the mass to a previous trauma. US depicts Morel-Lavallée lesion as a well-defined hypoanechoic collection located just superficial to the linear echogenic deep fascia (Parra et al. 1997; Mellado et al. 2004). An internal fluid-fluid level can occasionally be appreciated due to sedimentation of the cellular components of blood (Fig. 12.52) (Parra et al. 1997). Hyperechoic mural nodules and septations arising from dissection of fatty tissue by fluid can be demonstrated as well. An accurate scanning technique is required to detect Morel-Lavallée lesion with US. In fact, in acute lesions without a pseudocapsule, excessive pressure applied with the probe can squeeze the effusion away from the field-of-view of the transducer. When a Morel-Lavallée lesion is suspected on clinical grounds, a large amount of gel and extended field-of-view techniques are best used to accurately depict the full extent of the hematoma. US-guided aspiration of fluid followed by local compression helps to prevent local recurrence.

12.5.3 Posterior Hip Pathology

Soft-tissue disorders arising from the posterior hip essentially include traumatic injury at the insertion of the hamstring muscles, sciatic neuropathies and ischiogluteal bursitis. The coexisting involvement of the hamstrings' insertion at the ischium and the adjacent sciatic nerve is a common condition observed in athletes who present with pain near the ischial tuberosity. It is commonly referred to as

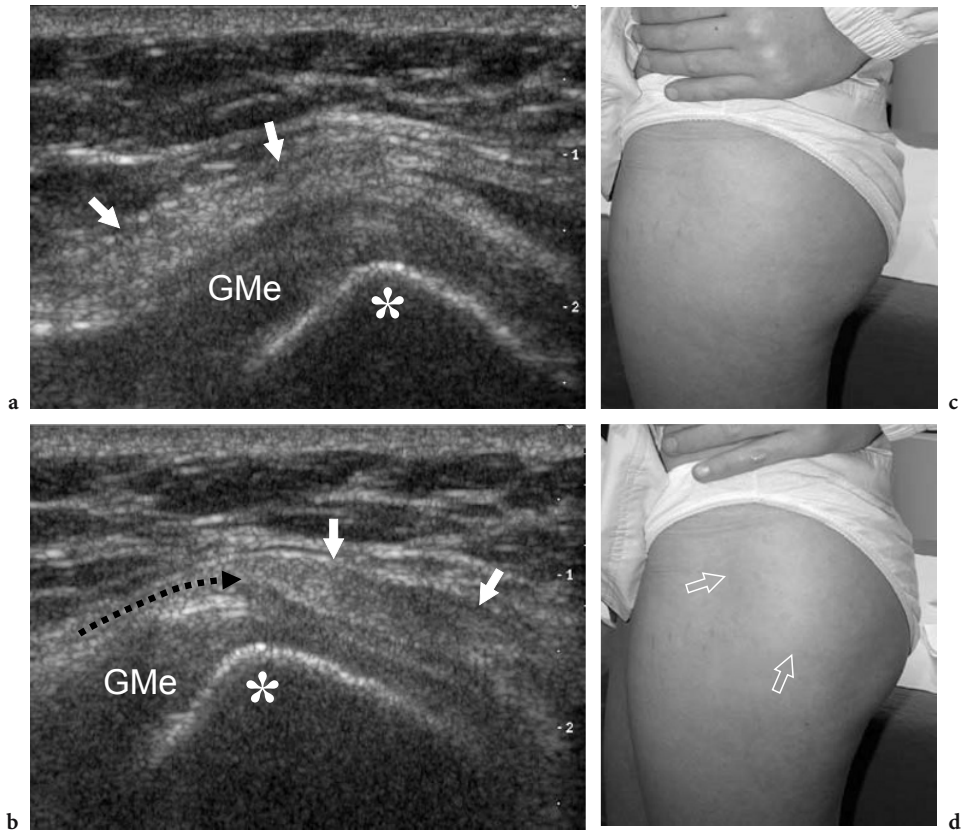

Fig. 12.51a–d. Snapping iliotibial band in a girl with bilateral clicking and a lump in the lateral hip visible during maximal hip extension and adduction. **a,b** Transverse 12–5 MHz US images obtained over the greater trochanter with the patient standing **a** in neutral position and **b** during maximal extension and adduction of the hip with **c,d** photographic correlation. **a** In neutral position, the fasciae latae (*white arrows*) lies anterior to the greater trochanter (*asterisk*). **b** When the hip is maximally extended, the iliotibial band abruptly jerks posterior to the greater trochanter. Dynamic scanning depicts this abnormal shifting movement (*dashed arrow*). Note that the fasciae latae is thicker than in normal conditions. *GMe*, gluteus medius tendon

the "hamstrings syndrome" and characterized by pain radiated down the posterior thigh or popliteal region and exacerbated by any activity that stretches the hamstrings.

12.5.3.1 Hamstrings Tendinopathy

Hamstrings tendons can be injured following chronic microtrauma or a single acute injury. In the former case, the proximal attachment of these muscles appears swollen and hypoechoic reflecting changes related to tendinopathy (Fig. 12.53). This pattern is similar to other overuse tendinopathies. Calcifications can be detected at the tendon insertion as irregular hyperechoic foci into the ischial tuberosity indicating a calcific enthesopathy. On the other hand, acute injuries are almost invariably the consequence of sport accidents in which a forceful extension of the leg against resistance, typically observed in basketball players, sprinters or soccer players, or an excessive lengthening, such as occurs in waterskiing, results in powerful stretching of the ischial insertion of the hamstrings tendons leading to their rupture or avulsion (Blasier and Morawa 1990). The proximal insertion of the long head of the biceps femoris and the semitendinosus is more commonly involved than that of the semimembranosus (Slavotinek et al. 2002). Patients complain of pain in the buttock area and inability to walk. In nondisplaced avulsions or partial tendon tears, conservative therapy with rest and restricted activity is the treatment of choice. When a displaced ischial avulsion takes place with detachment of a fragment of bone, fibrous union or heterotopic bone formation may occur resulting in functional disability. In these cases, surgery may be an option.

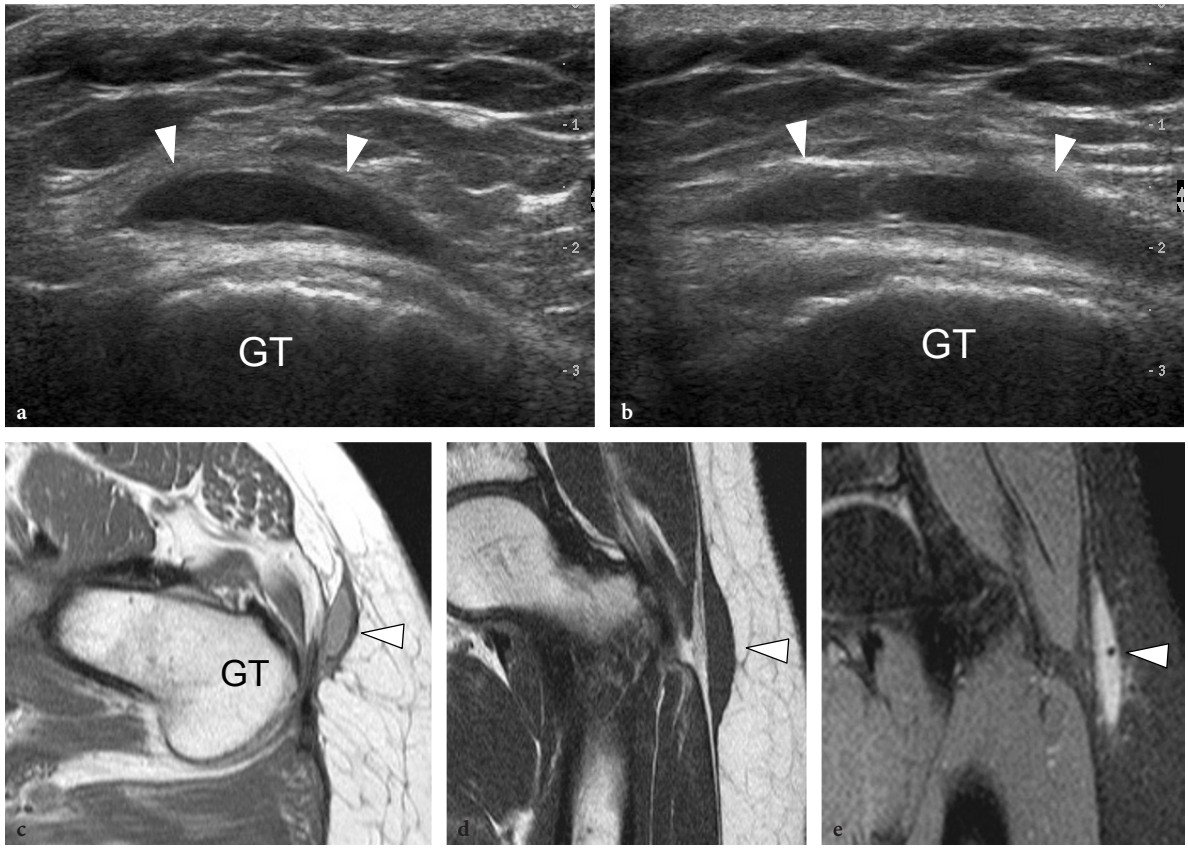

Fig. 12.52a-e. Morel-Lavallée lesion. **a** Transverse and **b** coronal 12–5 MHz US images in patient with a previous contusion trauma at the lateral aspect of the hip show a large fluid collection (*arrowheads*) with thickened walls at the level of the superficial fascia, just lateral to the fasciae latae. *GT*, greater trochanter. **c** Transverse proton density, **d** coronal T1-weighted and **e** coronal fast-STIR MR images confirm the US findings. Observe the intermediate (**c**), low (**d**) and high (**e**) signal intensity of the serous collection (*arrowhead*) in the different MR sequences used, which can be referred to a chronic stage of the hematoma

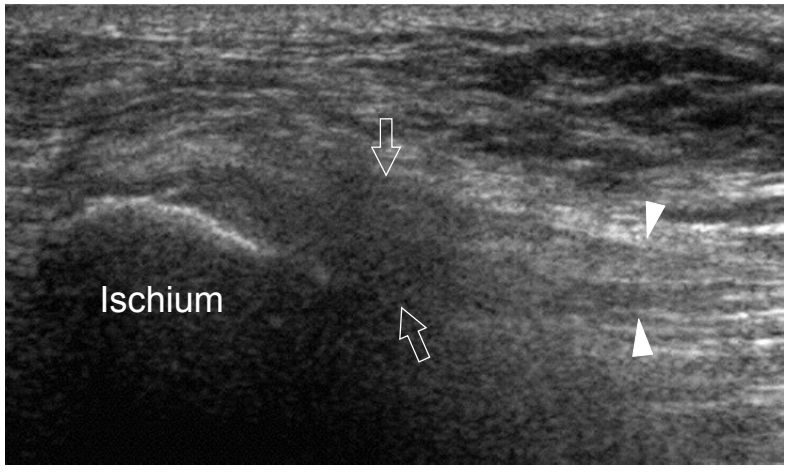

Fig. 12.53. Ischiocrural tendinopathy. Long-axis 12–5 MHz US image obtained over the insertion of the ischiocrural tendons on the ischial tuberosity reveals proximal swelling and hypoechoic changes of these tendons reflecting insertional tendinopathy (*arrows*). On a more distal level, these tendons (*arrowheads*) appear normal

US assessment of proximal hamstrings lesion can be difficult in cases of hypertrophied thighs because the insertion point is located deeply and the soft-tissues of the buttock may have a substantial thickness. In addition, any pressure exerted with the transducer in an attempt to reduce the distance between the affected tendons and the skin can be painful in acute phases. In complete tendon tears, US can demonstrate the discontinuity of the affected tendon, which appears retracted downward and surrounded by local hematoma, whereas the adjacent nonaffected tendon can be seen inserting normally into the hyperechoic cortex (Fig. 12.54). Partial tears can be more difficult to assess and differentiate from focal tendinopathy. In general, they extend more distally downward to reach the myotendinous junction (Fig. 12.55). In doubtful cases, we believe MR imaging can be helpful to delineate the size of the rupture with accuracy, and especially in young high-level sportsmen who are potential candidates for surgical treatment (Slavotinek et al. 2002). Most cases can be managed with rest, anti-inflammatory drugs and steroid injections followed by mobilization. In the event of a coexistent irritation of the adjacent sciatic nerve, tenderness over the ischial tuberosity is more manifest on clinical grounds and the Tinel sign in that region may reproduce the sciatic distribution of pain (Fig. 12.56). Depending on the severity of trauma, the sciatic nerve may appear normal or may be surrounded by hypoechoic fluid related to hematoma. In chronic phases, scarring with encasement of the nerve may

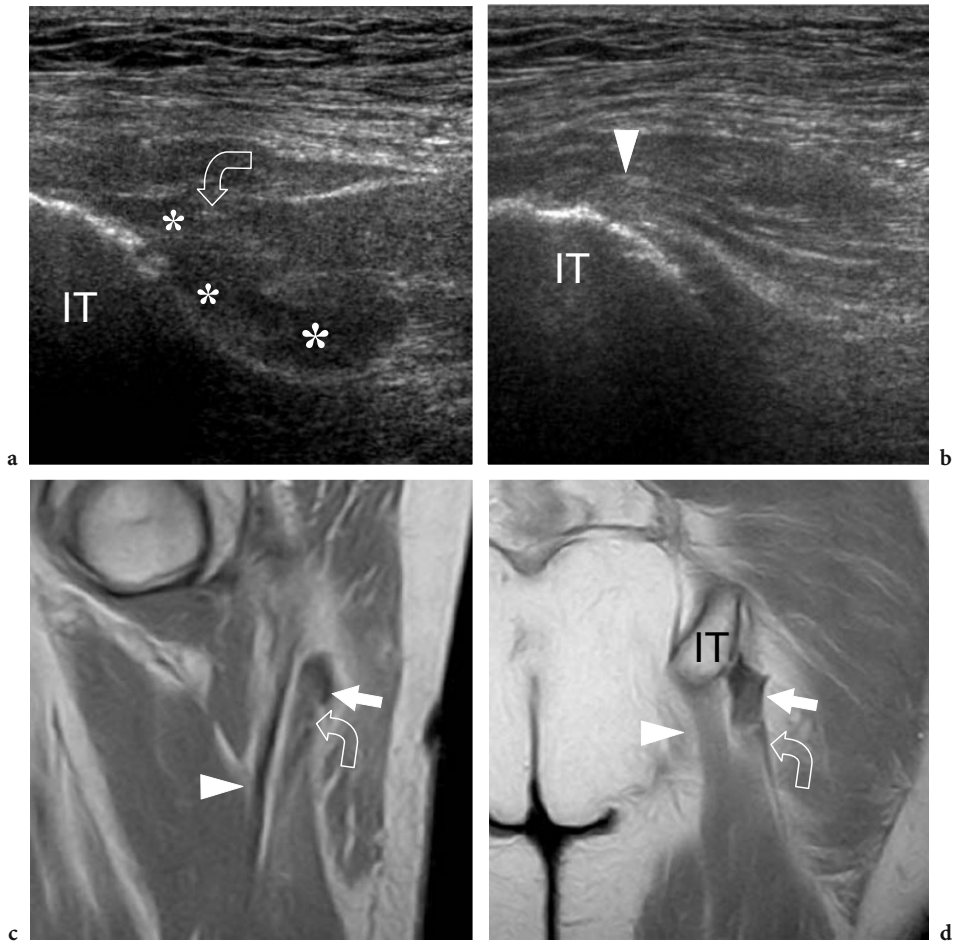

Fig. 12.54a–d. Avulsion tear of the semitendinosus-biceps tendon. **a,b** Long-axis 12–5 MHz US images over **a** the conjoined semitendinosus-biceps tendon and **b** the semimembranosus tendon. While the conjoined tendon (*curved arrow*) is avulsed from its insertion on the ischial tuberosity (*IT*) and appears surrounded by hypoechoic hematoma (*asterisks*), the semimembranosus tendon (*arrowhead*) appears intact. **c,d** Coronal Gd-enhanced T1-weighted MR images confirm the complete tear of the semitendinosus-biceps tendon complex (*curved arrow*) and the hematoma (*straight arrow*) which separates it from the ischial tuberosity (*IT*). In both MR images, note the normal-appearing semimembranosus tendon (*arrowhead*)

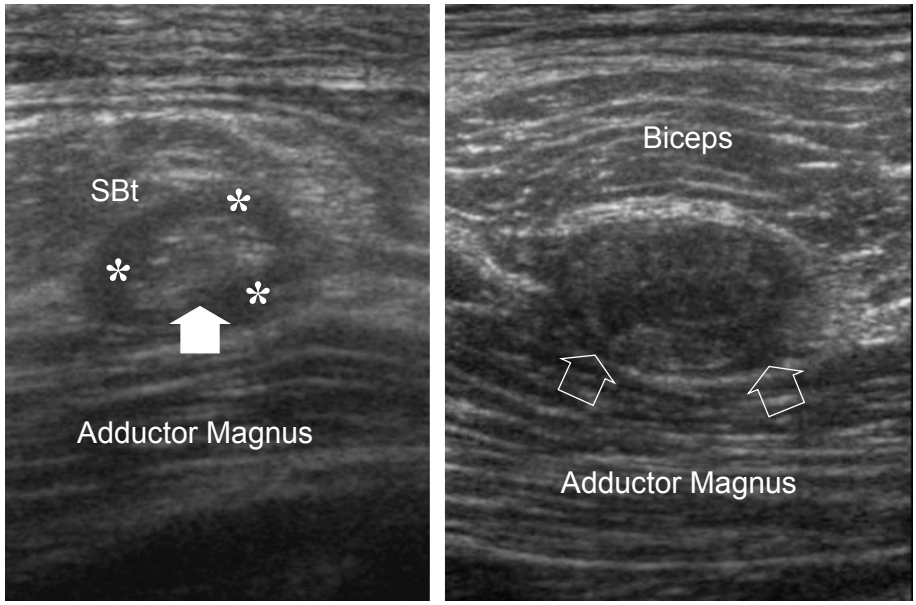

a b

Fig. 12.55a,b. Partial tears of the semimembranosus tendon. Spectrum of US findings in two different patients with **a** acute and **b** chronic trauma. **a** Transverse 12–5 MHz US image over the posterior hip demonstrates a thickened semimembranosus tendon (*arrow*) surrounded by anechoic effusion (*asterisks*), adjacent to the semitendinosus-biceps tendon (*SBt*). **b** Transverse 12–5 MHz US image over the posterior hip reveals a markedly hypoechoic and heterogeneous tendon (*arrows*)

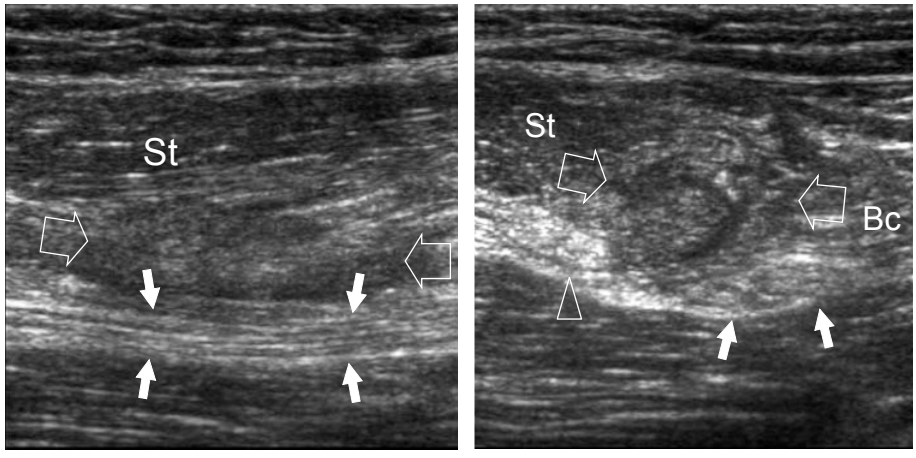

a b

Fig. 12.56a,b. Hamstrings syndrome. **a** Long- and **b** short-axis 12–5 MHz US images obtained over the posterior hip in a patient with ischiocrural tendon tear associated with the acute onset of symptoms resembling sciatica. The close relationship between the injured conjoined tendon (*open arrows*) of the semitendinosus (*St*) and biceps (*Bc*) and the sciatic nerve (*white arrows*) is responsible for symptoms related to nerve irritation. Observe the normal semimembranosus tendon (*arrowhead*)

occur. In these instances, surgical debridement and release of the nerve is necessary.

12.5.3.2 Sciatic Neuropathy

Distally to the sciatic notch, most sciatic nerve lesions arise from significant trauma, such as fracture dislocations of the hip joint, and as a complication of hip replacement procedures. Other causes include prolonged periods of immobilization in bed, scarring in the region of the ischial tuberosity in the hamstrings syndrome when exuberant callus formation occurs during healing or when an avulsed bone fragment directly impinges on the nerve, space-occupying masses and the piriformis syndrome. From the clinical point of view, a complete lesion of the sciatic nerve

leads to palsy of the hamstrings muscles and of all the muscles below the knee with sensory loss in the cutaneous distribution of the peroneal and tibial nerves. In general, the lateral trunk of the sciatic nerve is more commonly involved leading to the onset of a false common peroneal neuropathy. In patients with total hip arthroplasty, lengthening of the leg by >4 cm, dislocation of the hip during the surgical intervention, local hemorrhage and direct injuries by a retractor may be implicated as the cause of nerve injury. Clinical findings include posterior hip pain irradiated downstream in the thigh and impairment of walking ability. In these cases, US may help to reveal focal nerve abnormalities and compression by scar tissue and hematoma (Fig. 12.57). The examiner should, however, be aware of the low sensitivity of US for detecting subtle lesions in this deep area, especially in obese patients, and for revealing more proximal abnormalities at the level of the piriformis muscle and the sciatic foramen. In particular, the piriformis syndrome, a rare cause of lower back pain and sciatica secondary to sciatic nerve entrapment at the greater sciatic notch, cannot be revealed with US due to the deep course of the nerve underneath the gluteus muscles. Similarly, the increased size and the occurrence of possible anomalies of the piriformis muscle cannot be reliably identified with US. For this purpose, MR imaging is superior to correctly diagnose piriformis syndrome and differentiate it from other possible causes of lower lumbar pain (Lee et al. 2004).

12.5.3.3 Ischiogluteal Bursitis

Fluid distention of the ischiogluteal bursa, a condition also known as "weaver's bottom", is mainly encountered in neoplastic patients affected by cachexia and severe weight loss. It is assumed that reduction in the thickness of subcutaneous fat in the buttock region may result in repetitive minor trauma on the bursa causing its inflammation and fluid distention (van Mieghem et al. 2004). Clinically, ischiogluteal bursitis presents with pain over the midline of the buttock irradiating along the hamstrings and possibly mimicking other diseases, such as lumbar disk herniation and piriformis syndrome. US may be helpful to identify this condition.

12.5.4 Joint and Bone Disorders

Differentiation of hip joint disorders from paraarticular pathologies is of the utmost importance because their treatment and prognosis are different. While advanced inflammatory states and degenerative conditions limit joint motion and are readily evident on standard radiographs, therapy is more effective if started early, before the occurrence of advanced joint damage. In general, physical examination of patients with disorders affecting the hip joint is characterized by stiffness and local pain–

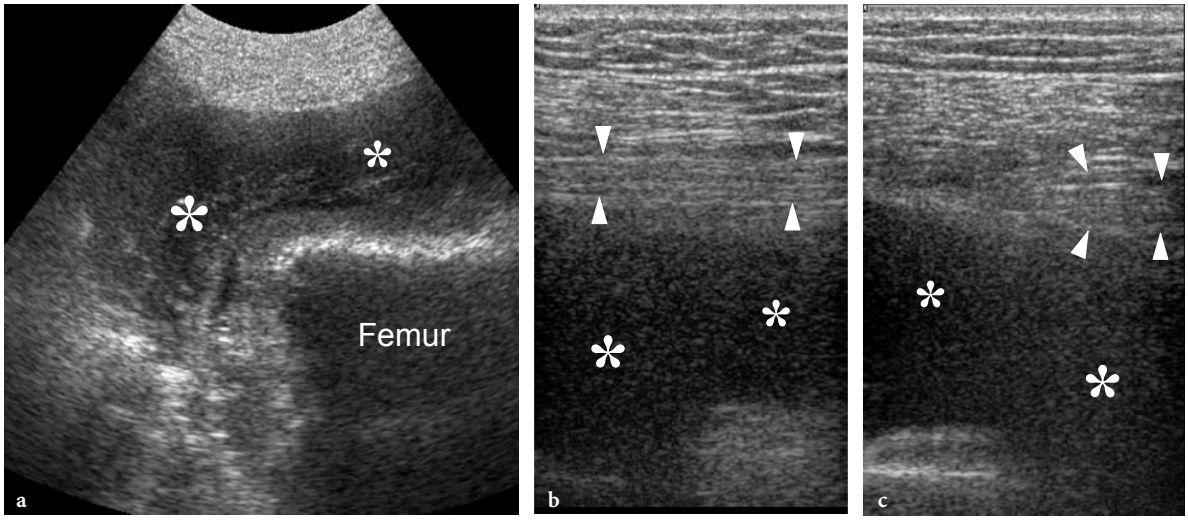

Fig. 12.57a–c. Postoperative sciatic neuropathy following total hip replacement. **a** Sagittal 2–4 MHz US image over the posterior hip demonstrates a large partially organizing hematoma (*asterisks*) following the procedure of hip replacement. **b** Long- and **c** short-axis 12–5 MHz US images of the sciatic nerve demonstrate a displaced and stretched nerve (*arrowheads*) over the blood collection (*asterisks*)

nonspecific symptoms which may be difficult to distinguish from those of tendinopathy.

12.5.4.1 Joint Effusions in Adult Hips

Demonstration of an intra-articular effusion is definite proof of a joint disorder. US plays an important role in detecting intra-articular effusion of the hip because distension of the joint cannot be palpated due to its deep position. As discussed before, the best imaging planes for this purpose are those obtained longitudinally over the anterior femoral neck (Fig. 12.12) (Zieger et al. 1987). Similar to the situation in other joints, an articular effusion appears as a hypoanechoic collection which shows variable echogenicity depending on the nature of the fluid content (serous, bloody, infectious). An increased thickness (≥7 mm) of the anterior joint capsule and asymmetric (≥1 mm) distension of the recess compared with the opposite side indicate hip effusion (Koski et al. 1989). Nevertheless, a recent prospective study on the effectiveness of US in the detection of hip effusions in both native and postoperative adult hips using arthrocentesis as a gold standard revealed that anterior recess distension as seen on US is not an accurate sign of hip effusion in adults (Weybright et al. 2003). In this study, fluid was found to be present with an anterior distension of only 5 mm or absent for distension >10 mm (Weybright et al. 2003). An explanation for this finding is that hypertrophied synovium appears hypoechoic and may distend the anterior recess in the absence of joint effusion (Fig. 12.58). Theoretically, color and power Doppler imaging might be helpful to distinguish synovium from fluid. In a recent paper, a significant correlation between synovial membrane thickness and power Doppler US signal has been reported (Walther et al. 2002). In addition, these authors found a significantly higher power Doppler US signal in patients with rheumatoid arthritis compared with the signal in patients with osteoarthritis (Walther et al. 2002). Synovitis, however, does not always exhibit a hypervascular pattern and, at least in patients with large body habitus, the anterior recess may be located too deep to achieve good sensitivity in the detection of flow signals. On the other hand, complicated hip joint effusions in the anterior recess may mimic hypoechoic synovium. Identification of even minimal scattered blood flow signals would suggest synovitis in these cases (Weybright et al. 2003). Using a posterior approach, spectral Doppler, color Doppler imaging and, more recently, contrast-enhanced color Doppler US seem to be promising in the diagnosis of active sacroiliitis and follow-up after treatment (Arslan et al. 1999; Klauser et al. 2005). US can also guide sacroiliac joint injections in patients with sacroiliitis (Pekkafali et al. 2003)

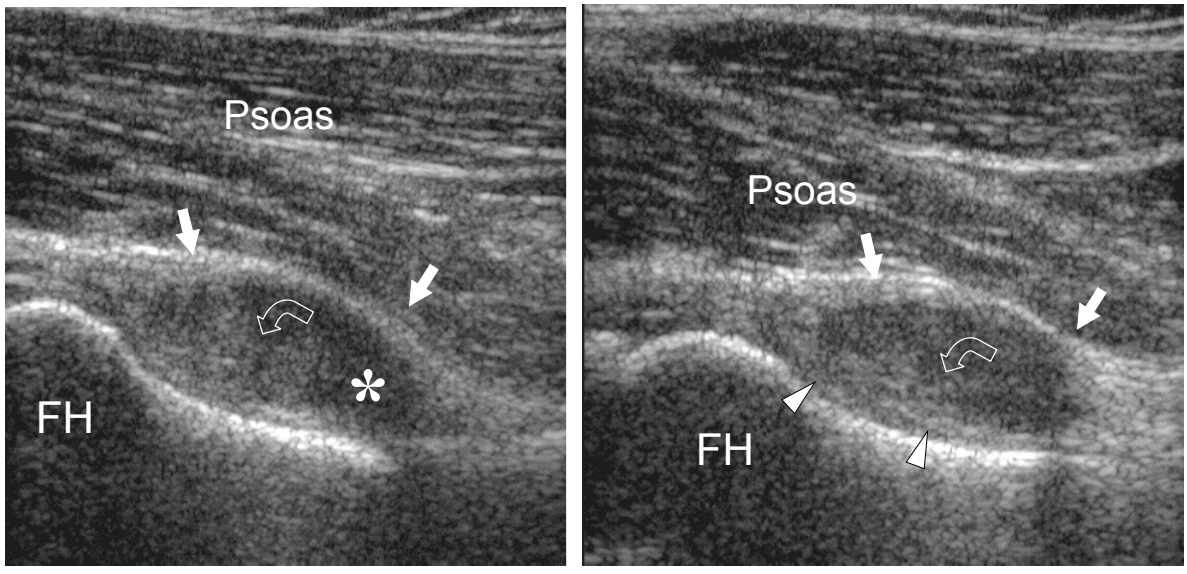

a b

Fig. 12.58a,b. Intra-articular synovial hypertrophy in a patient with rheumatoid arthritis. **a,b** Transverse oblique 12–5 MHz US images over the anterior femoral neck reveal distension of the anterior recess by hypoechoic fluid (*asterisks*) and echogenic pannus (*curved arrow*) leading to bulging of the capsular plane (*straight arrows*). Observe the anterior (*straight arrows*) and posterior (*arrowheads*) capsule. *FH*, femoral head

12.5.4.2 Synovitis and Arthropathies

In hip joint synovitis, hypertrophy of the synovial membrane can be demonstrated by presence of solid tissue or hyperechoic folds projecting inside the articular cavity filled by fluid. Although US can demonstrate marginal erosions located at the interface between bone and the articular cartilage which covers the femoral head and neck, standard radiographs, CT and MR imaging are more effective diagnostic modalities for this purpose. This can be explained by the inability of US to investigate the overall articular surface due to the posterior acoustic shadowing produced by the acetabular cover. Degenerative osteoarthritis is one of the most common hip disorders and is diagnosed on the basis of standard radiographs. US can demonstrate anterior osteophytes as hyperechoic projections arising from the junction between the head and the neck of the femur, but this technique does not have an important role in the diagnostic investigations (Figs. 12.59, 12.60). Intra-articular loose bodies can be demonstrated with US as well and should be differentiated from femoral osteophytes. The hip is one of the joints more frequently affected

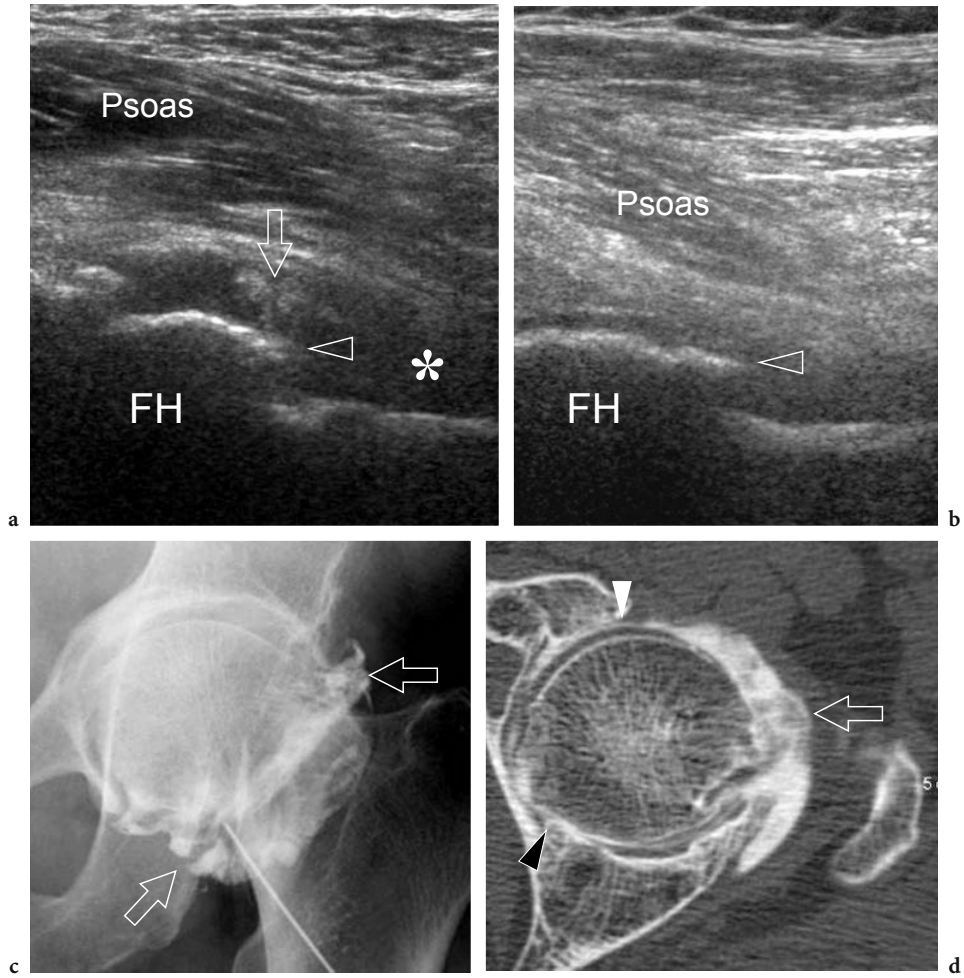

Fig. 12.59a-d. Intra-articular synovial hypertrophy in a woman with posterior osteoarthritis of the left hip. **a,b** Transverse oblique 12–5 MHz US images over the anterior hip show a fluid effusion (*asterisk*) filling the anterior synovial recess. Synovium hypertrophy (*arrow*) can be appreciated as echogenic folds projecting into the joint cavity. Note the anterior osteophytes (*arrowhead*) appearing as pointed hyperechoic projections lbetween the head (*FH*) and neck of the femur. **c** Arthrographic anteroposterior image displays contrast dye filling the synovial cavity. Multiple filling defects (*open arrows*) are due to the hypertrophied synovial folds developing inside the joint cavity. **d** Transverse CT-arthrographic image confirms the presence of hypertrophied synovium (*arrow*) within the joint. Note that the anterior cartilage of the femoral head is normal (*white arrowhead*), in contrast to the posteromedial cartilage (*black arrowhead*) which appears markedly thinned

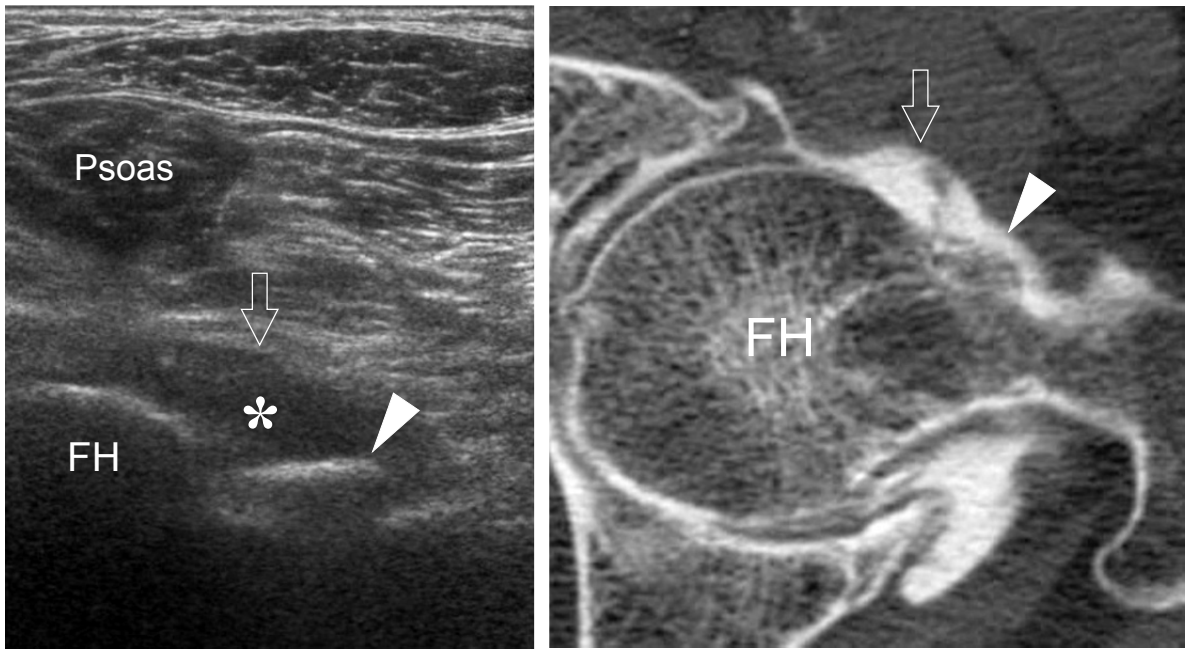

a b

Fig. 12.60a,b. Marginal femoral osteophytes. **a** Transverse oblique 12–5 MHz US image over the anterior hip reveals a fluid effusion (*asterisk*) in the anterior recess of the hip joint causing bulging of the anterior capsule (*arrow*). An anterior osteophyte (*arrowhead*) appears as a well-defined hyperechoic prominence with posterior acoustic shadowing located at the junction of the femoral head (*FH*) and neck. **b** Corresponding transverse oblique CT-arthrographic image confirms the presence of the femoral osteophyte (*arrowhead*)

by amyloid deposition disease. US can detect intra-articular amyloid infiltration (Fig. 12.61). The infiltrated synovium appears thickened and hypoechoic and can completely fill the joint space. Although these features are nonspecific for amyloidosis, in the proper clinical setting, such as in longstanding renal insufficiency or multiple myeloma, they are highly suggestive of this condition.

12.5.4.3 Prosthetic Hip Replacement

The most common complications of total hip replacement are aseptic resorption of bone with subsequent mechanical loosening and infection. Both conditions are associated with an effusion located inside the pseudocapsule of the joint. US can detect fluid collections as hypoanechoic areas with irregular borders located anteriorly to the femoral prosthetic neck on transverse oblique images (Fig. 12.62) (Foldes et al. 1992, 1995). A distension of the pseudocapsule of greater than 3.2 mm at the native lateral femoral neck has been indicated as an indicator of infection (Fig. 12.63) (van Holsbeeck et al. 1994). Nevertheless, a more recent study questioned the performance of US in the field (Weybright et al. 2003). One clear advantage of this technique is demonstration of para-articular collections which do not communicate with the prosthetic cavity. These collections cannot be diagnosed at arthrography. On the other hand, CT or MR imaging are not adequate in these patients because of metallic artifacts caused by the implanted material. In doubtful cases, US-guided aspiration of the collection can be performed (Weybright et al. 2003).

An uncommon and often unrecognized complication of total hip replacement is damage to the para-articular tendons (Fig. 12.64) (Lequesne et al. 1991). In this field, the anterior impingement of the iliopsoas can be secondary to chronic friction of the posterior aspect of the iliopsoas against the acetabular cup of the prosthesis. This most often occurs in spiral screwed cup models (Fig. 12.65a–c). The impingement more likely occurs in cases of anterior protrusion of the cup that can be secondary to its excessive anteversion or excessive size (Figs. 12.65d–f, 12.66). As a result of local repetitive friction and mechanical rubbing, an inflammatory reaction and effusion in the bursa can be appreciated. In addition, partial tears, fraying and blood infiltration of the deep portion of the iliopsoas muscle and tendon have been

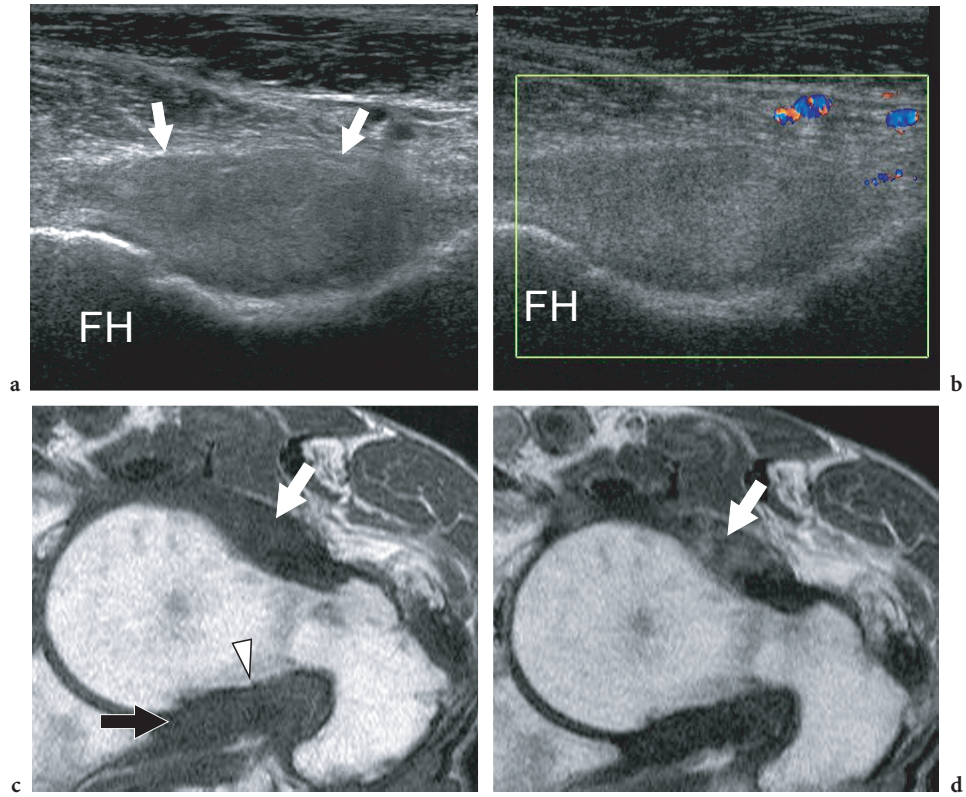

Fig. 12.61a-d. Intra-articular amyloidosis. **a,b** Transverse oblique **a** gray-scale and **b** color Doppler 12–5 MHz US images over the anterior hip show the anterior joint recess (*arrows*) filled with solid hypoechoic material. Note that this material does not exhibit a discrete internal vasculature. **c,d** Transverse oblique T1-weighted MR images obtained **c** before and **d** after intravenous injection of gadolinium. Images confirm the presence of hypointense material within the anterior (*white arrow*) and posterior (*black arrow*) recesses. Subtle erosions (*arrowhead*) can be seen on the posterior femoral neck. After contrast administration, weak irregular enhancement is evident within the anterior recess (*arrow*)

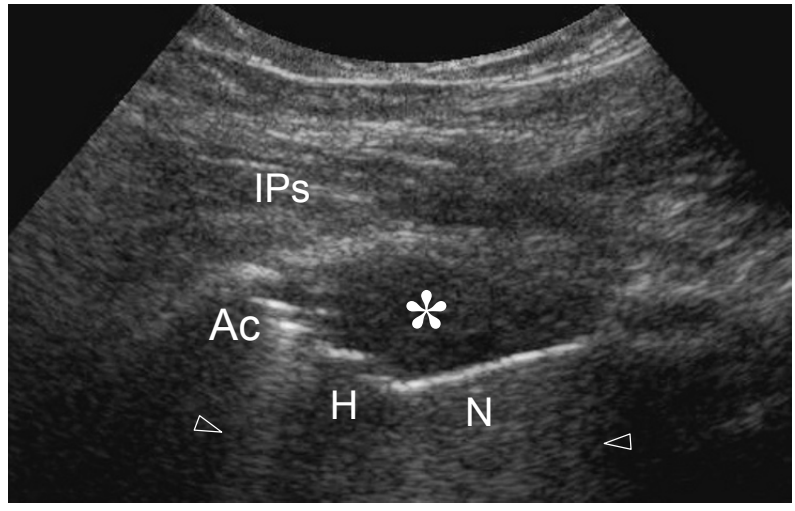

Fig. 12.62. Total hip replacement. Longitudinal oblique 12–5 MHz US image obtained over the anterior aspect of the hip joint in a patient with a hip prosthesis. The prosthetic components are well depicted with US, including the acetabular part (*Ac*), the head (*H*) and the neck (*N*). Posterior reverberation artifacts are manifest (*arrowheads*). A discrete amount of fluid (*asterisk*) distends the anterior recess of the pseudocapsule. *IPs*, iliopsoas muscle

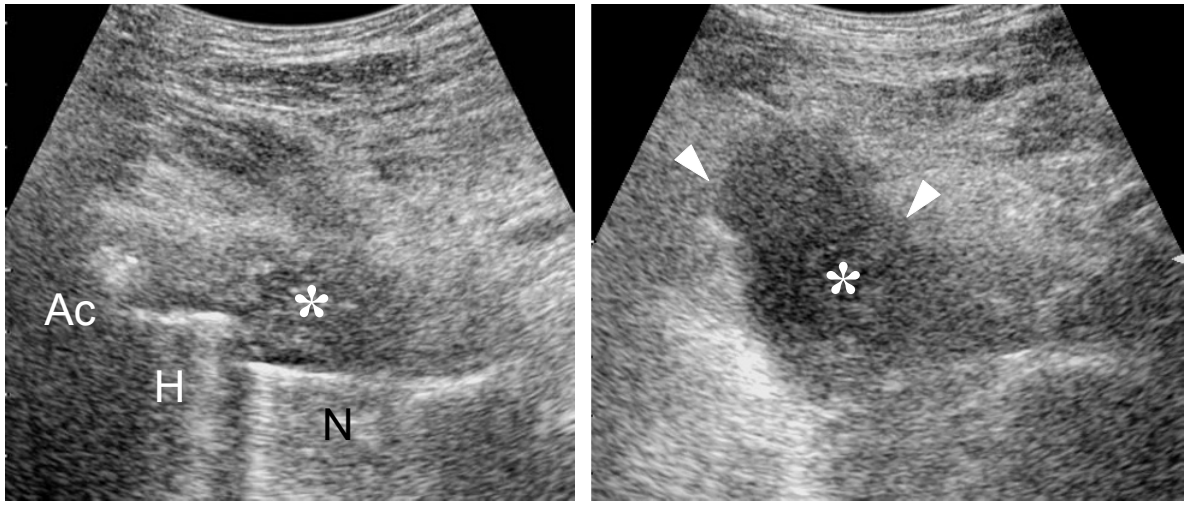

Fig. 12.63a,b. Infection after total hip replacement. Transverse oblique 2–4 MHz US images obtained over **a** the anterior and **b** the posterior aspect of the hip in a patient with a suspected infection of the hip prosthesis. In **a**, an irregular effusion (*asterisk*) containing echogenic material is found within the anterior recess of the pseudocapsule. *Ac*, acetabular component; *H*, head; *N*, neck of the prosthesis. In **b**, the posterior US image shows a para-articular fluid collection located posterior to the femur. A US-guided puncture was performed with sampling of purulent material

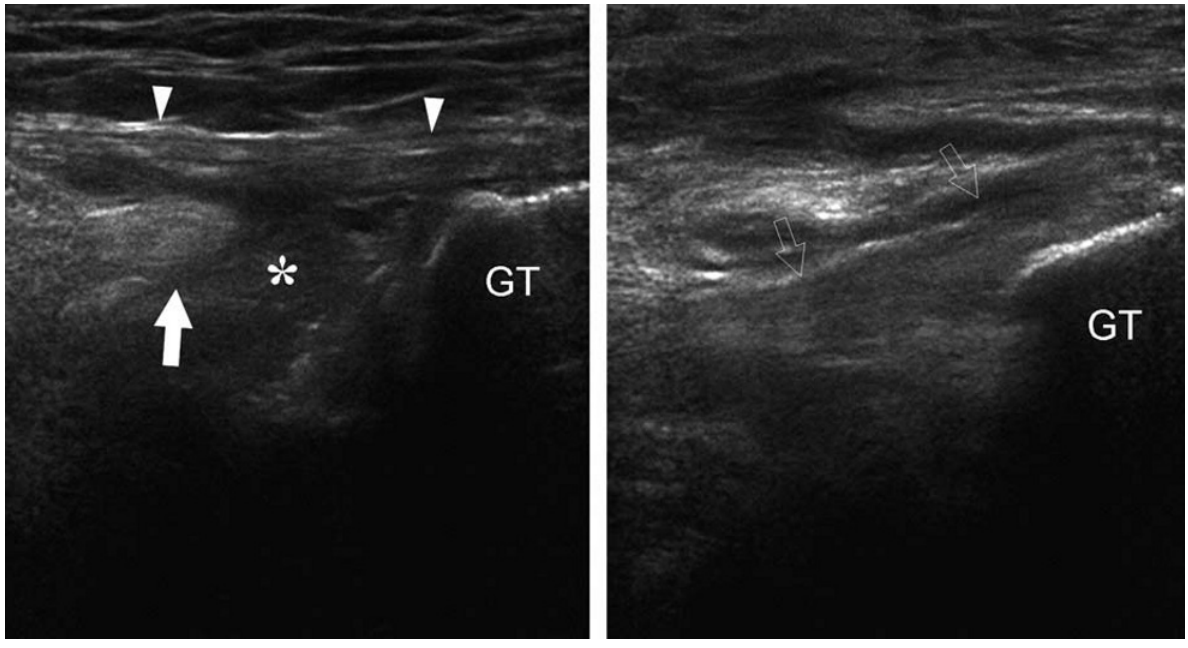

Fig. 12.64a,b. Gluteus medius tendon tear in total hip replacement. **a** Coronal 12–5 MHz US image over the lateral hip in a patient with total hip replacement shows complete detachment of the anterior tendon of the gluteus medius (*arrow*) and a hematoma (*asterisks*) filling the space between the retracted tendon and the greater trochanter (*GT*). Observe the associated thickening of the fasciae latae (*arrowheads*). **b** A more posterior coronal 12–5 MHz US image identifies the intact posterior tendon of the gluteus medius (*open arrows*) inserting into the trochanter

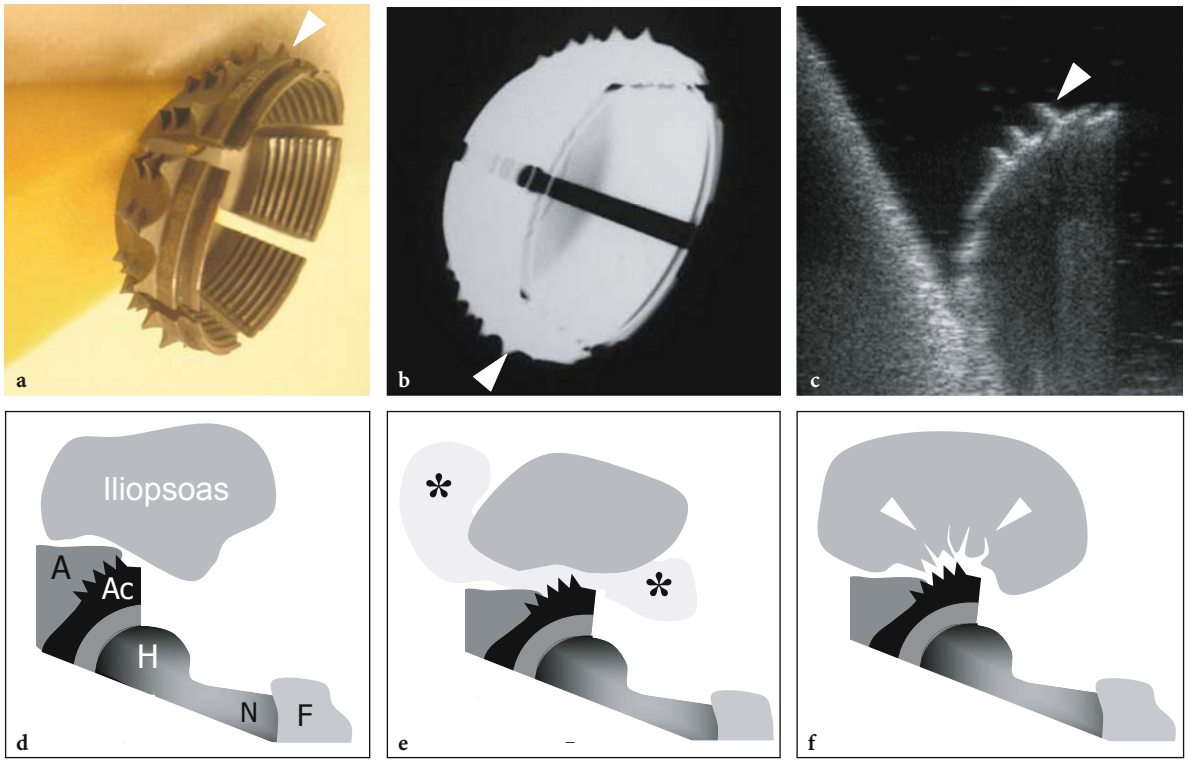

Fig. 12.65a–f. Acetabular cup for hip replacement. **a** Photograph, **b** standard radiograph and **c** in vitro US appearance of an acetabular spiral screwed cup. US depicts the cup as a hyperechoic structure with reverberation artifact characterized by a series of external "teeth" (*arrowhead*). **d–f** Schematic drawings of a sagittal view through the anterior hip illustrate **d** a normally positioned cup, **e,f** an anterior protruding cup resulting in **e** iliopsoas bursitis (*asterisks*) and **f** tears of the undersurface of the iliopsoas muscle (*arrowheads*). *A*, native acetabulum; *Ac*, acetabular cup; *H*, head of the prosthesis; *N*, neck of the prosthesis; *F*, femoral bone

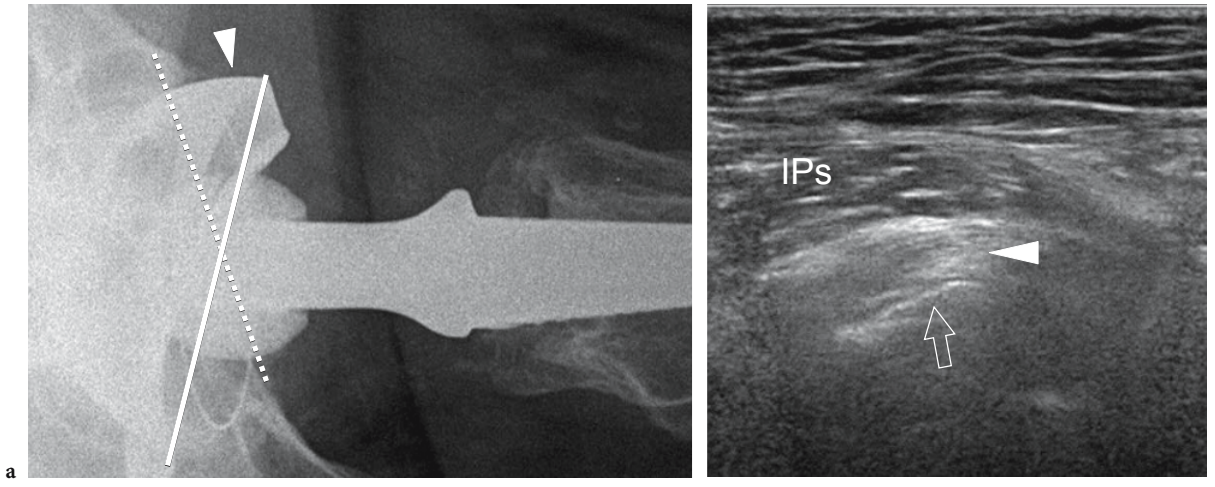

Fig. 12.66a,b. Acetabular cup anteversion. **a** Arcelin X-ray view of the right hip in a patient who underwent total hip replacement. Note the anterior rotation and protrusion of the anterior edge (*arrowhead*) of the cup. **b** Longitudinal 12–5 MHz US image demonstrates the impingement of the protruding cup (*arrow*) with the iliopsoas tendon (*arrowhead*). In this particular case, there was no tendon lesion. *IPs*, iliopsoas muscle

described followed by fibrotic changes. Both bursitis and partial tear of the iliopsoas can cause a ill-defined groin pain that worsens on active flexion or passive extension of the hip, a feature that can alert the clinician to the possibility that iliopsoas impingement may be present. US is able to detect the exact site of the impingement and to assess the iliopsoas damage (Rezig et al. 2004). The most useful scanning planes to demonstrate such impingement are those obtained along the long-axis of the iliopsoas tendon (Figs. 12.67, 12.68). US shows an effusion inside the iliopsoas bursa, focal hypoechoic changes in the iliopsoas muscle and hematoma. Dynamic US assessment of the impingement can be obtained at rest

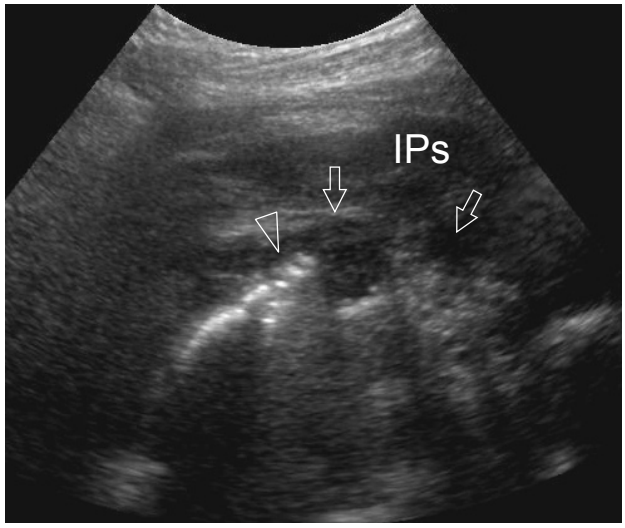

a

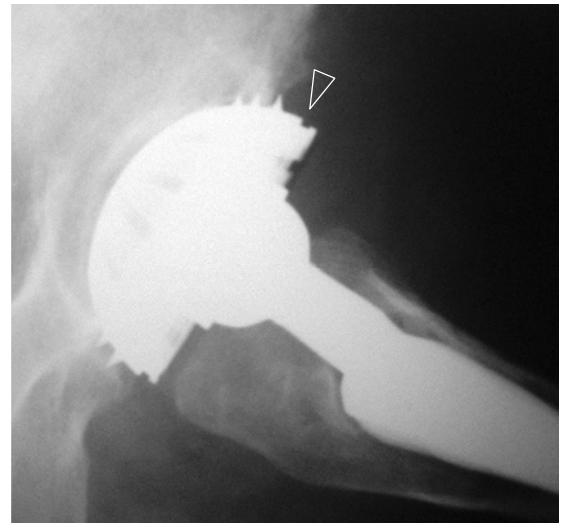

b

Fig. 12.67a,b. Iliopsoas impingement by an acetabular cup. **a** Transverse oblique 12–5 MHz US image obtained over the anterior hip region shows protrusion of the acetabular cup (*arrowhead*) and resulting damage to the undersurface (*arrows*) of the iliopsoas muscle (*IPs*) caused by the "teeth" of the cup. An echogenic effusion is found within the pseudocapsule. **b** Arcelin X-ray view confirms incorrect positioning of too large a cup which resulted in anterosuperior protrusion (*arrowhead*)

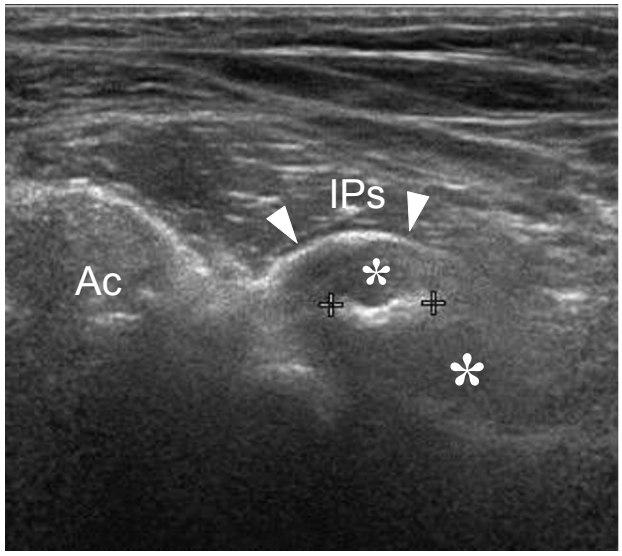

a

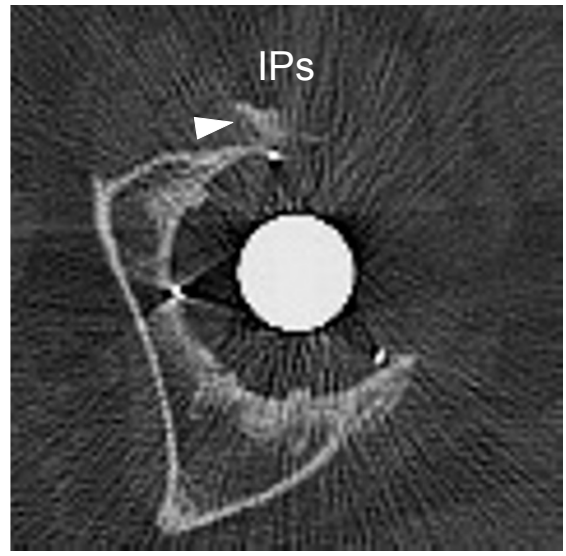

b

Fig. 12.68a,b. Iliopsoas impingement by an acetabular cup. **a** Transverse oblique 12–5 MHz US image obtained over the anterior hip shows a beak-shaped hyperechoic projection (*arrowheads*) on the anterior border of the acetabular cup surrounded by an effusion (*asterisks*). *Ac*, acetabulum. *IPs*, iliopsoas muscle. **b** Correlative transverse CT image demonstrates a hyperdense anterior structure (*arrowhead*) which impinges on the posterior aspect of the iliopsoas muscle (*IPs*), representing cement leakage following the hip replacement procedure

and during contraction of the iliopsoas muscle. The most appropriate therapy includes rest, nonsteroidal anti-inflammatory drugs and local steroid-lidocaine injection. US is effective in accurately guiding anesthetic injections (Wank et al 2004). If conservative therapy fails, iliopsoas tenotomy or surgical revision of the cup can be necessary.

12.5.4.4 Occult Fractures

Due to the anatomic complexity of the hip, some undisplaced fractures or bone avulsion injuries at the tendon attachments on the bone may go unnoticed on plain films, even when additional projections are performed. In these cases, the patient may be submitted to US examination of the hip due to persistent pain and disability in order to rule out soft-tissue abnormalities. With careful scanning technique, US is able to identify occult fractures around the hip based on detection of either a step-off deformity or focal discontinuity or fragmentation of the hyperechoic cortical line (Fig. 12.69). In these instances, additional radiographic or CT studies should always be obtained to confirm the US diagnosis.

12.5.5 Hip Masses

Both solid and cystic masses can be encountered in the soft tissues around the hip joint as incidental findings (Fig. 12.70). Most are benign and have a indolent behavior, such as lipomas, ganglion cysts, bursal distension, lymphadenopathies and neural tumors, and can be easily diagnosed with US based on previously described criteria. The pseudohypertrophy of the tensor fasciae latae muscle can present as a pseudomass arising on the anterolateral aspect of the hip and warrants additional brief discussion here.

12.5.5.1 Pseudohypertrophy of Tensor Fasciae Latae Muscle

Unilateral pseudohypertrophy of the tensor fasciae latae muscle is an uncommon clinical entity that may simulate a soft-tissue neoplasm. This condition is incidentally discovered in elderly women who present with an asymptomatic and unilateral lump in the hip area. A clinical history of hip arthoplasty and peripheral neuropathies is often associated (Ilaslan et al. 2003). US demonstrates a fusiform enlargement of the tensor fasciae latae muscle which assumes a hyperechoic appearance due to an increased amount of fatty tissue interspersed between the muscle fibers (Fig. 12.71). If the examiner is not aware of this condition, the oval shape and hyperechoic appearance of the mass could simulate a soft-tissue lipoma. However, the typical striations of muscle echotexture should avoid any diagnostic confusion. Familiarity with this condition and the characteristic features of tensor fasciae latae hypertrophy on US may aid in making an accurate diagnosis and avoiding unnecessary biopsy or surgical intervention.

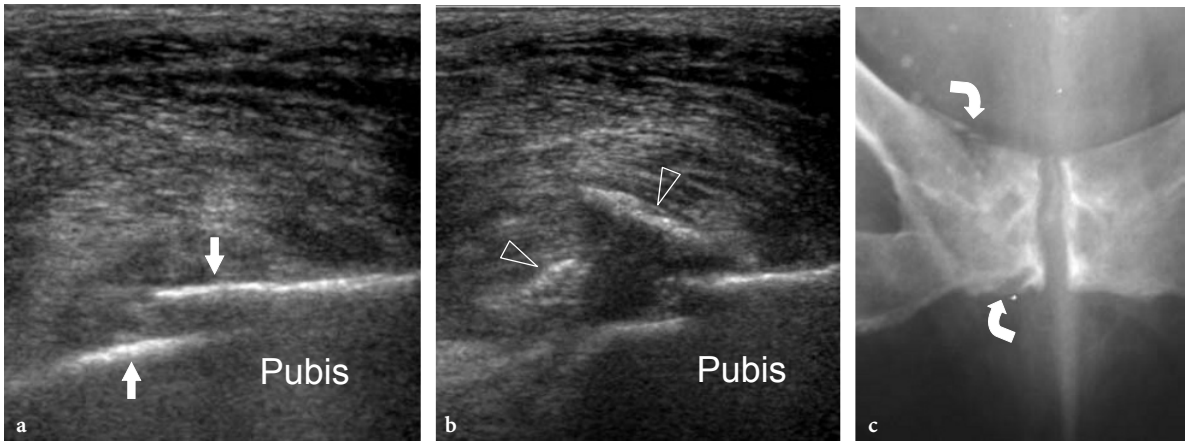

Fig. 12.69a–c. Fracture of the pubis. **a,b** Sagittal 12–5 MHz US images obtained in a middle-aged woman presenting with persistent groin pain after a fall show a discontinuity (*arrows*) of the bright echogenic line of the bony cortex of the right pubis and elevation of some fragments of bone (*arrowheads*) consistent with a fracture. **c** After US examination, the patient was submitted to a radiographic study which confirmed the fracture (*curved arrows*) of the pubis

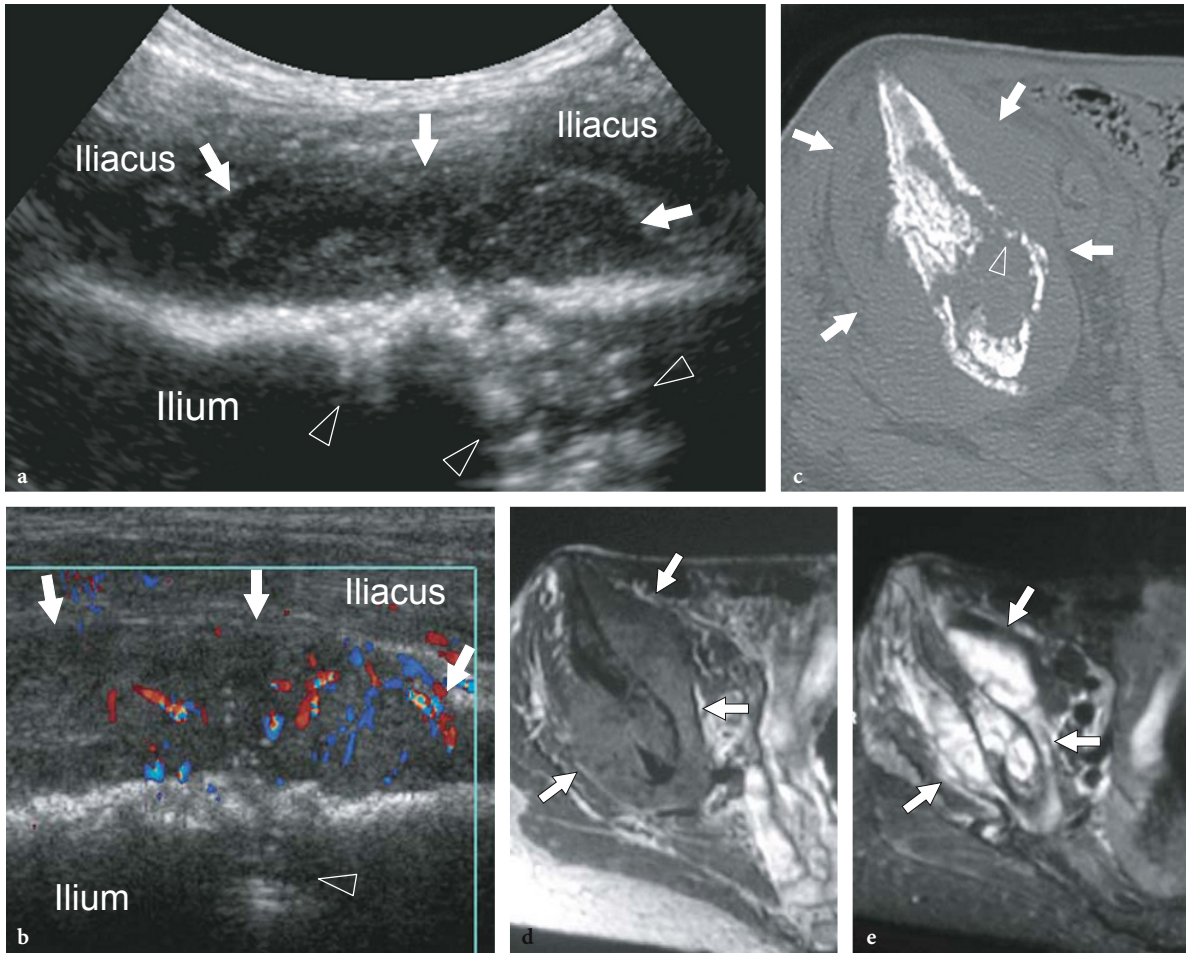

Fig. 12.70a–e. Bone lymphoma. Sagittal **a** gray-scale and **b** color Doppler 12–5 MHz US of the right pelvis in a patient complaining of increasing hip pain for 6 months reveal a solid heterogeneous hypoechoic soft-tissue mass (*arrows*) underlying the iliacus muscle associated with signs of bone destruction (*arrowheads*) of the ilium, resembling a pathologic fracture. The mass exhibits a hypervascular pattern with diffuse and irregularly distributed color flow signals. **c** Transverse CT scan confirms the presence of a large osteolytic lesion of the ilium with pathologic fracture (*arrowhead*). **d** T1-weighted and **e** fat-suppressed T2-weighted MR images show the full extent of the lesion in the ilium and the surrounding soft tissues

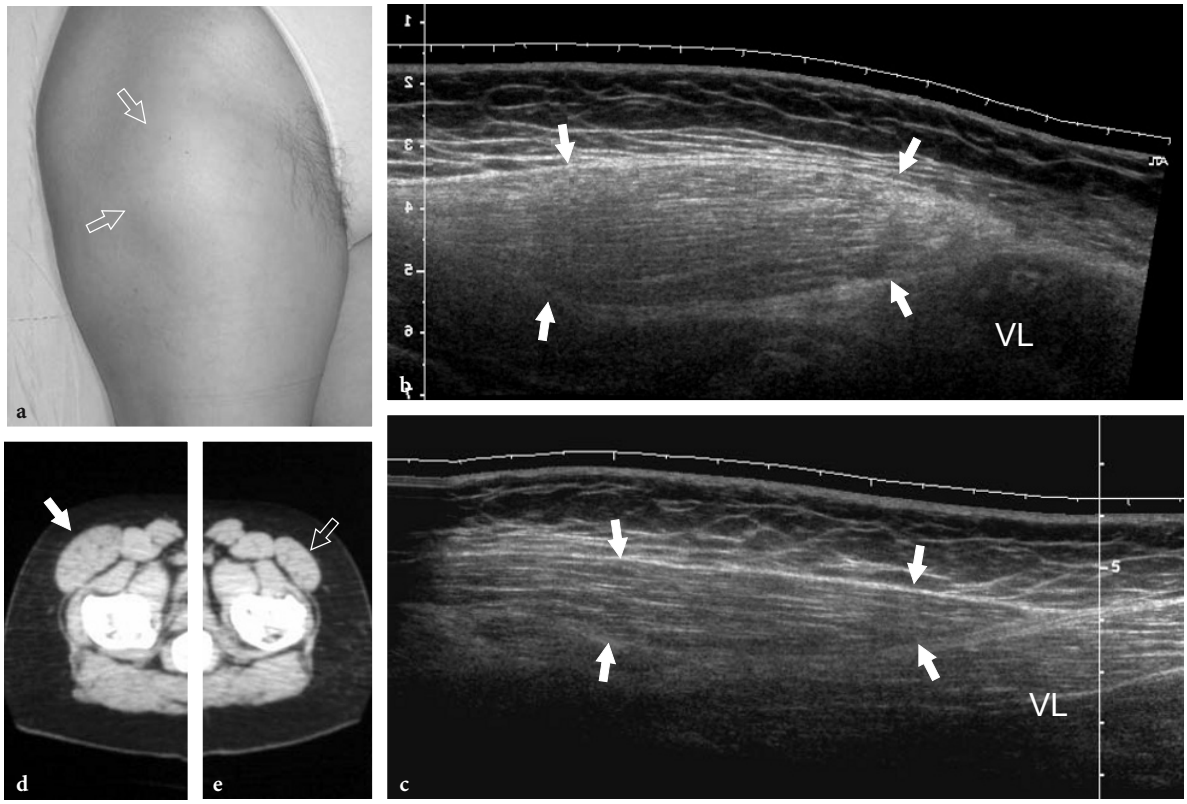

Fig. 12.71a–e. Benign pseudohypertrophy of the tensor fasciae latae muscle. **a** Photograph of the anterior right thigh of a middle-aged woman presenting with a palpable, non-tender anterolateral lump in the thigh which had been gradually enlarging for a decade. Note that the overlying skin appears normal. **b** Longitudinal extended field-of-view 12–5 MHz US image obtained over the mass reveals enlargement and increased echogenicity of the right tensor fasciae latae muscle (*arrows*). **c** Correlative extended field-of-view 12–5 MHz US image obtained on the contralateral side shows a normal tensor fasciae latae muscle (*arrows*). *VL*, vastus lateralis muscle. **d,e** Parts of a transverse CT scan of the lower pelvis confirm the unilateral hypertrophy of the right tensor fasciae latae muscle (*white arrow*) in comparison with the left (*open arrow*)

References

Anda S, Svenningen S, Slordhal J et al (1986) Voluntary hip dislocation examined by computed tomography. Acta Orthop Scand 57:94–95

Arslan H, Sakarya ME, Adak B et al (1999) Duplex and color Doppler sonographic findings in active sacroiliitis. AJR Am J Roentgenol 173:677-680

Bass CJ, Connel DA (2002) Sonographic findings of tensor fasciae latae tendinopathy: another cause of anterior groin pain. Skeletal Radiol 31:143–148

Bianchi S, Martinoli C, Peiris Waser N et al (2002a) Rectus femoris central tear. Skeletal Radiol 31:581–586

Bianchi S, Martinoli C, Keller A et al (2002b) Giant iliopsoas bursitis: ultrasound findings with MRI correlations. J Clin Ultrasound 30:437–441

Blasier RB, Morawa LG (1990) Complete rupture of the hamstrings origin from a water skiing injury. Am J Sports Med 18:435–437

Choi YS, Lee SM, Song Byet et al (2002) Dynamic sonography of external snapping hip syndrome. J Ultrasound Med 21:753–758

Cohen M (2002) Echoanatomie des ichio-jambiers. Gel Contact 9:4–8

Coley BD, Roberts AC, Fellmeth BD et al (1995) Postangiographic femoral artery pseudoaneurysms: further experience with US guided compression repair. Radiology 194:307–311

Connell DA, Bass C, Sykes CA et al (2003) Sonographic evaluation of gluteus medius and minimus tendinopathy. Eur Radiol 13:1339–1347

Cvitanic O, Henzie G, Skezas N et al (2004) MRI diagnosis of tears of the hip abductor tendons (gluteus medius and gluteus minimus). AJR Am J Roentgenol 182:137–143

Fellmeth BD, Roberts AC, Bookstein JJ et al (1991) Postangiographic femoral artery injuries: nonsurgical repair with US guided compression. Radiology 178:671–675

Foldes K, Gaal M, Balint P et al (1992) Ultrasonography after hip arthroplasty. Skeletal Radiol 21:297–299

Foldes K, Balint P, Balint G et al (1995) Ultrasound-guided aspiration in suspected sepsis of resection arthroplasty of the hip joint. Clin Rheumatol 14:327–329

Ginesty E, Dromer C, Galy-Fourcade D (1998) Iliopsoas bursopathies. A review of twelve cases. Rev Rhum Engl Ed 65:181–186

Graif M, Seton A, Nerubai J et al (1991) Sciatic nerve: sonographic evaluation and anatomic-pathologic considerations. Radiology 181:405–408

Gruber H, Peer S, Kovacs P et al (2002) The ultrasonographic appearance of the femoral nerve and cases of iatrogenic impairment. J Ultrasound Med 22:163–172

Hashimoto BE, Green TM, Wiitala L (1996) Ultrasonographic diagnosis of hip snapping related to iliopsoas tendon. J Ultrasound Med 16:433-435

Hasselman CT, Best TM, Hughes C 4th, Martinez S, Garrett WE Jr (1995) An explanation for various rectus femoris strain injuries using previously undescribed muscle architecture. Am J Sports Med 23:493–499

Heller (2003) Anatomy of the trochanteric bursae (letter). Radiology 226:922–922

Ilaslan H, Wenger DE, Shives TC et al (2003) Unilateral hypertrophy of tensor fasciae latae: a soft-tissue tumor simulator. Skeletal Radiol 32:628–632

Janus C, Hermann G (1982) Enlargement of the iliopsoas bursa: unusual cause of cystic mass on pelvic sonogram. J Clin Ultrasound 10:133–135

Janzen DL, Partridge E, Logan PM et al (1996) The snapping hip: clinical and imaging findings in transient subluxation of the iliopsoas tendon. Can Assoc Radiol J 47:202–208

Kang SS, Labropoulos N, Mansour A et al (1998) Percutaneous ultrasound guided thrombin injection: a new method for treating postcatheterization femoral pseudoaneurysms. J Vasc Surg 27:1032–1038

Karpinski MRK, Piggott H (1985) Greater trochanteric pain syndrome. J Bone Joint Surg Br 67:762–763

Klauser A, Halpern EJ, Frauscher F et al (2005) Inflammatory low back pain: high negative predictive value of contrast-enhanced color Doppler ultrasound in the detection of inflamed sacroiliac joints. Arthritis Rheum 53:440-444

Koski JM, Anttila PJ, Isomaki HA (1989) Ultrasonography of the adult hip joint. Scand J Rheumatol 18:113–117

Lee EY, Margherita AJ, Gierada DS et al (2004) MRI of piriformis syndrome. AJR Am J Roentgenol 183:63-64

Lequesne M, Dang N, Montagne P et al (1991) Conflict between psoas and total hip prosthesis. Rev Rhum Mal Osteoartic 58:559–564

Mellado JM, Pérez del Palomar L, Diaz L et al (2004) Long standing Morel-Lavallée lesions of the trochanteric region and proximal thigh: MRI features in five patients. AJR Am J Roentgenol 182:1289–1294

Morel-Lavallée (1863) Décollements traumatiques de la peau et des couches sous-jacentes. Arch Gen Med 1:20–38, 172–200, 300–332

Pai VR, van Holsbeeck M (1995) Synovial osteochondromatosis of the hip: role of sonography. J Clin Ultrasound 23:199–203

Parra JA, Fernández MA, Encinas B et al (1997) Morel-Lavallée effusions in the thigh. Skeletal Radiol 26:239–241

Paulson EK, Sheafor DH, Kliewer MA et al (2000) Treatment of iatrogenic femoral arterial pseudoaneurysms: comparison of US-guided thrombin injection with compression repair. Radiology 215:403–408

Paulson EK, Nelson RC, Mayes CE et al (2001) Sonographically guided thrombin injection of iatrogenic femoral pseudoaneurysms: further experience of a single institution. AJR Am J Roentgenol 177:309–316

Pekkafali MZ, Kiralp MZ, Basekim CC et al (2003) Sacroiliac joint injections performed with sonographic guidance. J Ultrasound Med 22:553-559

Pellman E, Kumari S, Greenwald R (1986) Rheumatoid iliopsoas bursitis presenting as unilateral leg edema. J Rheumatol 13:197–200

Pelsser V, Cardinal E, Hobden R et al (2001) Extraarticular snapping hip: sonographic findings. AJR Am J Roentgenol 176:67–73

Pfirrmann CWA, Chung CB, Theumann NH et al (2001) Greater trochanter of the hip: attachement of the abductor mechanism and a complex of three bursae-MR imaging and MR bursography in cadavers and MR imaging in asymptomatic volunteers. Radiology 221:469–477

Rezig R, Copercini M, Montet X et al (2004) Ultrasound diagnosis of anterior iliopsoas impingement in total hip replacement. Skeletal Radiol 33:112–116

Rizio L, Salvo JP, Schurhof MR et al (2004) Adductor longus rupture in professional football players: acute repair with suture anchors. A report of two cases. Am J Sports Med 32:243–245

Robben SGF, Lequin MH, Diepstraten AFM et al (1999) Anterior joint capsule of the normal hip in children with transient synovitis: US study with anatomic and histology correlation. Radiology 210:499–507

Robinson P, Barron DA, Parsons W, Grainger AJ, Schilders EMG, O'Connor PJ (2004) Adductor-related groin pain in athletes: correlation of MR imaging with clinical findings. Skeletal Radiol 33:451–457

Salmeron I, Cardenas JL, Ramirez-Escobas MA et al (1999) Idiopathic iliopsoas bursitis. Eur Radiol 9:175

Sener RN, Alper H, Ozturk L et al (1991) Retroperitoneal part of the femoral nerve. Normal ultrasound features. Neuroradiology 33:159–161

Slavotinek JP, Verrall GM, Fon GT (2002) Hamstrings injury in athletes: using MR imaging measurements to compare extent of muscle injury with amount of time lost from competition. AJR Am J Roentgenol 179:1621–1628

Van Holsbeeck MT, Eyler WR, Sherman LS et al (1994) Detection of infection in loosened hip prostheses: efficacy of sonography. AJR Am J Roentgenol 163:381–384

Van Mieghem IM, Boets A, Sciot R et al (2004) Ischiogluteal bursitis: an uncommon type of bursitis. Skeletal Radiol 33:413-416

Wank R, Miller TT, Shapiro JF (2004) Sonographically guided injection of anesthetic for iliopsoas tendinopathy after total hip arthroplasty. J Clin Ultrasound 32:354-357

Wahl CJ, Warren RF, Adler RS et al (2004) Internal coxa saltans (snappping hip) as a result of overtraining. A report of 3 cases in professional athletes with a review of causes and the role of ultrasound in early diagnosis and management. Am J Sports Med 32:1302–1209

Walther M, Harms H, Krenn V et al (2002) Synovial tissue of the hip at power Doppler US: correlation between vascularity and power Doppler US signal. Radiology 225:225–231

Weybright PN, Jacobson JA, Murry KH et al (2003) Limited effectiveness of sonography in revealing hip joint effusion: preliminary results in 21 adult patients with native and postoperative hips. AJR Am J Roentgenol 181:215–218

Yoon TR, Song EK, Chung JY et al (2000) Femoral neuropathy caused by enlarged iliopsoas bursa associated with osteonecrosis of femoral head: a case report. Acta Orthop Scand 71:322–324

Zieger MM, Dörr U, Schulz RD et al (1987) Ultrasonography of hip joint effusions. Skeletal Radiol 16:607–611